AN ABSTRACT OF THE DISSERTATION OF

Sasmita Tripathy for the Doctor of Philosophy in Nutrition presented on July 11, 2012.

Title: Polyunsaturated Fatty Acid Synthesis and Type 2 Diabetes Complications

Abstract approved:

Donald B Jump

Type 2 diabetes mellitus (T2DM) is a disease of multi-complications affecting more than 20 million US adults. Hyperglycemia is the classic clinical feature of diabetes, and uncontrolled hyperglycemia leads to deadly health complications. Thus, control of blood glucose represents a major goal for diabetics. Human and rodent studies revealed another clinical feature; diabetics have low tissue and plasma levels of polyunsaturated fatty acids (PUFAs), an effect often attributed by impaired endogenous PUFA synthesis. In this context, rodent studies have revealed a possible link between PUFA synthesis and high fat diet induced obesity and diabetes. These studies have shown that obese and diabetic mice have low hepatic expression and activity of fatty acid elongase-5 (Elovl5), a key enzyme involved in the PUFA synthesis pathway. Over-expression of Elovl5 in livers of chow fed C57BL/6J mice decreased fasting blood glucose and increased hepatic glycogen contents. Therefore, my hypothesis for the current work is that elevated hepatic Elovl5 activity or improved hepatic PUFA synthesis will improve systemic and hepatic

carbohydrate metabolism in a mouse model of diet induced obesity and diabetes.

Using a recombinant adenovirus approach, we over-expressed Elovl5 in livers of high fat diets (60% calories derived from fat as lard, Research Diets) induced obese-diabetic mice. Elevated hepatic Elovl5 activity increased hepatic and plasma C_{20-22} PUFA contents, reduced homeostatic model assessment for insulin resistance (HOMA-IR), improved glucose tolerance and lowered fasting blood glucose to euglycemic levels in obese-diabetic mice. The mechanism for insulin mimetic effect of Elovl5 on hepatic glucose metabolism was correlated with increased phosphorylation of Akt-S^{473}, FoxO1-S^{256} and PP2Acat-Y^{307}, decreased nuclear content of FoxO1, and decreased expression of Pck1 and G6Pase; important enzymes involved in gluconeogenesis (GNG) and glucose production. Phospho-FoxO1 is excluded from nuclei, ubiquitinated and degraded by the proteasome. Loss of nuclear FoxO1, due to its increased phosphorylation, leads to the reduction in the expression of key genes involved in gluconeogenesis, i.e., Pck1 and G6Pase.

Using obese-diabetic mice liver extracts and HepG2 cells, I established that Elovl5 uses two mechanisms to control hepatic GNG. The first mechanism involves Elovl5 mediated increased Akt2-S^{473} and FoxO1-S^{256} phosphorylation via mTORC2-rictor pathway. The second mechanism involves Elovl5 mediated attenuation of de-phosphorylation of FoxO1 via PP2A inhibition. Together, these mechanisms increase FoxO1 phosphorylation status in livers of fasted

obese-diabetic mice, lower hepatic FoxO1 nuclear abundance and FoxO1 capacity to sustain transcription of GNG genes and inhibit GNG and restore blood glucose levels in fasted obese-diabetic mice.

Results of these studies showed Elovl5 corrected high fat diet induced hyperglycemia in C57BL/6J mice, identified the molecular mechanism of Elovl5 control of GNG and explained how Elovl5 or PUFA synthesis controls GNG. Therefore, these findings will be eventually helpful in developing a therapeutic target to combat hyperglycemia.

Polyunsaturated Fatty Acid Synthesis and Type 2 Diabetes Complications

by
Sasmita Tripathy

A DISSERTATION

submitted to

Oregon State University

in partial fulfillment of
the requirements for the
degree of

Doctor of Philosophy

Presented July 11, 2012
Commencement June 2013

Doctor of Philosophy dissertation of Sasmita Tripathy
Presented on July 11, 2012.

APPROVED:

Major Professor, representing Nutrition

Co-Director of the School of Biological and Population Health Sciences

Dean of the Graduate School

I understand that my dissertation will become part of the permanent collection of Oregon State University libraries. My signature below authorizes release of my dissertation to any reader upon request.

Sasmita Tripathy, Author

ACKNOWLEDGEMENTS

I would like to acknowledge the people who helped me directly or indirectly throughout my PhD career. At first, it is my privilege to express my sincere appreciation to my major advisor Dr. Donald B Jump for his sustained interest, meticulous guidance, constructive criticism, tireless supervision, moral support and valuable suggestions shown during the period of my investigation, that made it possible to complete my PhD degree successfully. It is a great honor for me to work under the supervision of one of the best scientists in lipid area. I greatly appreciate your time you have invested in me. Thank you so much for not losing faith on me during my lowest point of my career.

I am extremely grateful to my doctoral committee members; Dr. Maret G Traber, Dr. Emily Ho, Dr. Urszula Iwaniec and my graduate council representative Dr. Jean Hall who have been very instrumental throughout my PhD career. Their constructive criticism, guidance and valuable suggestions helped me in many aspects of PhD career. Thank you all for your time and efforts and encouraging me to work harder.

I would like to acknowledge past and present members of the Jump lab. I would like to thank first Dr. Moises Torres-Gonzalez; it was a great experience working with him in Elovl5 project. I would like to thank Karin Hardin for her excellent technical help throughout the PhD career. I would like to thank Chris Depner and Kelli Lytle for their friendships and sharing graduate school experiences with me.

I would like to acknowledge the Nutrition graduate program, School of Biological and Population Health Sciences, College of Public Health and Human Sciences and the Linus Pauling Institute for providing me great research facilities, financial support and opportunities. I would like to thank my friends Anna, Jill, John, Carmen and Laura for their invaluable friendships and support throughout my career.

I would like to thank my parents and brothers for their love and support. Thank you for being good listeners and patiently waiting for me to complete my PhD degree. I would also like to thank my in-laws for their moral support.

At last I would like to thank two very important persons of my life; my husband Siba Das and our daughter Ella. Thank you Siba for being such a good listener, caring and loving husband. I would also like to thank my husband Siba for inspiring me to join graduate school in US, teaching me various lab techniques and supporting me throughout my PhD career. Finally I would like to thank our daughter Ella; she is a constant motivation for me these past two years. It is so much fun watching her growing up. I am so proud of you Ella.

CONTRIBUTION OF AUTHORS

The author's responsibilities were as follows:

Chapter 1: Sasmita Tripathy wrote and Dr. Donald B Jump edited it.

Chapter 2: Sasmita Tripathy, Dr. Moises Torres-Gonzalez and Dr. Donald B Jump contributed to the study concept, research design, data interpretation, manuscript preparations and manuscript revisions. Sasmita Tripathy contributed to the protein data, Dr. Donald B Jump contributed to the enzyme activity data and Dr. Moises Torres-Gonzalez contributed to the RT-PCR data.

Chapter 3: Sasmita Tripathy and Dr. Donald B Jump contributed to the study concept, research design and data interpretation. Sasmita Tripathy generated the data, analyzed the data and wrote manuscript and Dr. Donald B Jump edited the manuscript.

Chapter 4: Sasmita Tripathy wrote and Dr. Donald B Jump edited it.

TABLE OF CONTENTS

TABLE OF CONTENTS (Continued)

TABLE OF CONTENTS (Continued)

Page

TABLE OF CONTENTS (Continued)

Page

LIST OF FIGURES

LIST OF FIGURES (Continued)

LIST OF FIGURES (Continued)

LIST OF TABLES

Dedicated to my beloved father Mr. Ramesh Chandra Tripathy

Chapter 1

Introduction

1.1. Type 2 diabetes mellitus

Diabetes mellitus, a disorder of metabolism, has been recognized as a disease for over two thousand years (source: www.who.int). Type 2 diabetes mellitus (T2DM) makes up about 90% of all diabetic cases, whereas, the other 10% are due to type 1 and gestational diabetes mellitus (1). T2DM affects more than 200 million people worldwide and is a major public health concern in the US, affecting ~ 20 million adults and resulting in diabetes care cost of ~$200 billion annually (1). The prevalence of T2DM has increased at an alarming rate over the past few decades both in the US and around the world. It is known to be associated with obesity, and is often accompanied by non-alcoholic fatty liver disease (NAFLD) and metabolic syndrome (2-4). Approximately 70% of individuals with type 2 diabetes have a fatty liver, in which cases the disease follows a more aggressive course with necro-inflammation and fibrosis (2-4). T2DM also increases the risk for cardiovascular disease, stroke, hypertension and cognitive dysfunction (5).

The immediate symptom observed in T2DM is the impairment in insulin signaling. Impairment in insulin signaling leads to persistent increase in glucose production, glucose output from the liver, and decrease in glucose uptake by muscle and adipose tissue, ultimately leading to excessive blood glucose level, a condition known as hyperglycemia (2-4, 6). Uncontrolled hyperglycemia further causes metabolic changes that can damage many body organs and also lead to life threatening micro-vascular complications such as

retinopathy, nephropathy and neuropathy (7-9). Thus, T2DM is a deadly disease of multi-complications, and control of blood glucose represents a major goal for patients with T2DM.

The type and quantity of dietary fatty acids play significant roles in onset and progression of T2DM and its associated complications (10-12). Excessive dietary consumption of saturated fatty acids (SFA) or an imbalance in SFA and polyunsaturated fatty acids (PUFA) intakes have been shown to increase the risk of obesity, insulin resistance and fatty liver disease (10-12). Population studies suggest that subjects with T2DM and fatty liver have low plasma and tissue C_{20-22} polyunsaturated fatty acids, which could be attributed to either impaired endogenous PUFA synthesis or less dietary PUFA intake (13-16). Supplementation studies with dietary PUFAs in subjects with T2DM showed no significant improvement on blood glucose control and insulin resistance, indicating that the diabetics have impaired endogenous PUFA synthesis pathway (17, 18). Despite significant advancement in T2DM research, the role of endogenous PUFA synthesis in hyperglycemia and progression of T2DM is still not clear. The current work examines the link between endogenous PUFA synthesis and hyperglycemia.

1.2. Endogenous fatty acid synthesis

The liver acts as the central organ that controls whole body fatty acid metabolism. Fatty acids have several important physiological functions such as, source of energy, constituent of structural and bioactive lipids,

maintenance of cell membrane fluidity, energy metabolism, and regulation of gene expression and signaling pathways (19). Regulation of these physiological functions is governed by many endogenous metabolic pathways such as *de novo* lipogenesis (DNL), fatty acid elongation, desaturation and β-peroxidation (20-22). DNL is a metabolic process used for synthesis of saturated fatty acids from glucose, whereas elongation, desaturation and β-peroxidation are used for modification of fatty acids to generate endogenous unsaturated fatty acids (20-22).

Most cells have the capacity to synthesize saturated fatty acids from glucose via DNL by using two enzymes; acetyl CoA carboxylase (ACC) and fatty acid synthase (FASN) (20-23). DNL pathway **(Fig. 1.1)** is mediated by key transcription factors, sterol regulatory element binding protein (SREBP)-1 and carbohydrate regulatory element binding protein (ChREBP) / max like factor X (MLX) heterodimer (21, 22).

Fatty acid elongation is the enzymatic metabolic process of elongating fatty acids by two carbon atoms (23, 24) with help of the elongase enzyme. Elongases act as condensing enzymes interacting with 3-keto acyl-CoA reductase, a dehydratase and trans-2,3-enoyl-CoA reductase to elongate fatty acids (23, 25). There are seven fatty acid elongases (Elovl 1-7) described in rodent and human genomes (22, 24, 25), four of which are expressed in liver (Elovl1, 2, 5 and 6) (20, 21). Fatty acid elongation takes place in microsome,

where malonyl-CoA is used as a substrate for adding two carbon atoms to fatty acyl-CoA along with other substrate NADPH (23, 25).

Desaturation is a process of removing two hydrogen atoms from an organic compound, creating a carbon-carbon double bond with the help of the enzyme, desaturase. Desaturases are classified as delta, indicating that the double bond is created at a fixed position from the carboxyl group of a fatty acid (21, 22). There are three different desaturase enzymes; stearoyl CoA desaturase-1 (SCD-1) or delta-9 desaturase (Δ^9D), fatty acid desaturase-1 (FADS1) or delta-5 desaturase (Δ^5D) and fatty acid desaturase-2 (FADS2) or delta-6 desaturase (Δ^6D) (21, 22). Fatty acid elongases function together with fatty acid desaturases to generate long chain MUFA (**Fig. 1.1**) and PUFAs (**Fig. 1.2**) (20-22, 25).

Peroxisomal β-oxidation (pβ-Ox) is a process in which long chain fatty acids break down to shorter length. It is a metabolic pathway in PUFA synthesis, which takes place in the peroxisome (22).

1.2.1. Regulation of DNL, MUFA and PUFA synthesis

The liver regulates fatty acid metabolism by controlling endogenous fatty acid synthesis and oxidation, as well as gene expression involved in carbohydrate metabolism and the insulin signaling pathway (21, 22). Regulation of these processes by liver is carried out by a variety of transcription factors, which alter the genes involved in fatty acid metabolism. Some of the key transcription factors involved in fatty acid metabolism are

peroxisome proliferator activated receptor (PPAR)-α, liver X receptor (LXR), sterol regulatory element binding protein (SREBP)-1 and carbohydrate regulatory element binding protein (ChREBP)/max like factor X (MLX) heterodimer. These transcription factors are involved in various steps of fatty acid metabolism; PPAR-α induces fatty acid oxidation, whereas LXR, SREBP-1 and ChREBP/MLX heterodimer induce DNL and MUFA synthesis **(Fig. 1.3)** (12, 22, 26, 27). LXR, SREBP-1 and ChREBP/MLX heterodimer regulate this regulation of DNL and MUFA synthesis by induction of key enzymes, ACC1, ACC2, FASN, SCD-1 and Elovl6. These key enzymes are also coordinately controlled by insulin, dietary carbohydrate, fasting and refeeding condition (20, 21). In addition to regulating the MUFA pathway, SREBP1 also regulates the PUFA synthesis by modest induction of enzymes FADS1, FADS2, Elovl2 and Elovl5 (21). PUFA synthesis is strongly controlled by the transcription factor PPAR-α, which is responsible for the strong induction of enzyme Elovl5. Enzymes involved in PUFA synthesis are less responsive to insulin, fasting or refeeding conditions as compared to the ones involved in DNL and MUFA synthesis (20, 21).

1.2.2. Impact of diabetes and obesity on enzymes involved in DNL, MUFA and PUFA synthesis

Transcription factors controlling the enzymes involved in DNL, MUFA and PUFA synthesis also play important role in obesity, metabolic syndrome and diabetes (28-31). These three metabolic disorders have been examined in

rodent models; streptozotocin-induced diabetic rat, high fat diet induced obese-diabetic mice and obesity induced by leptin deficient mice (21). Studies on streptozotocin-induced diabetes in male Sprague-Dawley rats have revealed that these rats have a decline in the hepatic nuclear protein abundance of SREBP-1 and MLX which is associated with the decline in expression of ACC1 and 2, FASN, Elovl6 and SCD-1, enzymes involved in DNL and MUFA synthesis pathways (21). Expression of Elovl5, Elovl2, FADS1 and FADS2, enzymes involved in PUFA synthesis are unaffected in streptozotocin induced diabetic rodents (21).

Studies with leptin deficiency induced obese C57BL/6J mice ($Lep^{ob/ob}$ mice) showed that these mice are massively engorged with lipid, predominantly neutral lipid in liver and have massive increase in hepatic nuclear expression of SREBP-1 and MLX (21). The increase in SREBP-1 and MLX correlates with strong induction of enzymes in DNL and MUFA synthesis such as ACC1 and 2, FASN, SCD-1 and Elovl6. These mice also had a modest induction of enzymes involved in PUFA synthesis; FADS1, FADS2 and Elovl2 and strong induction of Elovl5 (21).

High fat diet (60% calories derived from fat as lard) induced obese-diabetic mice have a lower nuclear abundance of SREBP-1 and MLX in the liver but no effect on hepatic nuclear abundance of PPAR-α (21). These changes in hepatic transcription factor abundance is associated with suppression of enzymes, ACC1 and 2, FASN, SCD-1 and Elovl6, involved in

the DNL and MUFA synthesis and Elovl5, involved in PUFA synthesis (21). Results from these three rodent models suggest that obesity and diabetes modulate endogenous fatty acid synthesis pathways.

1.3. Role of endogenous fatty acid synthesis in T2DM and associated complications

1.3.1. Role of DNL and MUFA synthesis

Rodent studies on manipulation of enzymes in DNL and MUFA synthesis have defined the crucial role of DNL and MUFA synthesis in obesity, diabetes and their associated complications. Knockout studies of ACC1 in rodents have shown decreased DNL and triglyceride synthesis (32, 33), whereas, studies with ACC2 knockout mice (34, 35) have shown decreased bodyweight and increased fatty acid oxidation, glucose uptake and insulin sensitivity. SCD-1 knockout rodents have severe impairments in the biosynthesis of lipids rich in MUFA such as triacylglycerol, cholesterol ester and wax ester etc. (36, 37). Liver specific SCD-1 knockout mice are lean and are protected from diet-induced obesity, fatty liver and insulin resistance (36, 37). Transient suppression of SCD-1 by using an antisense oligonucleotide in $LDLR^{-/-}$, $ApoB^{100/100}$ mice has protected them from diet induced obesity, fatty liver and insulin resistance (38). Global knock down of Elovl6 in C57BL/6J mice, an enzyme in MUFA synthesis, protected the mice from hyperglycemia, hyperinsulinemia and hepatic insulin resistance (39). Studies in humans also suggested a positive correlation between SCD-1 activity and risk of metabolic syndrome and T2DM (40). All the above studies either confirmed or suggested

that over-expression or increases in activity of ACC1, ACC2, SCD-1 and Elovl6 have detrimental effects on metabolic syndrome, obesity, fatty liver and T2DM.

1.3.2. Role of PUFA synthesis

Studies on obese humans or patients with T2DM and metabolic syndrome have suggested that obese and diabetic subjects have low blood and tissue levels of $C_{20\text{-}22}$ PUFAs compared to healthy humans, an effect attributed to impaired endogenous PUFA synthesis (13-16, 41, 42). These studies showed that obese and type 2 diabetic subjects had increased serum palmitic acid levels, decreased FADS1 (low 20:4,n-6/20:3,n-6 ratio) and FADS2 (low 18:3,n-6/18:2,n-6 ratio) activity as compared to the healthy subjects, suggesting that obesity and T2DM modulate endogenous PUFA synthesis pathway (13-16, 41, 42). Although, these population studies underline an association between endogenous PUFA synthesis and T2DM, the metabolic basis and physiological consequences of low tissue and blood levels of PUFAs on blood glucose control and insulin resistance still remain unclear.

Studies on rodents give a clear picture for the link between PUFA synthesis and obesity, T2DM and metabolic syndrome (21, 43, 44). By knocking out FADS2, a gene involved in PUFA synthesis, researchers have shown that PUFA synthesis is very essential for multiple physiological functions such as cell membrane function, cell signaling, vision, brain

development, inflammation and reproduction etc. (45-47). Mice fed with high fat diets for 10 weeks to induce obesity and diabetes also had suppressed PUFA synthesis, which corresponded with suppression of Elovl5, an enzyme responsible for elongation of the PUFAs (21). Incidentally, high fat diets had no impact on other enzymes such as Elovl2, FADS1 and FADS2 involved in the PUFA synthesis pathway, suggesting that Elovl5 is the only enzyme that controls PUFA synthesis during obesity and diabetes (21). In another study, using A/J and C57BL/6J strains of mice, which are resistant and sensitive respectively to high fat diet induced obesity, hepatosteatosis and T2DM despite the same food intake, it was observed that the A/J mice had decreased hepatic triglyceride content, decreased blood glucose, and increased hepatic Elovl5 expression, as compared to high fat diet induced obese-diabetic C57BL/6J mice (43). These findings suggest that the increased expression of hepatic Elovl5 may have been responsible for the resistance to obesity and T2DM observed in the A/J strain of mice. Mice with knocked out Elovl5 develop fatty liver, have decreased hepatic arachidonic acid, and increased hepatic nuclear protein abundance of SREBP-1 (44). These rodent studies provide evidence for a possible link between endogenous PUFA synthesis, Elovl5 and complications associated with obesity and T2DM.

1.4. Elovl5, PUFA synthesis and blood glucose control

Elovl5 is a 28 KD microsomal enzyme involved in elongation process of PUFA synthesis. Among the elongases, it is the most abundantly expressed

enzyme in human and rodent livers (20-22). The transcription factor SREBP-1, modestly induces Elovl5 expression in liver (21). Fish oil and high fat diets suppress Elovl5 expression and PUFA synthesis, whereas, PPAR-α agonist, and leptin deficiency induces its expression (20, 21).

Mice fed high fat diets are obese-diabetic, hyperglycemic, have suppressed PUFA synthesis and suppressed expression and activity of the enzyme Elovl5 (21). To understand the role of Elovl5 in hyperglycemia, chow fed C57BL/6J mice were injected with a recombinant adenovirus expressing Elovl5 or the control gene luciferase (22). Increased hepatic Elovl5 expression resulted in reduced fasting blood glucose and increased fasting hepatic glycogen content. These events are also shown to be independent of PPAR-α, SREBP1, ChREBP/MLX heterodimer control. In addition, increased hepatic Elovl5 activity improved insulin action in livers of fasted mice leading to suppression in gluconeogenesis and glycogen breakdown and thereby, decreased blood glucose levels and increased hepatic glycogen content (22).

1.5. Mechanism of hepatic insulin action

Insulin plays a major role in controlling hepatic and whole body carbohydrate, protein and lipid metabolism (5). Insulin binds to the insulin receptor present on the cell membrane, and this binding event leads to several phosphorylation events inside the cell **(Fig. 1.4)**. Phosphorylation of insulin receptor substrate (IRS), phosphatidylinositol 3-kinase (PI3-kinase) and Akt promotes storage of nutrients in the form of glycogen, lipid and protein, and

suppresses gluconeogenesis and hepatic glucose production (48). Phosphorylation or dephosphorylation state of each component in insulin signaling determines their activity (48-50). These events are tightly regulated by kinases, phosphatases and other regulatory components (5, 51-59). Fasting and refeeding conditions regulate hepatic insulin signaling. During fasting, there is suppression in the insulin mediated inhibition of gluconeogenesis and glycogen breakdown, whereas during refeeding insulin inhibits gluconeogenesis and promotes glycogen synthesis (5). Studies in my dissertation will address the insulin signaling components leading towards the control of gluconeogenesis.

1.5.1. Insulin regulation of hepatic gluconeogenesis

The liver produces glucose via gluconeogenesis (GNG) from non-carbohydrate substrates such as lactate, pyruvate, glycerol and alanine (60). The rate of GNG is controlled by the expression of key regulatory enzymes such as phosphoenolpyruvate carboxykinase (PepCk or Pck1), glucose-6 phosphatase (G6Pase or G6Pc) and the availability of gluconeogenic precursors (e.g. lactate, pyruvate, glycerol and alanine) (5). GNG and hepatic glucose production are mainly regulated by opposing effects of insulin and glucagon. Insulin suppresses gluconeogenic gene expression while glucagon induces them (5). Insulin controls gluconeogenic gene expressions via the transcription factor forkhead box O1 (FoxO1) and its co-activator peroxisome proliferator activated receptor γ co-activator 1α (PGC1α), whereas, glucagon

regulates the gluconeogenic gene expressions via c-AMP response element binding protein (CREB) and its co-activator CREB regulated transcription co-activator 2 (CRTC2) (61). FoxO1 controls hepatic gluconeogenesis via insulin signaling pathway (62). Thus, focus of my dissertation is FoxO1 control of gluconeogenesis and hepatic glucose production via insulin signaling pathway.

1.5.2. FoxO1

FoxO1 is a key transcription factor controlling GNG genes expression via insulin signaling pathway (62-65). Akt mediated phosphorylation of FoxO1 through the insulin signaling pathway excludes FoxO1 from nuclei, decreases its nuclear abundance and decreases GNG gene expression. Thus, increased phosphorylation of FoxO1 is associated with the suppression of hepatic GNG (54, 60, 66). During fasting, the active dephosphorylated form of FoxO1 is translocated from the cytoplasm to nucleus; where it binds promoters of its target genes and increases the transcription of genes such as Pck1 and G6Pase (54, 60, 66). Increased expression of these genes, coupled with increased substrate availability, i.e., gluconeogenic precursors, increases glucose production by the liver (5, 54, 55, 60, 66-68). In addition, many other covalent modifications of FoxO1 such as acetylation (69), O-linked-β-N-acetyl glucosamine (70) and ubiqutination (63) also play major roles in the control of gluconeogenesis. My focus here will be FoxO1 phosphorylation control of GNG and hepatic glucose production.

1.5.3. Role of protein kinases in regulation of FoxO1 phosphorylation

Akt is the protein kinase that directly phosphorylates FoxO1 (25). Akt is a serine/threonine protein kinase and has two phosphorylation sites; S^{473} and T^{308} (71, 72). Phosphorylation of Akt at S^{473} precedes T^{308} phosphorylation and is required for full activation of Akt (71, 72). Several kinases such as mTOR, mammalian target of rapamycin; ILK, integrin-linked kinase; MK-2, MAP kinase-activated protein kinase-2; p38MAP kinase; NEK6, the NIMA-related kinase-6 and DNK-PK, double stranded DNA-dependent protein kinase, are reported to phosphorylate Akt at the S^{473} site. The T^{308} site gets phosphorylated by phosphoinositide dependent kinase-1 (PDK1), which is a component in PI3 kinase pathway, dependent on insulin receptor for its regulation (73).

1.5.4 mTOR

Among the kinases phosphorylating the S^{473} site of Akt, mTOR has been reported as the only kinase that phosphorylates the S^{473} site in both *in vitro* and *in vivo* models (73-75). mTOR is a highly conserved serine/threonine protein kinase that integrates nutrient availability with hormonal/growth factor signaling to regulate cell growth, proliferation, viability and function (76, 77). Thus, it is a central controller of growth and energy homeostasis and acts as a switch between anabolic and catabolic pathways. mTOR plays a major role in cancer, diabetes and aging (76, 77). Hyper-stimulated mTOR signaling fuels cancer growth, whereas, the physiological activation of mTOR can be

beneficial for diabetes (76). mTOR is a catalytic subunit of two multi-component complexes: mammalian target of rapamycin complex 1 (mTORC1) and mammalian target of rapamycin complex 2 (mTORC2). mTORC1 is composed of mTOR, regulatory protein raptor and GβL (G-protein β-subunit-like), whereas, mTORC2 is composed of mTOR, rictor, mSIN1 (mammalian stress-activated protein kinase-interacting protein 1) and GβL (6, 56, 76, 78). Both complexes participate in different signaling pathways and recognize distinct substrates depending on the interaction of mTOR with its regulatory components, raptor or rictor (**Fig. 1.5**) (6, 76). Interaction of mTOR with rictor or raptor determines mTOR dominance in a particular pathway (6, 76). Raptor is the rapamycin sensitive component and rictor is the rapamycin insensitive component (6, 76). Both complexes have multiple downstream targets and thereby, they interact with many signaling pathways (**Fig. 1.5**) (6, 76). Insulin signaling (**Fig. 1.6**) is one of the pathways mTOR interacts and controls protein synthesis via mTORC1 and carbohydrate metabolism including both glucose and glycogen metabolism via mTORC2 (6, 76). mTOR as a catalytic subunit of mTORC2 phosphorylates Akt at S^{473} site and facilitates insulin signaling (6, 76).

1.5.5. Role of phosphatases in the regulation of Akt and FoxO1 phosphorylation

In addition to kinases, phosphatases also regulate Akt and FoxO1 phosphorylation. It has been reported that protein phosphatase 2A (PP2A), a serine/threonine phosphatase consisting of a catalytic subunit C, controls Akt

and FoxO1 phosphorylation status by mediating their dephosphorylation (25, 57, 79). A second protein phosphatase, MAP kinase phosphatase-3 (MKP-3), has been found to regulate FoxO1 phosphorylation (58). MKP-3 belongs to the family of dual specificity phosphatases, which dephosphorylates both serine/threonine and tyrosine residues in target proteins (80). PP2A and MKP-3 remove phosphate from FoxO1 and induce the accumulation of FoxO1 in the nucleus, leading to increased GNG. Phosphorylation and dephosphorylation of Akt and FoxO1 mediated by various kinases and phosphatases are important in controlling their physiological functions (5).

Overall, my dissertation will address the Elovl5 mediated suppression of GNG and fasting blood glucose via induction of FoxO1 phosphorylation and will examine the molecular mechanisms through which Elovl5 increases FoxO1 phosphorylation and suppresses GNG in diet induced obese-diabetic C57BL/6J mouse model and HepG2 cells.

1.6. Models for T2DM

1.6.1. C57BL/6J mice

Human T2DM is characterized by hyperglycemia and increased secretion of insulin, and closely associated with obesity and fatty liver (81). Multiple factors such as genetic, environmental and dietary factors in particular dietary fat play role in onset and progression of human T2DM (81-84). Thus, appropriate animal models are needed to resemble these phenotypes and pathogenesis of human T2DM. In this regard, male C57BL/6J mice are the

best choices to study the human T2DM compared to *db/db* mice or pharmaceutical compounds induced diabetic rodents (81-84). Feeding high fat diets for 10 weeks (45-60% calories derived from fat as lard) induces obesity, hyperglycemia and fatty liver in C57BL/6J mice, and these phenotypes resemble human T2DM phenotypes (21, 84). Therefore, I used C57BL/6J mice to examine the effects of Elovl5 on blood glucose control in high fat induced obesity, T2DM and fatty liver condition.

1.6.2 Human hepatoma cell lines (HepG2 cells)

Regulation of gluconeogenesis is important to control blood glucose (5, 85). Thus, it is required to examine the molecular basis of Elovl5 control of gluconeogenesis. Primary hepatocytes are an excellent choice to study hepatic gluconeogenesis and glucose production because those cells resemble best the *in vivo* conditions (85, 86). But using hepatocytes on the scale required for these studies was too expensive. Thus, HepG2 cells were selected to perform our mechanism studies of Elovl5 regulation of hepatic gluconeogenesis.

HepG2 cells are adherent epithelial-like cells growing as monolayer and in small aggregates (source: www.hepg2.com). HepG2 cell line was derived from the liver tissue of fifteen-year-old male with differentiated hepatocellular carcinoma. These cells are mortalized and not tumorigenic (source: www.hepg2.com). Also they respond well to stimulation with insulin and other growth hormones (source: www.hepg2.com). Moreover, treatment with

palmitate makes HepG2 cells insulin resistant and thereby increases expression of GNG genes Pck1 and G6Pase expression (85). More importantly, HepG2 cells have the differentiated properties like primary hepatocytes and thereby, these cells are often used as an alternative to primary hepatocytes in many *in vitro* studies (85, 86). HepG2 cells, however, express very low levels of G6Pase at basal state, and therefore, these cells are not appropriate for the study of glucose production (86).

1.7. Significance

Persistent high blood glucose or hyperglycemia is a classic metabolic feature in diabetes posing a tremendous health and economic burden (1, 5). Despite vast amounts of effort, maintaining a blood sugar level close to normal remains a major challenge for diabetics. My preliminary study established that elevated hepatic Elovl5 activity increased PUFA synthesis and decreased blood glucose in chow-fed mice (22). The outcome of my dissertation is that it has provided strong evidence that Elovl5 corrects hyperglycemia in high fat diet induced obese-diabetic rodent models and provided novel insight into the molecular and metabolic basis of Elovl5 and PUFA synthesis regulation of the carbohydrate metabolism. It also established a connection between PUFA synthesis and carbohydrate metabolism in T2DM. This information may be helpful in developing new therapeutic strategies to combat hyperglycemia in diet induced obesity and T2DM.

1.8. Summary

T2DM is a major metabolic disease affecting more than 200 million people worldwide (1). It is closely linked to obesity epidemic, fatty liver disease, and cardiovascular diseases (5). Hyperglycemia and insulin resistance are the classic hallmarks of diabetes (87). In T2DM, impairment of insulin signaling leads to gradual and persistent increase in glucose production and output from the liver and decrease in glucose uptake by muscle and adipose tissue, which are the major contributing factors for hyperglycemia (55). Uncontrolled hyperglycemia further leads to deadly micro-vascular complications and thereby blood glucose control remains a major goal for every diabetic (7-9). Liver is the central organ in control of the whole body metabolism, which tightly maintains blood glucose homeostasis (55). Previous studies from our lab have shown that dietary n-3 PUFA regulates many factors involved in hepatic carbohydrate metabolism, lipid metabolism, and insulin signaling (22, 26, 27). Regulation of these physiological processes by PUFA depends on the length of their chain and the degree of unsaturation, which are mediated by metabolic pathways such as *de novo* lipogenesis, elongation, desaturation, mono oxidation and β-peroxidation (22). Although the role of dietary fatty acids in onset and progression of insulin resistance and type 2 diabetes has been widely investigated, the role played by endogenous fatty acid synthesis has not been clearly elucidated. In one of our previous studies we have observed that endogenous PUFA synthesis was negatively

associated with hyperglycemia (21). C57BL/6J mice fed on a high fat diet become obese, hyperglycemic, glucose intolerant and develop fatty liver. This change is associated with a suppression of endogenous PUFA synthesis as reflected by a decline in the expression of enzyme involved in PUFA elongation (Elovl5) but not desaturation (21). Moreover, we observed a decline in the abundance of end products of PUFA synthesis (arachidonic acid [20:4,n-6] and docosahexaenoic acid [22:6,n-3]) in the liver (21). In another study, over-expression of hepatic Elovl5 affected both hepatic & plasma PUFA composition, decreased blood glucose level, and regulated phosphorylation status of downstream targets of insulin signaling, suggesting a possible link between PUFA synthesis, fatty acid elongation and carbohydrate metabolism (22).

The overall goal of my dissertation is to establish the mechanisms by which hepatic PUFA synthesis controls carbohydrate metabolism and blood glucose levels. The central hypothesis for my dissertation is that fatty acid elongation by Elovl5 regulates hepatic and systemic carbohydrate metabolism by controlling hepatic insulin action. The focus on Elovl5 is based on preliminary studies indicating that elevation of this enzyme in the liver lowers blood glucose levels (22). The following aims will test this hypothesis.

Aim1**:** To determine the impact of elevated hepatic Elovl5 activity on glucose metabolism in a mouse model of obesity and diabetes.

Aim2**:** To determine how increased fatty acid elongation alters hepatic & hepatocyte gluconeogenesis (focus on mechanism using HepG2, human hepatoma cells).

The outcome of these studies will provide novel information on links between PUFA synthesis, fatty acid elongation and carbohydrate metabolism. This information may be helpful in developing new strategies to combat dysregulation of carbohydrate metabolism in diabetes and obesity.

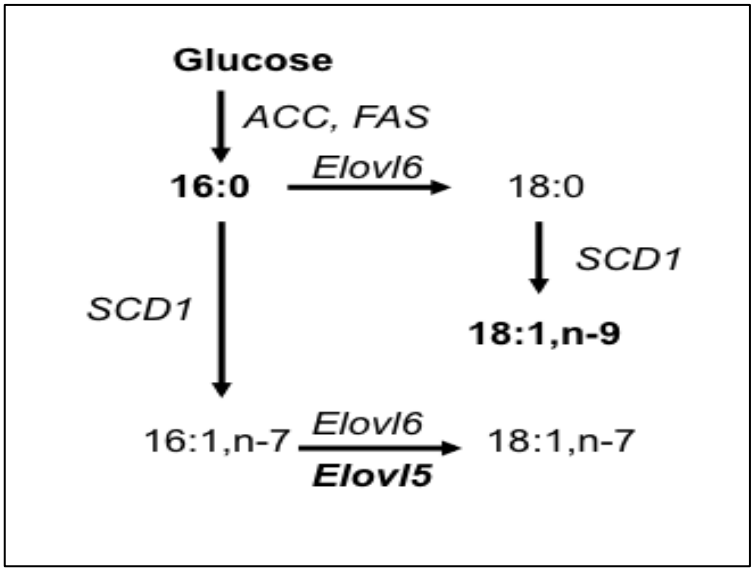

Fig.1.1. Scheme for DNL and MUFA synthesis. Glucose is converted to palmitate via DNL. Palmitate generated via DNL or obtained from dietary sources elongated (Elovl5 & Elovl6) and desaturated (stearoyl CoA desaturase) to form mono-unsaturated fatty acids. Palmitate (16:0), stearate (18;0), palmitoleate (16:1,n-7) and oleate (18:1,n-9). Enzymes involved in DNL and MUFA synthesis are acetyl CoA carboxylase (ACC); fatty acid synthase (FAS), elongases (Elovl5 & Elovl6), stearoyl CoA desaturase (SCD-1).

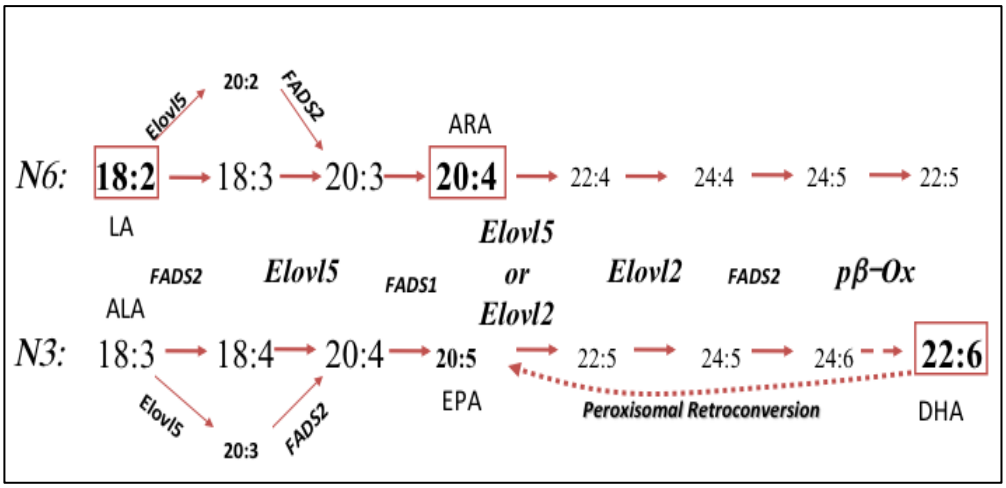

Fig. 1.2. Scheme for the synthesis of long chain PUFA from dietary essential fatty acids. Essential dietary fatty acids (18:2,n-6 and 18:3,n-3) are converted to arachidonic acid (20:4,n-6) and docosahexaenoic acid (22:6,n-3) by a series of desaturation (Δ^5D[FADS1] & Δ^6D[FADS2]), elongation (Elovl2 & Elovl5) and peroxisomal β-oxidation (pβ-Ox) steps. The boxed fatty acids, 18:2,n-6, 20:4,n-6 and 22:6,n-3, are the predominant PUFA appearing in hepatic membrane lipids. The elongation product of 18:2,n-6, i.e., 20:2,n-6, is an alternative route for generating 20:3,n-6 and 20:4,n-6. The elongation product of 18:3,n-3, i.e., 20:3,n-3, is an alternative route for generating 20:4,n-3 and 20:5,n-3. The enzymes involved in PUFA synthesis pathway are FADS1, FADS2, Elovl5, Elovl2.

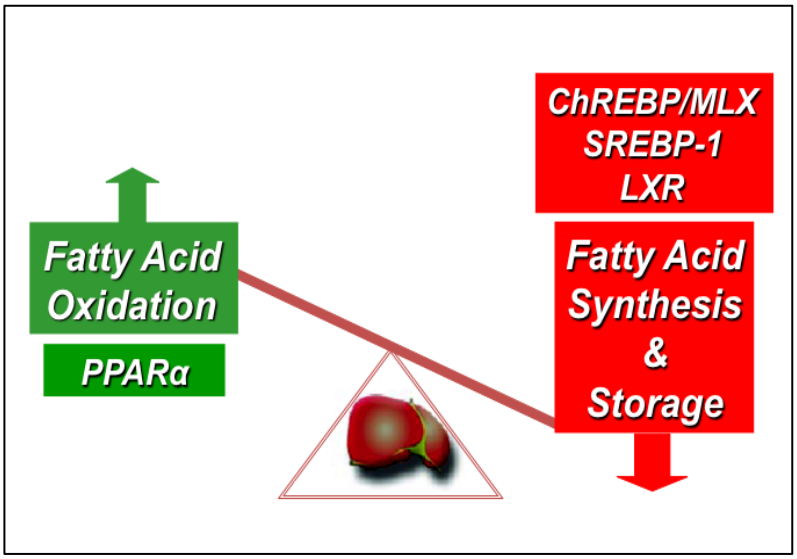

Fig. 1.3. Transcription factors regulation of hepatic fatty acid metabolism. Liver is the central organ regulating fatty acid metabolism both fatty acid oxidation and synthesis. SREBP-1, ChREBP/MLX heterodimer and LXR are the key transcription factors regulate fatty acid synthesis, whereas PPARα induces fatty acid oxidation genes.

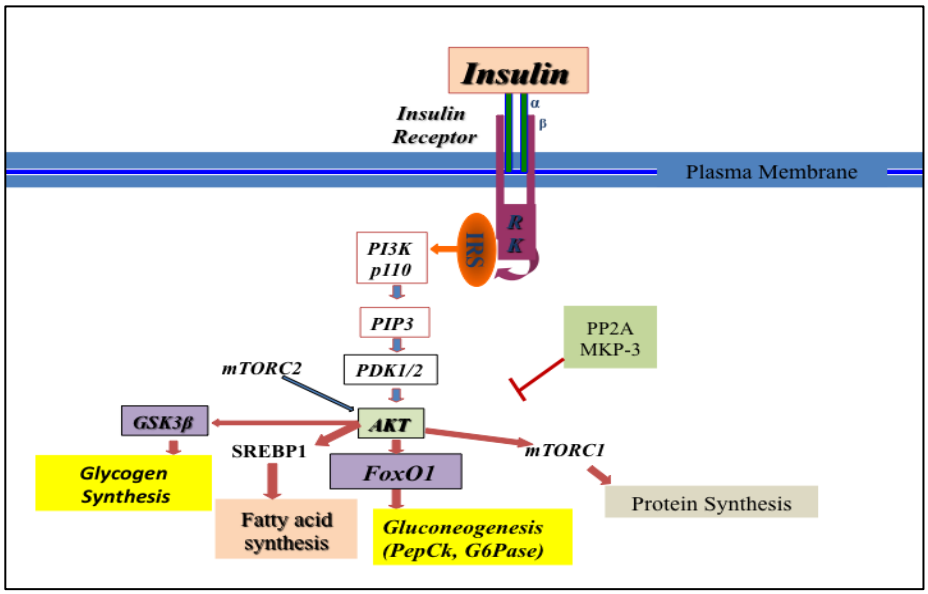

Fig. 1.4. Hepatic insulin signaling pathway. Insulin through PI3 kinase-Akt pathway controls the carbohydrate, lipid and protein metabolism. Insulin signaling leading to the control of carbohydrate metabolism is regulated by many kinases and phosphatases. Phosphatases such as PP2A and MKP-3 decrease Akt and FoxO1 activity by dephosphorylation. In the presence of insulin, gluconeogenesis is inhibited and glycogen synthesis is activated in liver. FoxO1 controls hepatic gluconeogenesis by regulating the expression of PepCk and G6Pase. GSK-3β controls glycogen synthesis. (PI3-kinase, phosphoinositidyl 3-kinase; GSK-3β, glycogen synthase kinase-3β; FoxO1, forkhead box O family transcription factor 1; PepCk, phosphoenolpyruvate carboxykinase; G6Pase, glucose-6-phosphatase, PP2A, protein phosphate 2A; MKP-3, MAP kinase phosphatase-3).

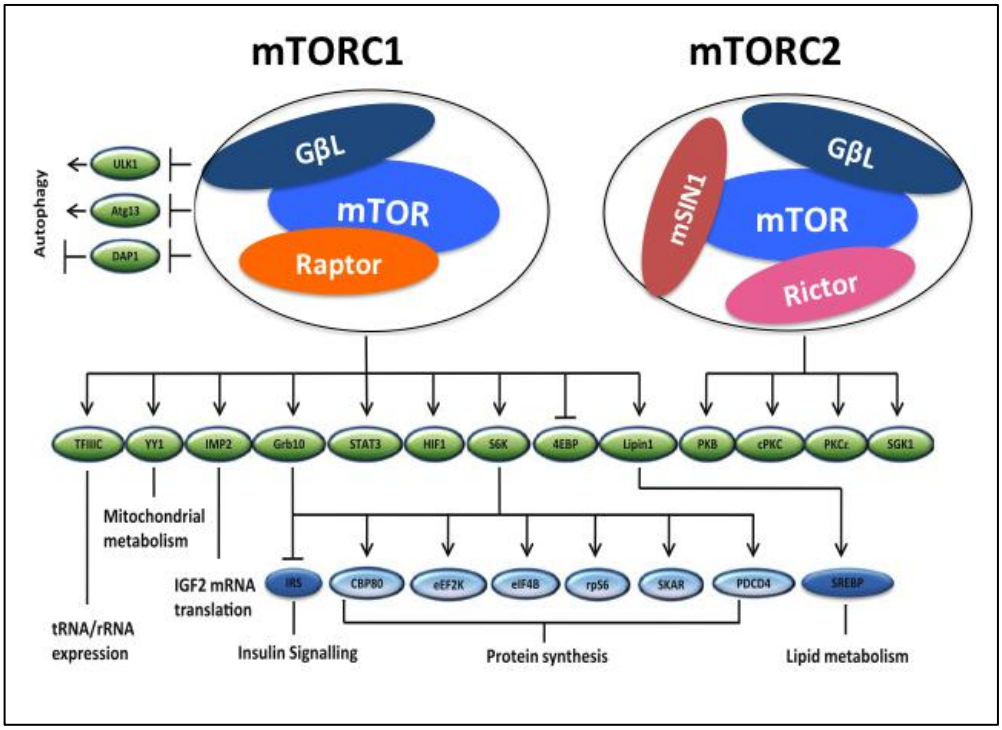

Fig. 1.5. mTOR signaling. mTOR is a conserved serine/threonine kinase. It is a catalytic subunit of two complexes: mTORC1 (consists of mTOR, regulatory protein raptor and GβL) and mTORC2 (consists of mTOR, regulatory protein rictor, GβL and mSIN1). Both complexes have their distinctive substrates. As such mTOR is a central controller of many pathways and regulates many biological functions such as insulin signaling, mitochondrial metabolism, protein, carbohydrate and lipid metabolism, cell growth, autophagy etc. in our body. Association of mTOR with rictor or raptor determines mTOR kinase dominance in a particular pathway. This figure is adapted from Xie & Herbert, 2012 (6).

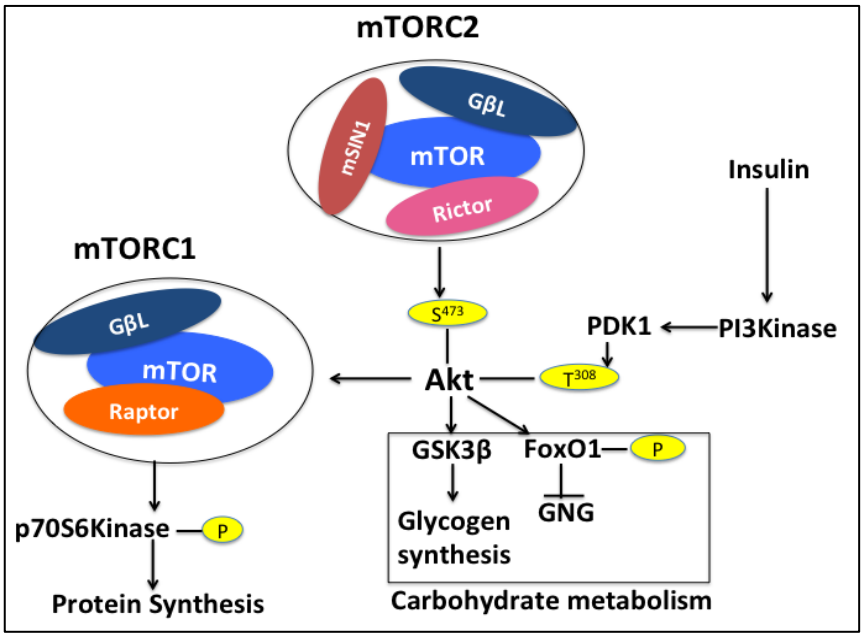

Fig. 1.6. mTOR signaling interaction with hepatic insulin signaling pathway. Insulin through PI3 kinase pathway phosphorylates Akt at T^{308} site and mTORC2 phosphorylates Akt-S^{473} site. Phosphorylation of Akt leads to increase phosphorylation of FoxO1 and glycogen synthase kinase 3β (GSK3β). Akt mediated FoxO1 and GSK3β phosphorylation leads to inhibition of GNG and augmentation of glycogen synthesis, respectively. Akt phosphorylates mTORC1 and regulates protein metabolism.

Chapter 2

Elevated hepatic fatty acid elongase-5 (Elovl5) activity corrects dietary fat induced hyperglycemia in obese C57BL/6J mice

Sasmita Tripathy, Moises Torres-Gonzalez and Donald B. Jump

Journal of Lipid Research
Publishers: American Society of Biochemistry and Molecular Biology.
September 2010, 51:2642-2654.

2.1. Abstract

Elevated hepatic fatty acid elongase-5 (Elovl5) activity lowers blood glucose in fasted chow fed C57BL/6J mice. Since high fat diets induce hyperglycemia and suppress hepatic Elovl5 activity, we tested the hypothesis that elevated hepatic Elovl5 expression attenuates hyperglycemia in high fat diet-induced obese mice. Increasing hepatic Elovl5 activity, by a recombinant adenoviral approach, restored blood glucose & insulin, HOMA-IR and glucose tolerance to normal values in obese mice. Elevated Elovl5 activity increased hepatic content of Elovl5 products (20:3,n-6, 22:4,n-6) and suppressed levels of enzymes (Pck1, G6Pc) and transcription factor FoxO1 & its co-activator PGC1α, but not transcription factor CREB and its co-activator CRTC2, involved in gluconeogenesis. Effects of Elovl5 on FoxO1 nuclear abundance correlated with increased phosphorylation of FoxO1, Akt & the catalytic unit of PP2A as well as a decline in cellular abundance of TRB3. Such changes are mechanistically linked to the regulation of FoxO1 nuclear abundance and gluconeogenesis. These results show that Elovl5 activity impacts the hepatic abundance and phosphorylation status of multiple proteins involved in gluconeogenesis. Our findings establish a link between fatty acid elongation and hepatic glucose metabolism, and suggest a role for regulators of Elovl5 activity in the treatment of diet-induced hyperglycemia.

Keywords: Elovl5, FoxO1, PGC1α, gluconeogenesis, fatty liver, diabetes

2.2. Introduction

Microsomal fatty acid elongation plays an important role in SFA, MUFA and PUFA synthesis. Microsomal fatty acid elongation utilizes specific substrates (malonyl CoA, NADPH and fatty acyl CoAs) and enzymes (3-keto acyl CoA synthase, 3-keto acyl CoA reductase, 3-hydroxy acyl CoA dehydratase and trans 2,3-enoyl CoA reductase) to catalyze the 2-carbon elongation of fatty acids (88-91). Specificity for fatty acyl CoA substrates and the rate of fatty acid elongation is determined by the first step in the pathway, i.e., the activity of the condensing enzyme, 3-keto acyl CoA synthase, and not the reductases or dehydratase (88, 92). As such, 3-keto acyl CoA synthase (also known as Elovl, elongation of long chain fatty acids) plays the key regulatory role in determining type and amount of elongated fatty acids found in cells.

Seven Elovl subtypes (Elovl 1-7) have been identified in the human, mouse and rat genomes. While Elovl1, Elovl3 & Elovl6 elongate SFA and MUFA, Elovl2, Elovl4 and Elovl5 elongate PUFA (20, 21, 89, 90, 93). Elovl5 also elongates some MUFA, like palmitoleic acid [16:1,n-7] (94) as well as PUFA e.g., linoleic acid (18:2,n-6), γ-linolenoyl-CoA (18:3,n-6) and 20:4,n-6 (20-22). Elovl2 and Elovl5 elongate 20-carbon PUFA to form 22 carbon PUFA, while Elovl2 exclusively elongates 22-carbon PUFA to form 24-carbon fatty acids (21). The formation of 24-carbon PUFA is required for docosahexaenoic acid (22:6,n-3) synthesis (95). Thus, Elovl2 and Elovl5 play an important role

in n-3 and n-6 PUFA synthesis. Human and rodent liver express five Elovl subtypes, Elovl5>Elovl1= Elovl2= Elovl6>Elovl3 (20, 21). Several of these elongases are regulated by stage of development, tissue-specific factors, hormones, dietary factors, pharmacologic compounds (20, 21, 89, 90, 93, 96). Consequently, changes in the activity of fatty acid elongases (Elovl) affects cellular fatty acid composition (89, 90). Changes in cellular fatty acid content impacts cell function through transcriptional and post-transcriptional regulatory mechanisms (12, 97, 98).

Recent studies suggest fatty acid elongases play a role in chronic metabolic diseases. Global ablation of fatty acid elongase-6 (Elovl6) protects mice from diet induced diabetes (39). Ablation of Elovl5 increases hepatic lipid content, at least in part, by inducing SREBP-1, a key transcription factor controlling *de novo* lipogenesis (44). Our studies established that induction of hepatic Elovl5 activity altered both plasma and blood lipid composition, but also affected glucose metabolism (22). Elevated hepatic Elovl5 activity induced a modest, but significant decline in blood glucose levels and significantly suppressed cytosolic phosphoenolpyruvate carboxykinase (Pck1) mRNA; Pck1 is a key enzyme involved in gluconeogenesis (22). While effects of fatty acid elongases on lipid metabolism can be predicted by the known action of these enzymes on cellular fatty acid composition (12), elongase effects on carbohydrate metabolism were not expected.

High fat diets induce obesity, hyperglycemia, insulin resistance and fatty liver in C57BL/6J mice. High fat diets also suppress hepatic Elovl5 activity (21). This report test the hypothesis that restoration of Elovl5 activity in livers of obese mice is sufficient to correct high fat diet-induced hyperglycemia. Our second goal was to determine how elevated Elovl5 activity controls the expression of Pck1 and other proteins involved in gluconeogenesis. Transcriptional control of Pck1 is very complex and involves multiple transcription factors [FoxO1, hepatic nuclear protein-4α (HNF4α), CREB, PPARα and other regulatory proteins [PGC1α, CRTC2, *tribbles*-related protein B3 (TRB3), sirtuin 1 (SIRT1)] (61, 99-101). PPARα controls the expression of multiple proteins involved in gluconeogenesis including, Pck1 (102), TRB3 (59) and fibroblast growth factor 21 (FGF21) (103). TRB3 inhibits Akt activity, while FGF21 regulates PGC1α (103). PGC1α interacts with FoxO1 and both factors bind to promoters of target genes, like Pck1 (64, 65). Phosphorylation of FoxO1 by Akt prevents phospho-FoxO1 (pFoxO1) from entering nuclei (62, 63). These mechanisms account for much of the insulin-mediated suppression of gluconeogenesis. The outcome of my studies will establish that hepatic Elovl5 activity regulates the expression of multiple enzymes and transcription factors involved in gluconeogenesis. This regulation is achieved by effects on PPARα-regulated gene expression and control of the phosphorylation status of key proteins controlling gluconeogenesis.

2.3. Materials and methods

2.3.1. Animals

All procedures for the use and care of animals for laboratory research were approved by the institution animal care and use committee (IACUC) at Oregon State University. Male C57BL/6J mice (stock# 000664, Jackson Laboratories, Bar Harbor, Maine), 2 months of age, were fed either a chow maintenance diet (Purina 5001), a low fat diet [10% calories as fat, D12450B] or high fat diet [60% calories as fat, D12492, Research Diets, Inc.] *ad lib.* Mice were fed the low & high fat diets for 12 weeks. The fatty acid composition of the Research Diets low and high fat diets is shown in **Fig. 2.1**.

2.3.2. Fasting and refeeding

Mice were fasted overnight (beginning 6 PM). The next morning (8 AM), food was returned to ½ of the mice. Fasted and refed animals were euthanized (isoflurane and exsanguination) at 8 AM (fasted) and noon (refed) for blood and tissue collection.

2.3.3. Glucose tolerance test

Mice maintained on a low or high fat diet were used for a glucose tolerance test. Five days prior to end of the study, mice were injected with recombinant adenovirus (see below). Three days later, mice were subjected to a glucose tolerance test. Mice were fasted overnight (beginning 6 PM). The next morning (~10 AM) mice were injected with glucose (2 g/kg, IP). Blood

was withdrawn from the tail vein prior to and after glucose treatment. Blood glucose was measured using a hand-held glucose meter (Contour, Bayer).

2.3.4. Recombinant adenovirus

The construction, purification and titering of the recombinant adenoviruses (Ad-Luc, luciferase and Ad-Elovl5, Elovl5) was described previously (21, 22). Mice were injected with adenovirus (2 x 10^{10} viral particles/mouse in PBS) by a retro-orbital route while under mild isoflurane anesthesia. Mice were maintained on food and water, *ad lib,* for the duration of the study. Body weight, food and water intake was monitored daily. All animals displayed no adverse effects from the adenovirus injection and gained weight equally for the 5 days period after injection.

2.3.5. RNA extraction and quantitative real time-polymerase chain reaction (qRT-PCR)

Total RNA was extracted from mouse liver and transcript levels were measured by qRT-PCR (22). Gene specific primers are listed in **Table 2.1**. Primers were designed using Primer Express software (Applied Biosystems, Foster City, CA). First strand cDNA was synthesized using the SuperScript III kit (Invitrogen Carlsbad, CA). Synthesized cDNA was mixed with SYBR green/ DyANmo (FL400), New England Biolabs. PCR quantification used a MJ Research Peltier ThermoCycler-200 (DNA Engine). All reactions were performed in triplicate. The relative amounts of mRNAs were calculated by using the comparative C_T method (User Bulletin #2, Applied Biosystems).

Cyclophilin was used as a control and all results were normalized to the abundance of cyclophilin mRNA.

2.3.6. Fatty acid elongation assay

Mouse liver microsomes were prepared and used for a fatty acid elongation assay (20, 21). The fatty acyl-CoA substrate used for this assay was 18:3,n-6-CoA, an Elovl5-specific substrate (Elovl5) (22).

2.3.7. Lipid extraction and fatty acid analysis

Total lipids were extracted from liver in chloroform:methanol (2:1) plus 1 mM butylated hydroxytoluene (22). 7-nonadecenoic acid (19:1) was added as a recovery standard at the time of extraction. Protein (Bio-Rad, Hercules, CA) was measured in extracts after the initial homogenization step in 40% methanol. Total lipids were saponified, converted to fatty acid methyl esters (FAME) in 1% H_2SO_4 in methanol and heating to 90^{o}C for 1 hr. FAME were extracted in hexane, dried and resuspended in hexane + 0.05% butylated hydroxytoluene and quantified using an Aligent 7890 GC gas chromatograph equipped with a flame ionization detector (FID) [conditions: column, 100 x 0.25 mm ID, 0.2 mm HP-88; inlet temperature = 250^{o}C; vol. injected 1 ml; split ratio varies from 1:5 to 1:50 depending on the concentration of FAME; carrier gas A = hydrogen; B = helium; head pressure 2 ml/min constant flow; oven To: 120^{o}C 1 min. 10^{o}C/min to 175^{o}C, 10 min 5^{o}C/min to 210^{o}C, 5 min 5^{o}C/min to 230^{o}C, 5 min; detector temperature, 280^{o}C; detector gases: 40 ml/min hydrogen; 450 ml/min air, Helium to make up gas 30 ml/min]. Fatty acid methyl

ester standards (GLC-642, GLC-643 & GLC-682) were obtained from Nu-Chek Prep.

2.3.8. Immunoblotting

Proteins were extracted from mouse liver as described previously (22) in the presence of protease (Roche Diagnostics, Indianapolis, IN) and phosphatase inhibitors (1mM β-glycerolphosphate, 2.5 mM Na-pyrophosphate, 1 mM Na_3VO_4). Cytosolic (post-nuclear) & nuclear protein fractions were separated electrophoretically by SDS-polyacrylamide gel electrophoresis (NuPAGE 4-12% polyacrylamide Bis-Tris, Invitrogen) and transferred to nitrocellulose (BA83) membranes.

Antibodies used for immunoblotting included: total FoxO1 & phospho-FoxO1, total PDK1 & phospho-PDK1, total PP2A catalytic unit & total CTMP (Cell Signaling, (Danvers, MA). HNF-4α (H-171); Na,K-ATPase; total Akt1 (C20); phospho-AKT1/2/3 (Ser 473)-R, PPARα (H98), MLX (N-17) PGC1, TRB3 and Pck1 (P14, Sc74825) were obtained from Santa Cruz Biotechnology (Santa Cruz, CA). SREBP1 (2A4), TATA-binding protein (TBP) were obtained from Abcam, Inc. (Cambridge, MA). Phospho-PP2A catalytic unit (Tyr-307) was obtained from Epitomics (Burlingame, CA). ChREBP (NB400135) was obtained from Novus Biologicals (Littleton, CO). The Elovl5 antibody was described previously (22). The IRDye 680 and IRDye 800 secondary antibodies (anti-mouse, anti-rabbit and anti-goat) were obtained from LiCor, Inc. (Lincoln, NB) or Rockland Immunologicals (Gilbertsville, PA).

Antigen-antibody reactions were detected and quantified using LiCor Odyssey scanner and software. Phospho-IRS2 was measured in liver extracts using an ELISA kit (Cell Signaling, Danvers, MA).

2.3.9. Measurement of plasma parameters

Plasma glucose, triglyceride, non-esterified fatty acids and cholesterol were measured using kits from Wako (Richmond, VA). Plasma β-hydroxybutyrate was measured using a kit from Stanbio (Boerne, TX). Plasma insulin and adiponectin were assayed by ELISA (Millipore, Watham, MA).

2.3.10. Measurement of hepatic protein, DNA, triglyceride, cholesterol & glycogen content

Liver (25-50 mg) was homogenized in 40% methanol + 0.1 mM HCl; a sample was collected for protein (Quick Start Bradford Assay, Bio-Rad, Hercules, CA) and DNA analysis (FluoReporter blue fluorometric dsDNA, Invitrogen, Carlsbad, CA). Total hepatic lipids were extracted with chloroform:methanol as described above. After centrifugation of the extract, the aqueous phase was used to measure glycogen. The aqueous phase was adjusted to 0.2 N NaOH, heated to 65^{o}C for an hour, cooled and neutralized with 5 N HCl. Glycogen was precipitated with ethanol, resuspended in water and hydrolyzed with amyloglucosidase (Sigma-Aldrich). Glucose released by amyloglucosidase was measured using the glucose assay kit (Wako, Richmond) (22). The organic phase was dried under nitrogen and *in vacuo*

and assayed for cholesterol and triglyceride using the total cholesterol and L-type TG H triglyceride assay kits from Wako (Richmond, VA) (22).

2.3.11. Statistical analysis

The statistical analysis performed in this work included Students t-test and ANOVA (two-way) plus post hoc Tukey honestly significant difference test (http://faculty.vassar.edu/lowry/VassarStats.html). A $p\text{-value} \leq 0.05$ was considered statistically different.

2.4. Results

2.4.1. Elevated hepatic Elovl5 activity induces FoxO1 phosphorylation in chow-fed mice

Previous studies with chow-fed C57BL/6J mice established that a 6-fold elevation in hepatic Elovl5 activity increased fasting levels of glycogen and suppressed hepatic Pck1 mRNA and plasma glucose (22). The effect on hepatic glycogen was attributed to the increased phosphorylation of Akt and GSK3β. The mechanism for Elovl5 control of Pck1and blood glucose was less clear. In this study, we determined whether Elovl5 controls FoxO1 nuclear abundance, a well established regulator of hepatic Pck1 expression and gluconeogenesis (64).

Using liver extracts from the previous study (22), the nuclear and cytoplasmic abundance of FoxO1, as well as phosphorylated FoxO1 (pFoxO1) was measured **(Fig. 2.2)**. Refeeding fasted mice suppressed hepatic nuclear FoxO1 by 60% **(Fig. 2.2, Panel A and B)**. A separate group of mice receiving

a saline injection gave similar results for FoxO1 following the fasting and refeeding study (not shown). Ad-Luc infection, alone, does not impact the fasting-refeeding effect on FoxO1 nuclear abundance.

Fasted mice infected with Ad-Elovl5 have a level of nuclear FoxO1 comparable to that seen in refed mice (**Fig. 2.2, Panel, A & B**). Refeeding Ad-Elovl5 infected mice had no additional effect on FoxO1 nuclear abundance. The Elovl5-mediated decline in nuclear FoxO1 correlated with a 4-fold increase in the phosphorylation status of cytoplasmic FoxO1, i.e., pFoxO1/cFoxO1 (**Fig. 2.2, Panel A & C**). FoxO1 is phosphorylated by Akt; elevated hepatic Elovl5 increases hepatic Akt phosphorylation 3-fold in fasted mice (22). By stimulating FoxO1 phosphorylation, increased hepatic Elovl5 suppresses FoxO1 nuclear abundance, presumably by inhibiting FoxO1 from entering nuclei (62, 63).

2.4.2. Effect of diet and adenovirus infection on hepatic Elovl5 activity

To gain further support for the notion that changes in hepatic Elovl5 activity impact glucose metabolism we used a mouse model of high fat diet induced obesity, hyperglycemia and insulin resistance. Previous studies established that feeding mice a high fat (lard) diet suppressed hepatic Elovl5 activity (21). Herein, male C57BL/6J mice were fed a low fat (10% calories as fat) or high fat (60% calories as fat) diet for 12 weeks as described (21). Five days before the end of the feeding trial, mice were infected with Ad-Luc or Ad-

Elovl5. High fat diets significantly increased body weight by 33-37% **(Table 2.2)**. Infection of mice with Ad-Elovl5 did not significantly affect body weight.

The high fat diet suppressed hepatic Elovl5 mRNA, protein and enzyme activity in Ad-Luc infected mice by ~50% **(Fig. 2.3, Panel A-C)**. This effect on Elovl5 is consistent with our previous study (21). Infection of high fat-fed mice with Ad-Elovl5 increased Elovl5 mRNA, Elovl5 protein and enzyme activity **(Fig. 2.3, Panel A-C)**. The level of Elovl5 enzyme activity in Ad-Elovl5 infected mice is ~40% above the level of Elovl5 activity in livers of low fat fed mice **(Fig. 2.3, Panel C)** (21, 22).

2.4.3. Elevated hepatic Elovl5 activity corrects hyperglycemia in obese mice

The effect of high fat diets and elevated Elovl5 activity on blood glucose and insulin levels in fasted mice was examined **(Fig. 2.4)**. As expected, mice fed the high fat diet are hyperglycemic **(Fig. 2.4, Panel A)** and have elevated blood insulin levels **(Fig. 2.4, Panel B)**. While the homeostatic model assessment for insulin resistance (HOMA-IR) score of 9.4 $\pm$ 6.3 reflects insulin resistance (HOMA-IR > 3.0) **(Fig. 2.4, Panel C)**, the lack of a significant effect on fasting plasma adiponectin and NEFA suggests these mice are not severely insulin resistant **(Table 2.2)**.

Since high fat fed mice are glucose intolerant (21), we examined glucose tolerance in fasted mice maintained on a high fat diet and infected with either Ad-Luc or Ad-Elovl5 **(Fig. 2.4, Panel D)**. Mice on the low fat diet for 12 weeks and not infected with Ad-Luc or Ad-Elovl5 served as a reference for

a normal glucose tolerance test. When compared to low fat-fed mice, mice fed the high fat diet were glucose intolerant. High fat fed mice infected with Ad-Elovl5, however, displayed glucose tolerance comparable to that seen in low fat-fed mice. Thus, elevated hepatic Elovl5 activity corrects high fat diet induced hyperglycemia and glucose intolerance.

2.4.4. The effect of diet and Elovl5 activity on plasma and liver composition

Fasting plasma triglycerides, NEFA and cholesterol were not significantly affected by diet **(Table 2.2)**. Fasting β-hydroxybutyrate was significantly decreased in high fat fed Ad-Luc infected mice; an effect that may be in response to elevated fasting insulin **(Fig. 2.4, Panel B)**. Ad-Elovl5 infection suppressed fasting triglycerides in low fat-fed mice (by 54%), but not in high fat-fed mice.

While high fat diets increased liver weight, this effect was not different when expressed as a percentage of body weight or mg protein/mg DNA. Infection of mice with Ad-Elovl5, however, significantly increased the liver weight (% body weight) by 44% and 33% in low and high fat-fed mice. This effect was not due to increased protein/mg DNA, but may be due to changes in hepatic lipid and glycogen. Hepatic triglyceride, but not cholesterol, was significantly elevated in mice fed the high fat diet **(Table 2.2)**. Hepatic triglycerides in livers of obese mice with elevated Elovl5 activity were not significantly different from mice fed the low fat diet. Changes in hepatic triglyceride induced by diet or Ad-Elovl5 did not correlate with changes in the

nuclear content of transcription factors controlling *de novo* lipogenesis e.g., SREBP1, ChREBP or MLX **(Fig. 2.5)**. Thus, factors controlling hepatic triglyceride content in this model likely involve triglyceride synthesis, VLDL assembly and secretion and fatty acid oxidation.

Hepatic glycogen content in fasted mice was significantly affected by diet and virus infection. In mice maintained on chow (22) or the low fat diet **(Table 2.2)**, elevated Elovl5 activity increased hepatic glycogen content. As reported by others (104), the high fat diet significantly increased hepatic glycogen content in fasted mice. Changes in hepatic glycogen content correlated with increased phosphorylation of glycogen synthase kinase 3β (GSK3β) **(Fig. 2.6)**. These studies established that elevated Elovl5 activity lowers hepatic triglyceride and glycogen in high fat diet-induced obese mice.

2.4.5. Effect of diet and Elovl5 activity on hepatic and plasma fatty acid composition

We next examined the effect of diet and Elovl5 activity on hepatic and plasma fatty acid composition. MUFA and PUFA fatty acyl CoAs are substrates for Elovl5-mediated fatty acid elongation **(Fig. 2.7, Panel A and B)** (20, 21). The dietary fatty acid profiles of the two diets are shown in **Fig. 2.1**. When expressed as fatty acid mole%, hepatic and plasma content of 16:0, 18:0 or 18:1,n-9 was not significantly affected by diet or elevated hepatic Elovl5 activity. The high fat diet significantly lowered hepatic 16:1,n-7 and 18:1,n-7 content. Elevated Elovl5 activity significantly increased the relative

abundance of 18:1,n-7 in livers of mice fed the low diet (Ad-Luc, 3.9 $\pm$ 0.73 mole% and Ad-Elovl5, 5.5 $\pm$ 0.72 mole%, $p<0.01$, ANOVA), but not in mice fed the high fat diet. Stearoyl CoA desaturase-1 (SCD1) converts 16:0 to 16:1,n-7 **(Fig. 2.7, Panel A)**; the high fat lard diet and elevated Elovl5 activity suppress hepatic SCD1 expression. Diet and Elovl5-induced changes in SCD1 expression correlate with changes in hepatic SREBP1 & ChREBP nuclear abundance **(Fig. 2.5)**. Both SREBP1 and ChREBP control SCD1 and Elovl6 gene expression (21). Elovl5 or Elovl6 catalyze the elongation of 16:1,n-7 to vaccenic acid (18:1,n-7) (21, 93) **(refer Fig. 1.1)**. Both low and high fat diets contain 16:1,n-7 and 18:1,n-7, but at low levels (<5 mole%, Fig. 2.1). The high fat diet suppresses hepatic & plasma abundance of these MUFA.

Linoleic acid (18:2,n-6) increased in liver and plasma of mice fed high fat diets, while hepatic and plasma content of 20:4,n-6 & 22:6,n-3 was not increased. As such, high fat diets suppress the ratio of 20:4,n-6 to 18:2,n-6 [liver: low fat: 0.54 $\pm$ 0.06; high fat: 0.28 $\pm$ 0.07, $p<0.05$, ANOVA]. This ratio reflects the conversion of dietary 18:2,n-6 to the major end products of PUFA synthesis, i.e., 20:4.n-6. This outcome may be due to the high level of 18:2,n-6 in the high fat diet or changes in PUFA synthesis and degradation.

Elevated Elovl5 significantly ($p \leq 0.05$) increased hepatic content of several low abundance $C_{20\text{-}22}$ PUFAs in mice fed the low and high fat diets. Cumulatively, $C_{20\text{-}22}$ PUFA increased $\geq$2-fold in livers of mice with elevated Elovl5 activity. A major fraction of this change is due to the 2- to 4-fold

increase in dihomo-γ-linolenic (20:3,n-6) and adrenic acid (22:4,n-6), respectively. These PUFA are well established products of Elovl5 (22). Elovl5 induced changes in hepatic C_{20-22} PUFA, however, were not seen in plasma lipids. Instead, plasma 22:4,n-6 levels were lower in Ad-Elovl5 infected mice.

Since the endoplasmic reticulum (ER) is the subcellular location for fatty acid elongation, we also examined the fatty acid composition of lipids associated with the ER **(Fig. 2.8)**. The high fat diet induced a similar reduction in microsomal 16:1,n-7 and 18:1,n-7 as seen in total fatty acids. Elevated Elovl5 activity, however, did not increase C_{20-22} PUFA content in the ER. As such, Elovl5 products do not accumulate in the ER. In fact, there is very little change in PUFA composition of the ER induced by either the high fat diet or elevated Elovl5 activity.

2.4.6. Effect of elevated Elovl5 activity on PPARα target genes

Elevated hepatic Elovl5 activity attenuates expression of several PPARα-regulated genes in livers of chow-fed mice (22) and in fasted mice maintained on the high fat diet **(Fig. 2.9)**. PPARα-target genes affected by increased Elovl5 activity include cytochrome P450 A10 (CYP4A10), acyl CoA thioesterase (ACOT1), HMG CoA synthase 2 (HS2) & Elovl2. Other PPARα target genes-hydroxyl-acyl-coenzyme A dehydrogenase/3-ketoacyl-Coenzyme A thiolase/enoyl-coenzyme A hydratase (trifunctional protein), α-subunit (HADHA), FADS1 and FADS2 however, were not significantly affected. This

outcome suggests that elevated Elovl5 activity affects a subset of PPARα target genes.

2.4.7. Effect of elevated Elovl5 activity on genes involved in gluconeogenesis

We next examined the effect of elevated Elovl5 activity on the expression of several proteins involved in gluconeogenesis, including enzymes [Pck1, pyruvate carboxylase (Pcx), G6Pc], a regulator of Akt activity (TRB3), transcription factor FoxO1 and its co-activator PGC1α and a growth factor (FGF21) (64, 68, 105) in livers of fasted mice maintained on the high fat diet **(Fig. 2.10)**. Elevated Elovl5 activity significantly suppressed hepatic expression of Pck1, G6Pc, FoxO1 and PGC1α mRNA in livers of mice fed high fat diets. Transcripts encoding TRB3, FGF21, LXRα and ApoC2, however, were not affected by elevated Elovl5 activity. Similar results were seen in mice fed low fat diets (not shown).

2.4.8. Effect of elevated Elovl5 activity on the abundance of proteins involved in gluconeogenesis

To determine if changes in gene expression were linked to changes in protein, we measured the cytosolic and nuclear abundance of several proteins. Elevated Elovl5 activity attenuated Pck1 protein abundance by 60% **(Fig. 2.11)**. The decline in Pck1 protein parallels the decline in Pck1 mRNA induced by Elovl5 **(Fig. 2.10)**.

The nuclear protein abundance of key transcription factors and co-activators (FoxO1, PGC1α, CREB, CRTC2, PPARα and HNF4α) controlling

gluconeogenic gene expression (64, 68, 105, 106) was measured **(Fig. 2.12, Panel A-D)**. High fat diets induced FoxO1 & PGC1α nuclear abundance by ~2-fold **(Fig. 2.12, Panel A, B & C)**. Elevated hepatic Elovl5 activity suppressed FoxO1 **(Fig. 2.12, Panel B)** & PGC1α **(Fig. 2.12, Panel C)** nuclear abundance by >50% in livers of high fat-fed mice. The decline in nuclear FoxO1 correlated with elevated phosphorylated FoxO1 (pFoxO1) **(Fig. 2.12, Panel A & D)**. Hepatic nuclear content of CRTC2, CREB, p-CREB, PPARα and HNF4α, however, was not affected by elevated hepatic Elovl5 activity. These studies establish that Elovl5 activity regulates the nuclear abundance of a subset of transcription factor and co-activator controlling gluconeogenic gene expression.

2.4.9. Effect of diet and Elovl5 on hepatic signaling pathways

Insulin suppresses gluconeogenesis by activating the PI3 kinase-Akt pathway. The active, phosphorylated form of Akt phosphorylates FoxO1 (65, 107); pFoxO1 fails to enter the nucleus and is degraded by the 26S proteasome (108). Elevated hepatic Elovl5 activity increased Akt phosphorylation in fasted chow fed mice (22), low and high fat-fed mice **(Fig. 2.13, Panel A and B)** by ~2-fold. The Elovl5-induced changes in Akt phosphorylation in the fasted state did not correlate with changes in IRS2 or PDK1/2 phosphorylation status **(Fig. 2.6)**. This outcome suggests that Elovl5 effects on Akt phosphorylation status are not due to activation of the insulin-insulin receptor-IRS2-PDK1/2 axis.

Accordingly, we turned our attention to other mechanisms that might regulate Akt phosphorylation. TRB3 (109) and C-terminal modulator protein [CTMP] (110) bind to and inhibit Akt phosphorylation and Akt activity. Hepatic TRB3 protein content is induced by fasting and suppressed by refeeding **(Fig. 2.13, Panel A & C)**. Elevated Elovl5 activity suppressed TRB3 protein content by $\geq$ 50% in livers of fasted mice maintained on both the low and high fat diets. CTMP was induced ~2-fold by high fat diets **(Fig. 2.13, Panel A)**. Elevated Elovl5 activity significantly (40%) suppressed hepatic CTMP levels in refed, but not fasted, high fat-fed mice **(Fig. 2.13, Panel D)**.

Protein phosphatase 2A (PP2A) is a multi-subunit enzyme that dephosphorylates Akt and FoxO1 (57, 111). Phosphorylation of Y^{307} in the PP2A catalytic subunit inhibits PP2A phosphatase activity (112). The amount PP2A catalytic unit and its phosphorylation status was not affected by diet or fasting **(Fig. 2.13, Panel A & E)**. The phosphorylation status of the PP2A-catalytic unit, however, increased > 2-fold in livers with elevated Elovl5 activity. These findings suggest that increasing hepatic Elovl5 attenuates PP2A activity thereby attenuating the dephosphorylation of key proteins [Akt (111) and FoxO1 (57)] controlling Pck1 expression and gluconeogenesis.

2.5. Discussion

Fatty acid elongases play well defined roles in saturate, mono- and polyunsaturated fatty acid synthesis (88-91). The notion that changes in fatty acid elongase activity impact carbohydrate metabolism and blood glucose

levels is novel. This study establishes that changes in hepatic Elovl5 activity impact blood glucose levels in high fat diet-induced obese mice. High fat diet-induced obesity, hyperglycemia, glucose intolerance and fatty liver correlates with low hepatic Elovl5 activity (21) **(Figs. 2.3, 2.4, 2.14)**. Restoration of hepatic Elovl5 activity to levels seen in mice maintained on low fat diets corrects the hyperglycemia, glucose intolerance and fatty liver, but does not abrogate obesity **(Table 2.2)**. The correction in blood glucose was correlated with reduced hepatic content of Pck1 protein and Pck1 and G6Pase mRNA, decreased nuclear content of FoxO1 and PGC1α, decreased hepatic glycogen content and increased phosphorylation of FoxO1, Akt & GSK3β **(Figs. 2.6, 2.10, 2.11, 2.12 & 2.13 and Table 2.2)**. These studies establish a mechanistic link between Elovl5 mediated changes in hepatic fatty acid composition **(Fig. 2.7)** and the control of hepatic glucose metabolism and blood glucose levels **(Fig. 2.14)**.

Not all transcription factors controlling Pck1 expression are sensitive to changes in Elovl5 activity; Elovl5 had no significant effect on the nuclear content of CRTC2, PPARα or HNF4α **(Figs. 2.12 & 2.14)**. Elovl5 regulation of FoxO1 and PGC1α involves at least two mechanisms: a) interference with PPARα-regulated gene expression **(Figs. 2.9 & 2.10)** and b) the control of the phosphorylation status and abundance of specific proteins (FoxO1, Akt, PP2A and TRB3) **(Figs. 2.2, 2.12, 2.13 & 2.14)**. Since Elovl5 had no effect on the phosphorylation status of IRS2 or PDK1/2 **(Fig. 2.6)**, we speculate that

elevated Elovl5 activity does not enhance insulin signaling through the insulin receptor-IRS-PDK pathway. Instead, elevated Elovl5 activity increased Y^{307} phosphorylation in the catalytic unit of PP2A **(Fig. 2.13, Panel E)**. Phosphorylation of Y^{307} has been linked to decreased phosphatase activity directed at Akt and FoxO1 (57). Elevated Akt phosphorylation enhances Akt activity, while elevated FoxO1 phosphorylation promotes its proteasomal degradation.

Other regulatory factors involved in gluconeogenesis include TRB3 and CTMP, two negative regulators of Akt activity (109). Elevated Elovl5 activity attenuates cellular content of TRB3 **(Fig. 2.13, Panel C)**, but did not impact hepatic CTMP levels in fasted mice **(Fig. 2.13, Panel D)**. Although TRB3 is regulated by PPARα and Elovl5 attenuates PPARα activity (22), TRB3 mRNA was amongst a subset of PPARα-regulated genes that was not affected by elevated Elovl5 activity **(Fig. 2.10)**. Cell levels of TRB3 are regulated through other mechanisms, like proteasomal degradation (113). Future studies will focus on defining mechanisms for Elovl5 control of PPARα function and TRB3 cellular abundance.

An unresolved issue is a full understanding of the molecular linkage between changes in hepatic Elovl5 activity and the control of hepatic TRB3 content, PPARα function and PP2A phosphorylation **(Fig. 2.14)**. Elevated Elovl5 activity induces a 2- to 4-fold increase in low abundance C20-22 PUFA, including 20:3,n-6 and 22:4,n-6 **(Fig. 2.7, Panel C)**. While these changes are

detected in total hepatic lipid extracts, they are not seen in microsomal (ER) or plasma lipids. We suspect these fatty acids are likely assimilated into membrane phospholipids. Twenty-two carbon PUFA are poor activators of PPARα (26). While this observation can explain some of the Elovl5 effects on PPARα-regulated genes **(Fig. 2.9 & 2.10)**, it cannot explain the Elovl5 regulation of the phosphorylation status of key proteins (Akt, GSK3β, PP2A) or hepatic TRB3 abundance. Enrichment of membranes with $C_{20\text{-}22}$ PUFA may affect specific signaling pathways (19, 114). Studies with human retinal endothelial cells provide one possible scenario. Increased docosahexaenoic acid (DHA, 22:6,n-3) content in cell membranes was linked to decreased levels of cholesterol and Src kinases (Fyn and c-Yes) in lipid rafts, as well as decreased expression of adhesion molecules (ICAM & VCAM) through an NFκB-mediated mechanism (115-118). PP2A phosphorylation at Y^{307} is regulated by Src-kinases and protein phosphotyrosine phosphatases (112). Additional studies are required to determine whether $C_{20\text{-}22}$ PUFA induced by elevated Elovl5 activity affects membrane lipid composition and cell signaling.

In contrast to high fat diet induced obesity and diabetes, streptozotocin-induced diabetes rapidly destroys β-cells and lowers plasma insulin. Hepatic Elovl5 mRNA and enzyme activity is not affected in this model of diabetes (21). As such, hyperglycemia in insulin-dependent diabetes is not linked to hepatic Elovl5 activity. Recent unpublished studies in our lab indicate that inhibition of acetyl CoA carboxylase (ACC) abrogates fatty acid elongation.

Acetyl CoA carboxylase activity is suppressed in insulin-dependent diabetes (32, 119). Thus, the availability of malonyl CoA for fatty acid elongation may be as important as elongase expression in controlling elongase function. Elevating hepatic Elovl5 activity would likely not improve blood glucose control because malonyl CoA remains limiting in the insulin-dependent diabetic.

In addition to effects on blood glucose and proteins involved in gluconeogenesis, elevated hepatic Elovl5 regulates hepatic glycogen **(Table 2.2)**. The effect of Elovl5 on hepatic glycogen is influenced by the diet. In chow and low fat diets, Elovl5 induces a modest, but significant increase in fasting glycogen content (22). The high fat-low carbohydrate diet also significantly increased hepatic glycogen content in fasted mice (104) **(Table 2.2)**. Elevated hepatic Elovl5 activity lowers hepatic glycogen. The effect of Elovl5 on hepatic glycogen is comparable to that seen with elevated expression of malonyl CoA decarboxylase (MCD) (104). Elevated Elovl5 activity, however, does not induce MCD mRNA (not shown). Effects of diet and Elovl5 on fasting hepatic glycogen can be explained, at least in part, by changes in the phosphorylation status of Akt **(Fig. 2.13)** and GSK3β **(Fig. 2.6)**.

It is unlikely that all of the effects of Elovl5 on the control of blood glucose in obese fasted mice can be explained by control of hepatic gluconeogenic gene expression. Recent studies have established that fasting blood glucose levels are not associated with increased Pck1 or G6Pc expression (120, 121). Moreover, studies in obese humans indicate that a

significant fraction of blood glucose in fasting is derived from whole body protein catabolism (122). While our studies establish that elevated Elovl5 activity improves blood glucose levels in high fat fed obese mice **(Fig. 2.4)**, addition studies are required to define the role whole body protein catabolism plays in Elovl5-mediated control of blood glucose.

Finally, mice fed high fat diet develop fatty liver, i.e., the accumulation of triglyceride **(Table 2.2)** (21). Mice with ablated Elovl5 also develop fatty liver, at least in part by increased levels of SREBP-1 in nuclei and induction of lipogenic gene expression (44). While elevated Elovl5 activity lowers hepatic nuclear SREBP-1 in mice fed the low fat diet, mice fed the high fat diets have suppressed levels of hepatic SREBP-1 content (21) **(Fig. 2.5)**. As such, fatty liver in high fat fed mice is not due to SREBP1-mediated induction of *de novo* lipogenesis. Moreover, there is no significant difference in nuclear SREBP-1 content in obese mice infected with Ad-Luc or Ad-Elovl5. Yet, hepatic triglycerides in non-obese mice and obese mice with elevated hepatic Elovl5 activity are not significantly different **(Table 2.2)**. The Elovl5 effect on hepatic triglyceride content is likely targeted elsewhere, such as triglyceride assembly or VLDL secretion. In this regard, our studies provide a clue to explain this mechanism. FoxO1 regulates hepatic triglyceride and VLDL metabolism by controlling the expression of microsomal transfer protein (MTTP) expression (123), a key protein involved in VLDL assembly and ApoCIII expression, a key protein involved in VLDL clearance (123, 124). Preliminary studies show that

elevated Elovl5 activity suppresses MTTP and ApoCIII mRNA abundance by >50% (not shown). By controlling FoxO1 nuclear abundance, Elovl5 regulates both carbohydrate and triglyceride metabolism.

In summary, high fat diets induce hyperglycemia, glucose intolerance and increased hepatic content of glycogen and triglyceride. High fat diets also suppress hepatic Elovl5 enzyme activity. Modest elevation of hepatic Elovl5 activity in obese mice is sufficient to restore euglycemia and lower hepatic glycogen and triglyceride to levels seen in non-obese mice. Under the conditions of this study, Elovl5 does not significantly affect body weight **(Table 2.2)**. The mechanism for these changes involves, at least in part, the suppression in the nuclear abundance of transcription factors (FoxO1, PGC1α) and the regulation of cell signaling pathways (Akt, GSK3β, PP2A) controlling gluconeogenesis and triglyceride metabolism. These studies establish a link between fatty acid elongation and hepatic glucose and triglyceride metabolism and suggest a role for regulators of Elovl5 activity in the treatment of diet induced hyperglycemia and fatty liver.

Acknowledgements: This research was supported by the National Institutes of Health (DK43220) and the National Institute for Food and Agriculture USDA (2009-65200-05846). We appreciate the excellent technical assistance of Karin Hardin.

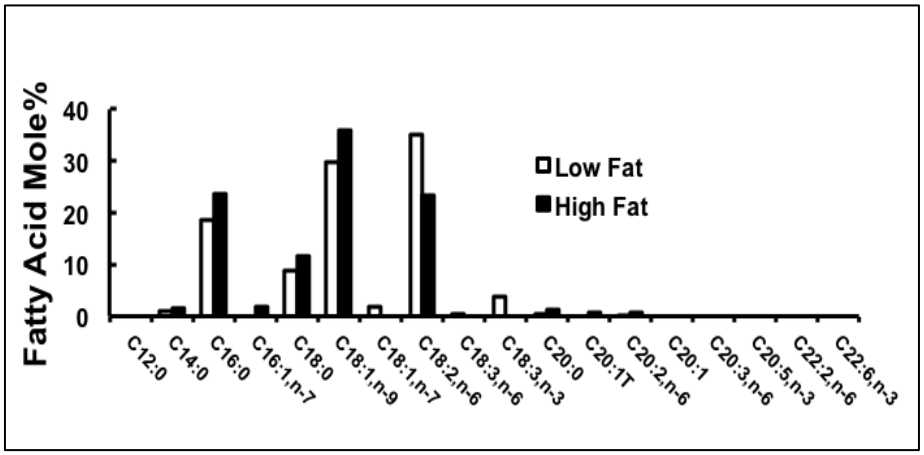

Fig. 2.1. Fatty acid composition of low and high fat diets. Fat in the low fat [(10% calories as fat, D12450B] and high fat [60% calories as fat, D12492] diets [Research Diets, Inc.] was saponified, converted to fatty acid methyl esters and quantified by gas chromatography. Results are expressed as Fatty Acid Mole %, mean of two separate determinations.

Table 2.1. Primer pairs for qRT-PCR

Gene	Accession	Forward	Reverse
ACOT1	NM_012006	CGCAGCCACCCCGAGGTAAA	TCTCAGGATGGTCACAGGGGGT
Cyclophilin	NM_008907	CTTCTTGCTGGTCTTGCCATTCCT	GGATGGCAAGCATGTGGTCTTTG
CYP4A10	NM_010011	TGTTTGACCCTTCCAGGTTT	CAATCACCTTCAGCTCACTCA
FADS1	NM_146094	TGTGTGGGTGACACAGATGA	GTTGAAGGCTGATTGGTGAA
FADS2	NM_019699	CCACCGACATTTCCAACAC	GGGCAGGTATTTCAGCTTCTT
Elovl2	NM_019423	ACGCTGGTCATCCTGTTCTT	GCCACAATTAAGTGGGCTTT
FGF21	NM_020013	TACACAGATGACGACCAAGAC	AAAGTGAGGCGATCCATAGAG
FoxO1	NM_019739	CAATGGCTATGGTAGGATGG	TTTAAATGTAGCCTGCTCAC
G6Pc	NM_008061	GCCTTCTATGTCCTCTTTCC	CAAACAGAATCCACTTGAAGAC
HS2	NM_008256	CCTTGAACGAGTGGATGAGA	CAGATGCTGTTTGGGTAGCA
Pck1	NM_011044	ACATTGCCTGGATGAAGTTTG	GGCATTTGGATTTGTCTTCAC
PCX	NM_008797	CGTGGTCTTCAAGTTCTGTG	CTAAGCCCATGTAGTACTCCAG
PGC1α	NM_008904	CTATGAAGCCTATGAGCACGA	ATAGCTGTCTCCATCATCCC
TRB3	NM_175093	GGCTCCAGGACAAGATGCGAGC	AGGGGCCACAGCAGGTGAC

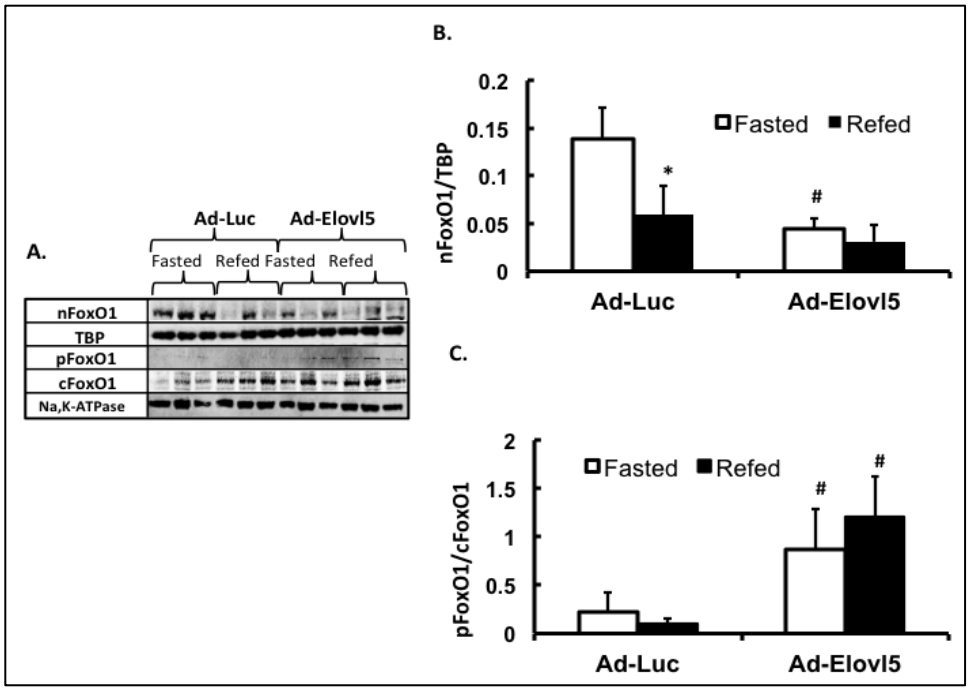

Fig. 2.2. Effects of elevated hepatic Elovl5 activity on FoxO1 nuclear content. Male C57BL/6J mice maintained on a chow diet were injected with Ad-Luc (control recombinant adenovirus) or Ad-Elovl5. Four days post injection animals were fasted overnight. At 8:00 AM the next day, ½ of the mice were euthanized for blood and tissue recovery (**Fasted**). The remaining mice were fed chow and euthanized 4 hours later (**Refed**). Hepatic nuclear and cytosolic (post-nuclear) proteins were prepared and levels of FoxO1, pFoxO1, TATA-binding protein (TBP) & Na,K-ATPase were measured by immunoblotting (Panel A); 3 animals/group. TBP and Na,K-ATPase are loading controls. Levels of nuclear FoxO1 were normalized to TBP, i.e., nFoxO1/TBP (Panel B). The level of cytosolic phosphorylated FoxO1 was normalized to total cytosolic FoxO1 (Panel C). Results are expressed as nFoxO1/TBP or pFoxO1/FoxO1, mean $\pm$ SD, n=3. ***,** $p \leq 0.05$ fasted versus refed animals; #, $p \leq 0.05$ Ad-Luc versus Ad-Elovl5 infected animals, ANOVA.

Table 2.2. Body weight, food intake, plasma and hepatic parameters

	Low Fat		High Fat	
	Ad-Luc	Ad-Elovl5	Ad-Luc	Ad-Elovl5
# Mice/group	8	8	8	8
Body Weight (g)				
Prior to Injection	30.9 ± 3.7	27.5 ± 1.2	42.5 ± 5.0*	39.2 ± 5.0*
After Injection	30.4 ± 3.6	27.4 + 1.6	40.9 ± 4.6*	36.3 ± 4.0*
Food Intake:				
grams/day	3.7 ± 0.8	3.3 ± 0.7	3.3 ± 1.6	2.5 ± 0.7
Kcal/day	14.1 ± 3.2	12.6 ± 2.6	17.2 ± 8.5	12.8 ± 3.9
Plasma Parameters				
Adiponectin (μg/ml)	5.2 ± 1.3	5.9 ± 0.3	6.6 ± 1.0	6.2 ± 1.1
NEFA (mEg/ml)	0.3 ± 0.1	0.4 ± 0.1	0.3 ± 0.1	0.3 ± 0.1
Cholesterol (mg/dl)	114.6 ± 42.3	173.9 ± 4.9	181.3 ± 46.6	159.0 ± 0.2
Triglycerides (mg/dl)	119.6 ± 4.7	55.9 ± 12.1#	91.5 ± 25.0	70.7 ± 18.0
β-hydroxybutyrate (μM)	1.54 ± 0.3	1.65 ± 0.4	0.6 ± 0.3*	1.5 ± 0.2
Liver Parameters:				
Weight (g)	1.2 ± 0.1	1.5 ± 0.1#	1.7 ± 0.3*	1.9 ± 0.3*
% of Body Weight	3.9 ± 0.4	5.5 ± 0.3#	4.2 ± 0.7	5.2 ± 0.3#
Liver Protein (mg protein/mg DNA)	24.3 ± 6.5	18.3 ± 4.2	29.0 ± 3.6	24.8 ± 4.8
Triglyceride (μg Triglyceride/mg protein)	49.2 ± 25.0	66.1 ± 22.6	156.9 ± 88.4*	91.0 ± 17.8
Cholesterol (μg Cholesterol/mg protein)	14.9 ± 2.1	13.3 ± 0.7	17.4 ± 7.1	17.0 ± 3.6
Glycogen (μg glucose/mg protein)	2.3 ± 2.1	4.9 ± 2.2#	31.9 ± 9.6*	10.8 ± 7.7#

Results are presented as mean ± SD. *$p \leq 0.05$, low fat versus high fat; #$p \leq 0.05$ Ad-Luc versus Ad-Elovl5, ANOVA, two-way.

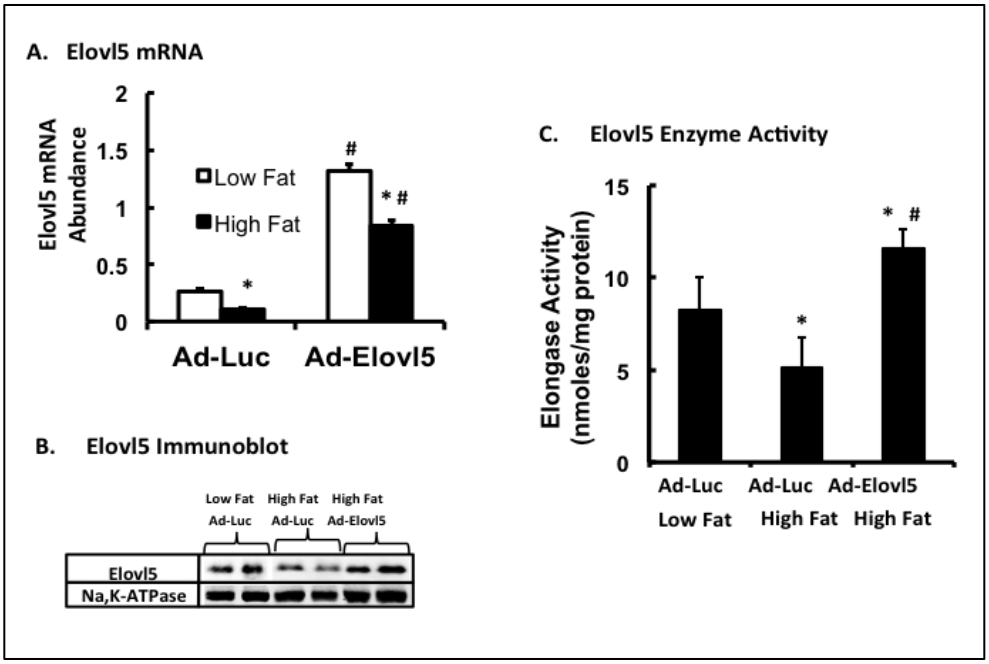

Fig. 2.3. Hepatic Elovl5 mRNA, protein and enzyme activity in C57BL/6J mice fed low and high fat diets. A. Elovl5 mRNA abundance. The abundance of Elovl5 and cyclophilin mRNA in livers of fasted mice infected with Ad-Luc and Ad-Elovl5 was quantified by qRT-PCR. Results are expressed as Elovl5 mRNA Abundance relative to cyclophilin, mean ± S.D., n=8 *****, p≤ 0.05 low fat versus high fat; #, p≤0.05 Ad-Luc versus Ad-Elovl5, ANOVA. B. Elovl5 Immunoblot. Hepatic Elovl5 and Na,K-ATPase (loading control) protein was measured by immunoblotting. Hepatic protein extracts are from 2 separate mice per group. C. Elovl5 Activity. Fatty acid elongase activity was measured using microsomes isolated from livers of fasted mice. 18:3,n6-CoA was used as substrate; 18:3,n6-CoA is a specific substrate for Elovl5. Results are expressed as Elongase Activity, nmoles ^{14}C-malonyl CoA incorporated in to fatty acids/mg protein, mean ± SD, 8 animals/group. *****, p≤ 0.05 low fat versus high fat; #, p≤0.05 Ad-Luc versus Ad-Elovl5, ANOVA.

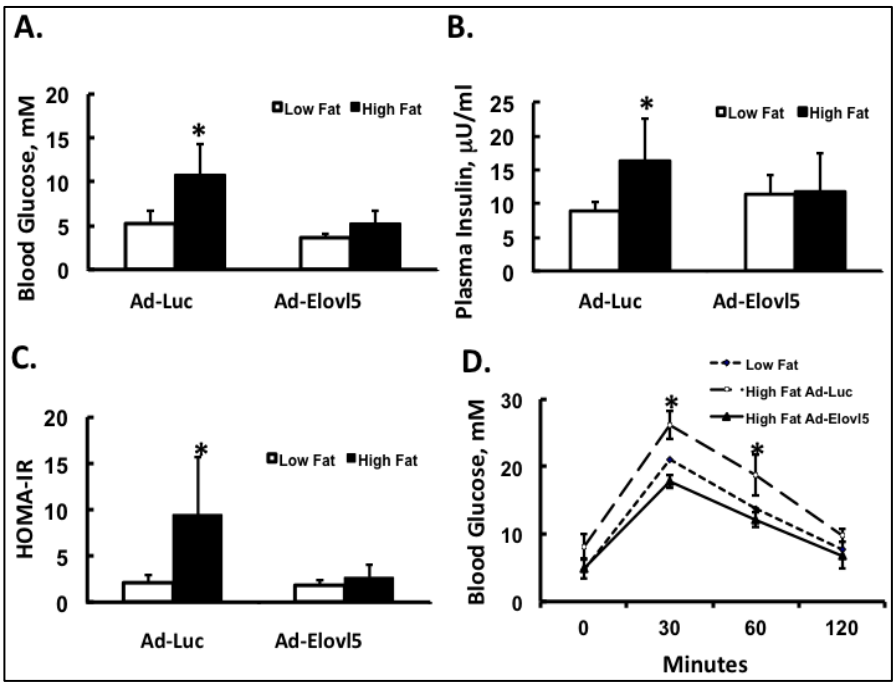

Fig. 2.4. Blood glucose, plasma insulin, HOMA-IR and glucose tolerance test in mice fed low and high fat diets. Fasting blood glucose (mM) [A] and plasma insulin (mU/ml) [B] were measured; these values were used to calculate HOMA-IR [C] [HOMA-IR = (Glucose X Insulin)/22.5]. Results are expressed as mean $\pm$ SD, n=4-8; *$p \leq 0.05$ Ad-Luc versus Ad-Elovl5, ANOVA. Panel D: Glucose Tolerance Test. Results are expressed as blood glucose (mM), mean $\pm$ SD, 4 animals were in each group; *****, $p \leq 0.05$ Ad-Luc versus Ad-Elovl5, ANOVA. The area under the curve was calculated using Sigmaplot v10 trapezoid rule. The values are: 1581 $\pm$ 168, 2044 $\pm$ 91, 1404 $\pm$ 132 mM glucose X min; for Low Fat, High fat-Ad-Luc and High fat–Ad-Elovl5, respectively. The high fat-Ad-Luc group was significantly different from the Low fat and High fat-Ad-Elovl5 groups; $p \leq 0.05$, ANOVA.

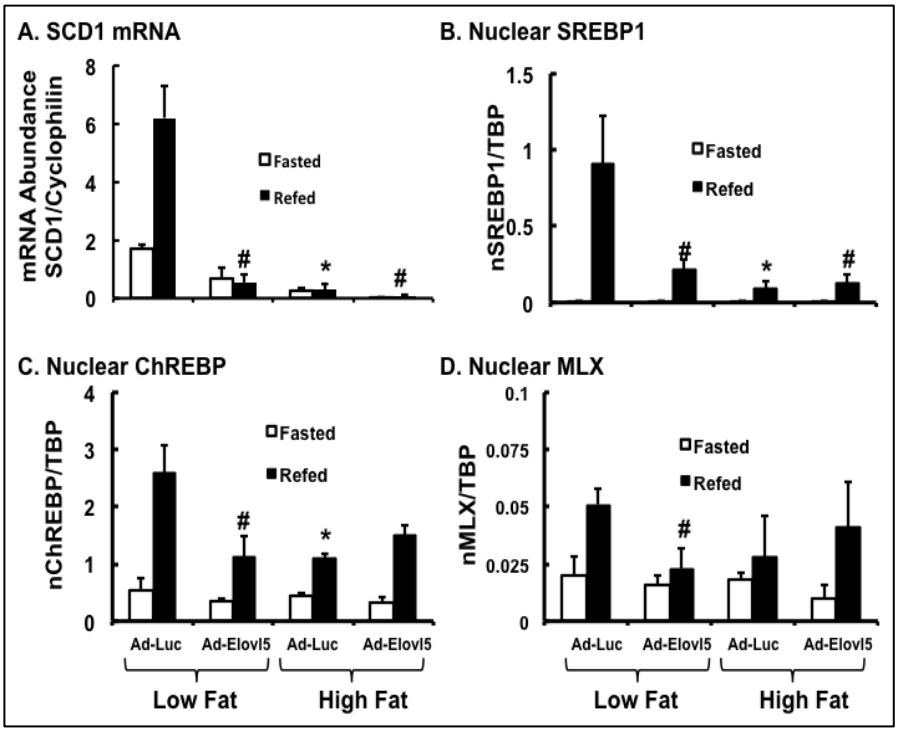

Fig. 2.5. Effect of diet and Elovl5 activity on hepatic stearoyl CoA desaturase (SCD1) mRNA and the nuclear protein content of SREBP1, ChREBP and MLX. Panel A. Transcript abundance for SCD1 was assayed by qRT-PCR; primers are listed in Table 2.1. Results are normalized to the transcript abundance of cyclophilin. Results are presented as mRNA abundance, SCD1/cyclophilin. Panels B-D. The nuclear protein abundance of SREBP-1 (nSREBP1), ChREBP (nChREBP) and MLX (nMLX) was measured by immunoblotting and quantified using a LiCor Odyssey. Nuclear levels of SREBP1, ChREBP and MLX were normalized to the loading control, TBP. All results are the mean $\pm$ SD, 4 mice/group. *, $p<0.05$ fasted versus refed; #, $p<0.05$ low fat versus high fat, ANOVA.

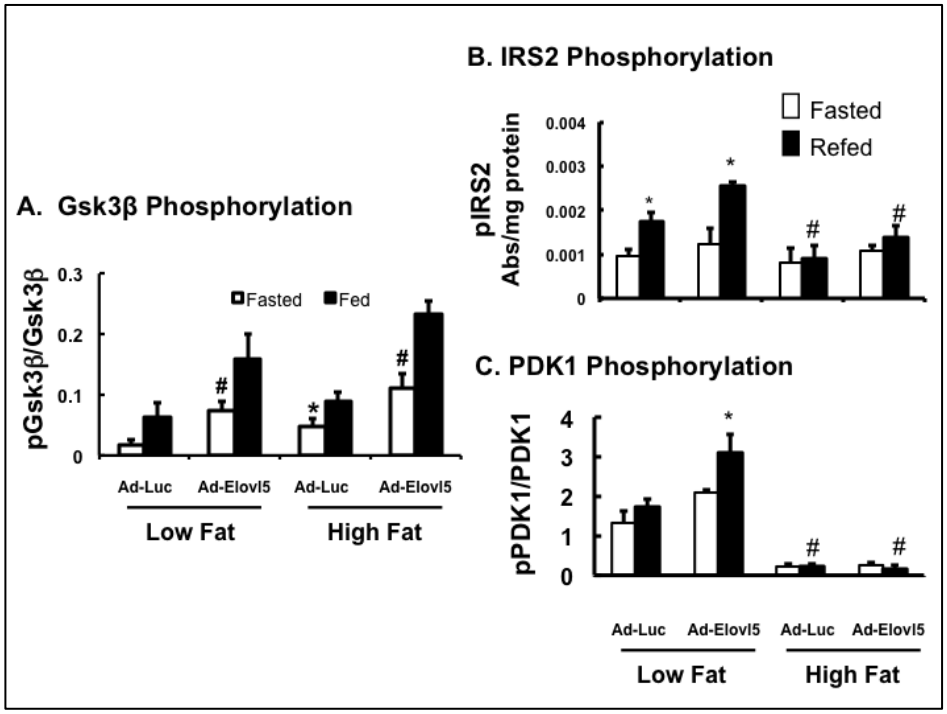

Fig. 2.6. Effect of diet and Elovl5 activity on the phosphorylation status of GSK3β, IRS2 and PDK1. Panel A. Phospho-GSK3β and total GSK3β was measured by immunoblotting and quantified using a LiCor Odyssey. The phosphorylation status is the amount of phosphorylated protein divided by the total protein (pGSK3β/GSK3β). Results are expressed the ratio of phospho-GSK3β to total GSK3β. Panel B. Phospho-IRS2 (pIRS2) was quantified using an ELISA assay. Panel C. Phospho- and total PDK1 was measured by immunoblotting and quantified using a LiCor Odyssey. The phosphorylation status is the amount of phosphorylated protein divided by the total protein (pPDK1/PDK1). Results are expressed as mean $\pm$ SD, 4-8 mice/group. *, $p<0.05$ fasted versus refed; #, $p<0.05$ low fat versus high fat, ANOVA.

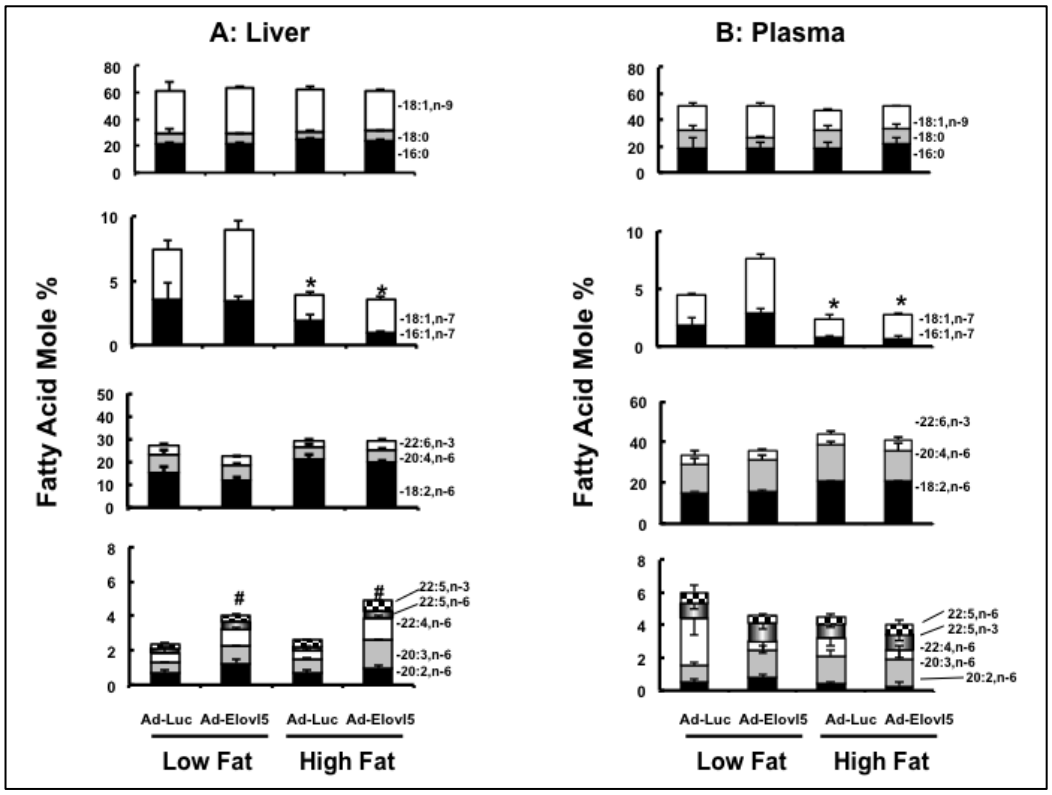

Fig. 2.7. Effect of dietary fat and Elovl5 on hepatic & plasma fatty acid composition. Fatty acid composition of mouse liver (A) and plasma (B) were measured on fasted mice. Lipids were extracted, saponified, converted to fatty acid methyl esters & quantified by gas chromatography. Results are expressed as Fatty Acid Mole%, mean $\pm$ SD, 4 mice/group. Statistical differences for the cumulative amount of fatty acids (e.g., 16:1,n-7 plus 18:1,n-7 or 20:2,n-6, 20:3,n-6, 22:4,n-6, 22:6,n-6, 22:5,n-3) are reported in panel A & B; *, $p \leq 0.05$ low fat versus high fat; #, $p \leq 0.05$ Ad-Luc versus Ad-Elovl5, ANOVA.

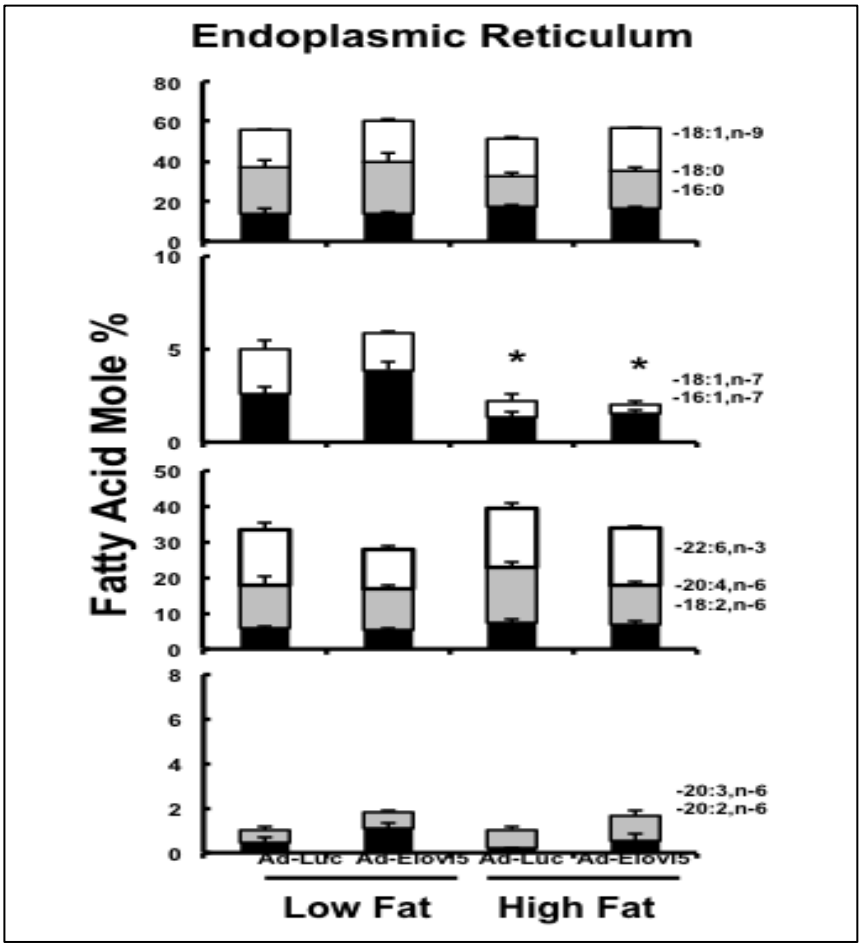

Fig. 2.8. Fatty acid composition of the endoplasmic reticulum (microsomes). Microsomes were prepared and lipids were extracted, saponified, converted to fatty acid methyl esters & quantified by gas chromatography. Results are expressed as Fatty Acid Mole%, mean ± SD, 4 mice/group.

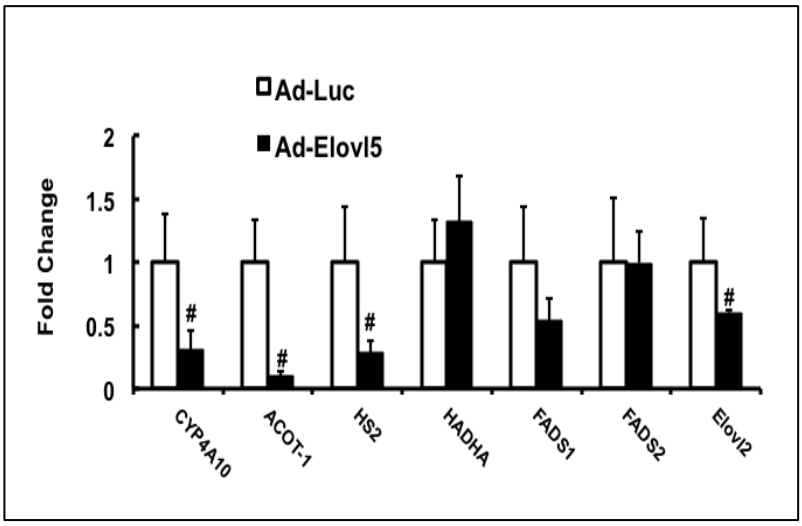

Fig. 2.9. Effect of Elovl5 on PPARα-regulated gene expression in mice fed a high fat diet. Transcript abundance was assayed by qRT-PCR using primers listed in Table 1. Results are normalized to the transcript abundance in Ad-Luc infected mice maintained on the high fat diet and fasted overnight. Results are presented as Fold Change induced by Ad-Elovl5, mean ± SD, 4 mice/group. #, $p \leq 0.05$, Ad-Luc versus Ad-Elovl5, *Students t-test*.

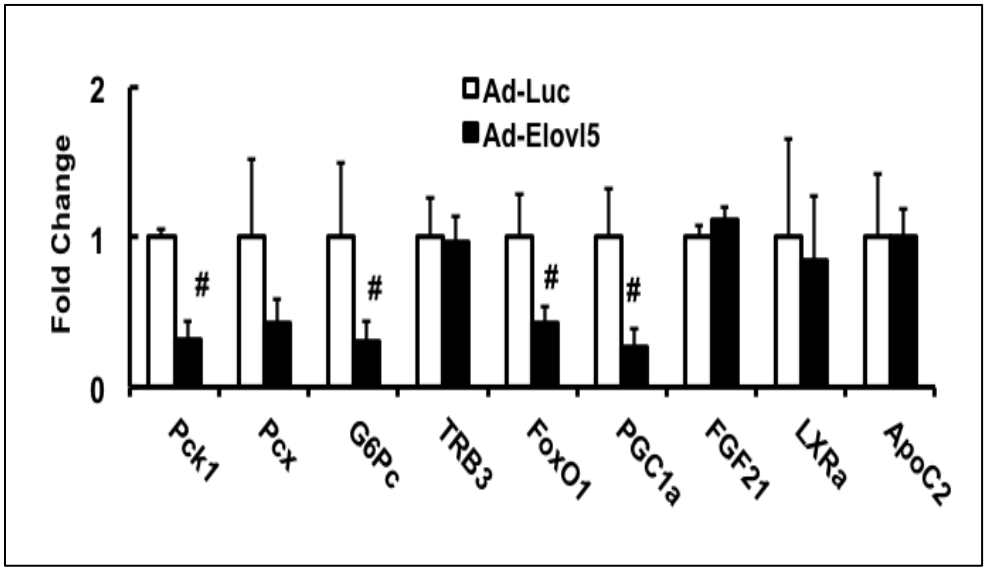

Fig. 2.10. Effect of elevated Elovl5 activity on mRNA levels of proteins involved in gluconeogenesis. Transcript abundance was assayed by qRT-PCR using primers listed in Table 2.1. Results are normalized to the transcript abundance in Ad-Luc infected mice maintained on the high fat diet and fasted overnight. Results are presented as Fold Change induced by Ad-Elovl5, mean $\pm$ SD, 4 mice/group. #, $p<0.05$, Ad-Luc vs Ad-Elovl5, *Students t-Test*.

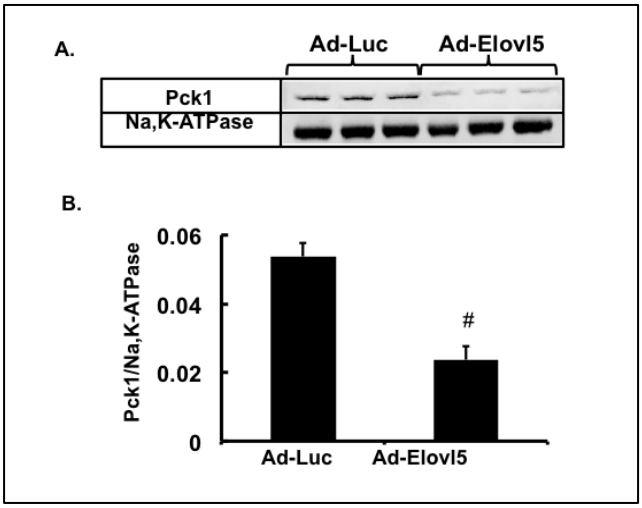

Fig. 2.11. Elevated Elovl5 activity suppresses cytosolic Pck1 abundance. Mouse liver post-nuclear (cytosolic) extracts were prepared from fasted mice maintained on the high fat diet and infected with either Ad-Luc or Ad-Elovl5. Protein abundance of Pck1 & Na,K-ATPase was measured by immunoblotting and quantified using a LiCor Odyssey. Panel A: Representative immunoblots for cytosolic Pck1 & Na,K-ATPase;Na,K-ATPase is the loading control; 3 mice/group. Panel B: Quantified results for cytosolic Pck1 were normalized to Na,K-ATPase. Results are expressed as mean $\pm$ SD, 6 mice/group. #, $p \leq 0.05$ Ad-Luc versus Ad-Elovl5, Students' t-test. The results are representative of 2 separate experiments.

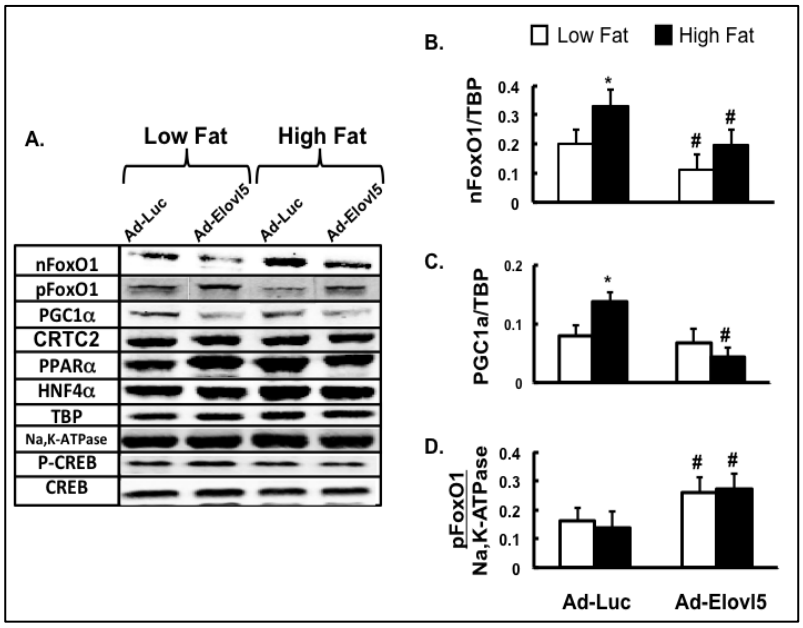

Fig. 2.12. Nuclear abundance and phosphorylation status of transcription factors controlling gluconeogenesis. Mouse liver nuclear and post-nuclear (cytosolic) extracts were prepared from fasted mice maintained on the low or high fat diets and infected with either Ad-Luc or Ad-Elovl5. Protein abundance was measured by immunoblotting and images were quantified using a LiCor Odyssey. Panel A: Representative immunoblots for nuclear FoxO1(nFoxO1), phosphorylated FoxO1 [cytosolic] (pFoxO1), PGC1α, CRTC2, PPARα, HNF4α, CREB, p-CREB & TBP; extracts from 1 mouse/group. Panels B-D: Quantified immunoblots for FoxO1, PGC1α and pFoxO1 (8 mice/group). FoxO1 and PGC1α were normalized to TBP; pFoxO1 was normalized to Na,K-ATPase. Results are expressed as mean $\pm$ SD, 8 mice/group. *****, $p<0.05$ low fat versus high fat; #, $p\leq0.05$ Ad-Luc versus Ad-Elovl5, ANOVA.

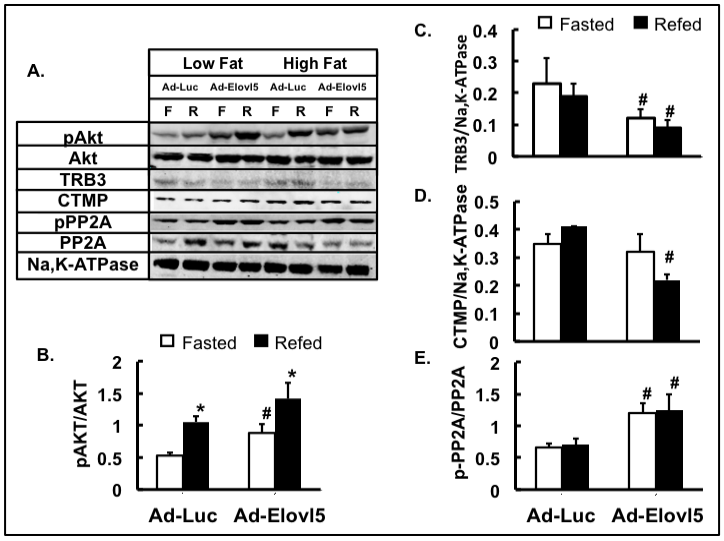

Fig. 2.13. Abundance and phosphorylation status of hepatic proteins involved in cell signaling. Mouse liver cytosolic extracts were prepared from fasted and refed mice maintained on low or high fat diets and infected with either Ad-Luc or Ad-Elovl5. Protein abundance was measured by immunoblotting and images were quantified using a LiCor Odyssey. Panel A: Representative immunoblots for cytosolic phosphorylated Akt (pAkt) and total Akt (Akt), TRB3, CTMP, phosphorylated PP2A catalytic unit (pPP2A), total PP2A catalytic units (PP2A) and Na,K-ATPase (a loading control); extracts from 1 mouse/group. Panel B-D: Quantified results for the phosphorylation status of Akt, i.e., pAkt normalized to total Akt (pAkt/Akt), total TRB3 normalized to Na,K-ATPase (TRB3/Na,K-ATPase), CTMP normalized to Na,K-ATPase and the phosphorylation status of PP2A catalytic unit, i.e., pPP2A normalized to total PP2A (pPP2A/PP2A). Results are expressed as mean $\pm$ SD, 8 mice/group. *****, $p<0.05$ low fat versus high fat; #, $p\leq0.05$ Ad-Luc versus Ad-Elovl5, ANOVA.

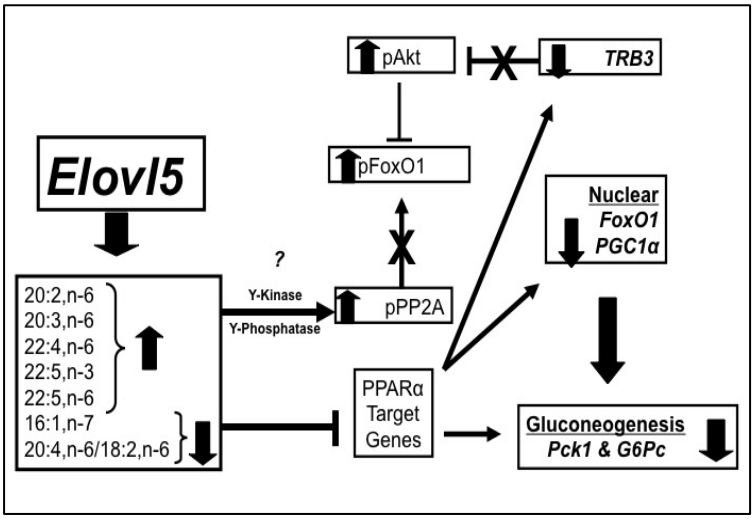

Fig. 2.14. Tentative model for Elovl5 effects on hepatic function. Elevated hepatic Elovl5 activity increased $C_{20\text{-}22}$ PUFA hepatic PUFA contents. Improved PUFA synthesis increased PP2A, Akt and FoxO1 phosphorylation, decreased FoxO1 and PGC1α nuclear content and suppressed Pck1 and G6Pc gene expressions.

Chapter 3

Fatty acid elongase-5 (Elovl5) regulates the mTORC2-FoxO1 pathway in livers of obese-diabetic C57BL/6J mice

Sasmita Tripathy and Donald B. Jump

Under review: Journal of Lipid Research
Publishers: American Society of Biochemistry and Molecular Biology.

3.1. Abstract

Fatty acid elongase-5 (Elovl5), a key enzyme involved in PUFA synthesis, was recently reported to regulate hepatic FoxO1; a major transcription factor controlling gluconeogenesis (GNG). This report focused on Elovl5 control of Akt and FoxO1 phosphorylation via rictor and PP2A. Induction of Elovl5 activity by using recombinant adenoviral approach in livers of high fat diet induced obese-diabetic mice and HepG2 cells increased phosphorylation of Akt2-S^{473} (mTORC2 site), but not Akt2-T^{308} (PDK1 site). Chemical inhibition of Akt2 activity blocked Elovl5 induction of FoxO1-S^{256} phosphorylation HepG2 cells. Elevated Elovl5 activity in liver and HepG2 cells induced rictor mRNA, rictor protein and rictor-mTOR interaction, but had no effect on other mTORC2 components (mSin1, GβL). Knockdown (siRNA) of rictor in HepG2 cells attenuated Elovl5 induction of Akt2-S^{473} and FoxO1-S^{256} phosphorylation. While PP242-mediated inhibition of mTORC1 and mTORC2 blocked the Elovl5 induction of FoxO1-S^{256} phosphorylation, rapamycin inhibition of mTORC1 had no effect on Elovl5 control of FoxO1-S^{256} phosphorylation. Two phosphatases (PP2A and MKP-3) regulate FoxO1. Inhibition of PP2A, but not knockdown of MKP-3 (shRNA), augmented Elovl5 induction of FoxO1-S^{256} phosphorylation. Taken together, Elovl5-mediated induction of rictor and inhibition of PP2A is required for Elovl5 control hepatic FoxO1 and genes involved in GNG.

Key words: Elovl5, Akt, FoxO1, mTORC2, rictor, gluconeogenesis

3.2. Introduction

Obese and diabetic humans (13, 125-127) and mice (21, 25) display evidence of impaired conversion of C_{18} essential fatty acids to C_{20-22} PUFA, i.e., low plasma ratio of 20:4n-6/18:2n-6. Until recently, the relationship between changes in plasma PUFA content and the onset and progression of type 2 diabetes was unclear. Our studies with a mouse model of high fat-low carbohydrate diet-induced obesity and diabetes established that the decline in the plasma and hepatic 20:4n-6/18:2n-6 was associated with the suppression of hepatic fatty acid elongase-5 (Elovl5) activity and expression. Elovl5 is a key enzyme involved in PUFA synthesis (21). Interestingly, other enzymes involved in PUFA synthesis, i.e., elongases (Elovl2) or desaturases (FADS1 or FADS2) were not affected by the high fat diet in this mouse model of diabetes and obesity (21, 25).

The physiological significance of this observation was revealed when hepatic Elovl5 activity in obese-diabetic mice was induced using a recombinant adenoviral approach. Restoration of hepatic Elovl5 activity in livers of obese-diabetic C57BL/6J mice increased hepatic and plasma C_{20-22} PUFA content, reduced homeostatic model assessment for insulin resistance (HOMA-IR), improved glucose tolerance and lowered fasting blood glucose to euglycemic levels, (25). Thus, elevated Elovl5 activity induced hepatic PUFA content and showed an insulin-mimetic effect on hepatic glucose metabolism i.e. decreased the hepatic gluconeogenesis and fasting blood glucose. The

mechanism for Elovl5 control of hepatic glucose metabolism was linked to increased phosphorylation of Akt-S^{473}, FoxO1-S^{256} and PP2Acat-Y^{307}, decreased nuclear content of FoxO1, and decreased expression of Pck1 and G6Pc; important enzymes involved in GNG and glucose production (25). Phospho-FoxO1 is excluded from nuclei, ubiquitinated and degraded by the proteasome (25, 62-65). Loss of nuclear FoxO1, due to its increased phosphorylation, leads to the reduction of expression of key genes involved in gluconeogenesis, i.e., Pck1 and G6Pc. While FoxO1 function is also regulated by other forms of covalent modification (acetylation and O-linked β-N-acetyl-glucosamine) (63, 69, 70), this report focuses on Elovl5 regulated mechanisms controlling FoxO1 phosphorylation.

Our previous studies suggest that both kinase and phosphatase pathways were involved in Elovl5 control of FoxO1 (25). Akt2 is a key regulator of hepatic FoxO1 and Akt2 is most abundant Akt isoform in rodent and human liver and other insulin sensitive tissues and cells (128-131). It plays a central role in T2DM and insulin resistance (128, 132). Akt is phosphorylated at two sites, T^{308} and S^{473} (71, 72). Phosphorylation of the Akt2-T^{308} is regulated by insulin through the PI3 kinase-PDK1 pathway, whereas Akt2-S^{473} site is phosphorylated by several kinases including, mammalian target of rapamycin complex 2 (mTORC2), integrin-linked kinase (ILK), MAP kinase-activated protein kinase-2 (MK-2), p38 MAP kinase, protein kinase C (PKCs), NIMA-related kinase-6 (NEK6), double stranded DNA-

dependent protein kinase (DNK-PK) and ataxia telangiectasia mutated gene products (56, 73, 77, 78, 133-135). Recently, mTORC2 was identified as a key regulator of Akt-S^{473} and FoxO1 phosphorylation, establishing a link between the mTOR pathway and GNG (74, 75, 136). Effects of PUFA synthesis or Elovl5 on mTORC2 and its components (mTOR, rictor, GβL, mSIN1) have not been reported.

Both PP2A and MKP-3 remove phosphate from FoxO1; this process promotes the nuclear accumulation of FoxO1 and the induction of GNG (57, 58). Elevated Elovl5 activity induces the phosphorylation of protein phosphatase-2A catalytic unit at Y^{307} (PP2Acat-Y^{307}), which inhibits PP2A catalytic activity (25). MKP-3 was recently reported to regulate FoxO1 phosphorylation status (58). MKP-3 belongs to the family of dual specificity phosphatases and dephosphorylates both serine/threonine and tyrosine residues in target proteins (80). Elovl5 or PUFA effects on MKP-3 have not been reported.

While my earlier studies revealed a complex interplay between kinases and phosphatases in the Elovl5-mediated control of FoxO1 and GNG (25), those studies did not establish the requirement for these regulatory components in the Elovl5 control of FoxO1. This study defined and established the molecular mechanisms such as Elovl5 mediated mTORC2/rictor induction and PP2A inhibition are required for the increase phosphorylation of FoxO1. Moreover, the involvement of mTORC2 in FoxO1 regulation is new.

Accordingly, these findings establish the requirement for FoxO1 phosphorylation, and the role key kinases and phosphatases play in the Elovl5-mediated control of FoxO1 and GNG.

3.3. Materials and methods

3.3.1. Materials

Dulbecco's modified essential medium (DMEM) with high glucose (25 mM) and antibiotics for cell culture were obtained from Invitrogen, Grand Island, NY. Hyclone fetal calf serum was purchased from Thermo-fisher scientific. Akt1/2 inhibitor or Akti1/2 (#124018) and PP242 (#475988) and rapamycin (#553140) were purchased from EMD Calbiochem, Philadelphia, PA. Microcystin-LR (#10007188) was obtained from Cayman Chemicals, Ann Arbor, MI. Human rictor siRNA (#8622) and control siRNA (#6568) were obtained from Cell Signaling, Danvers, MA. X-tremeGENE siRNA transfection reagent (#04476093001) was purchased from Roche Applied Science, Indianapolis, IN. Antibodies against rictor (#9476), phospho-rictor T^{1135} (#3806), raptor (#2280), GβL (#3274), p70S6-kinase (#9202), phospho-p70 S6 Kinase T^{389} (#9205), mTOR (#2972), phospho-mTOR S^{2448} (#2971), FoxO1(#9454), phospho-FoxO1S^{256} (#9461), GSK3β (#9315), phospho-GSK3α/β S^{21}/S^{9} (#9331), rictor sepharose bead conjugate (#5379), raptor sepharose bead conjugate (#5382) and IgG control sepharose bead conjugate (#3423) were obtained from Cell Signaling, Danvers, MA. Antibodies against Akt2 (sc-7127), phospho-Akt1/2/3-T^{308} (sc-16646-R), phospho-Akt1/2/3-S^{473}

(sc-7985), phospho-GSK3β-Y^{216} (sc-135653) and Na,K-ATPase (sc-21712) were purchased from Santa Cruz Biotechnology, Santa Cruz, CA. The antibody against TATA-binding protein (TBP) (ab818) was obtained from Abcam, Cambridge, MA. The mSIN1 (#07-2276) antibody was purchased from Millipore, Billerica, MA. The secondary antibodies, IRDye 680 and IRDye 800, (anti-mouse, anti-rabbit, and anti-goat) were obtained from LiCor, Inc., Lincoln, NE.

3.3.2. Recombinant adenovirus

The source, construction, purification, titration and use of the recombinant adenovirus expressing luciferase (Ad-Luc) and Elovl5 (Ad-Elovl5) were described previously (21, 25). Adenovirus expressing a form of FoxO1 that is resistant to phosphorylation control (ADA-FoxO1, Ad-ADA-FoxO1) was a generous gift from Dr. D. Accili (Columbia University Medical center, NY) (69). Adenoviruses expressing shRNA-MKP3-24 and shRNA-scrambled were generous gifts from Dr. Haiyan Xu (Brown Medical School, Providence, RI) (58).

3.3.3. Mouse liver extracts

The mouse hepatic protein extracts from whole liver, nuclei or cytosol used in this study were obtained from the lean and obese-diabetic C57BL/6J mice described previously (25). Briefly, male C57BL/6J mice were fed a low fat (10% calories as fat diet; Research Diets, D12450B) or a high fat (60% calories as fat diet, Research Diets, D12492) for 12 weeks. After 12 weeks on

these diets, mice fed the low fat diet were lean and euglycemic, while mice fed the high fat diet were obese, hyperglycemic and insulin resistant. Five days prior to termination of the experiment, mice were infected with Ad-Luc or Ad-Elovl5. Five days later, mice were fasted overnight; half of the fasted mice were refed their diets for 4 hours. Fasted and refed mice were euthanized at 8 AM and 12 noon for the recovery of blood and liver. Methods for liver recovery and preparation of protein extracts were described in our earlier report (25).

3.3.4. HepG2 Cells

Human hepatoma (HepG2) cells were obtained from American Type Culture Collection (Manassas, VA) and used to perform cell culture experiments. HepG2 cells were grown in Dulbecco's modified essential medium with high glucose (DMEM with 25 mM glucose) supplemented with 10% fetal calf serum. All experiments were carried out in cells grown on 6 wells or 12 wells plates (Corning Life Sciences, Corning, NY) in a humidified incubator at 37^0C and 5% CO_2. HepG2 cells were infected with recombinant adenovirus expressing either control viruses (Ad-Luc or Ad-shRNA-scrambled) or test viruses (Ad-Elovl5, Ad-ADA-FoxO1, Ad-shMKP3-24) at 20 infectious units (IU) per cell. In all HepG2 cell experiments, proteins were extracted as whole cell extract.

3.3.5. RNA extraction and quantitative real time polymerase chain reaction

Total RNA was extracted from mouse liver of our earlier study (25) and HepG2 cells using Triazol (Invitrogen). Transcript levels were measured by

qRT-PCR. Gene-specific primers are listed in **(Table 3.1)**. Primer design and qRTPCR methods were described previously (25). The relative amounts of mRNAs were calculated by using comparative C_T method (User Bulletin #2, Applied Biosystems). Cyclophilin was used as a control gene. Levels of target gene mRNA abundance were normalized to the abundance of cyclophilin mRNA.

3.3.6. Immunoblotting

Proteins were extracted from mouse liver and HepG2 cells as described previously (22, 25) in the presence of protease (Roche Applied Science, Indianapolis, IN) and phosphatase inhibitors (1 mM β-glycerol phosphate, 2.5 mM Na-pyrophosphate, 1 mM Na_3VO4). Cytosolic (post-nuclear), nuclear protein fractions and whole cell protein extracts were separated electrophoretically by SDS-polyacrylamide gel electrophoresis (NuPAGE 4–12% polyacrylamide Bis-Tris, Invitrogen) and transferred to nitrocellulose (BA83) membranes. Blots were incubated with primary antibodies against various proteins overnight at 4^0C. Next day blots were washed and incubated with secondary antibody for one hour at room temperature. Antigen-antibody reactions were detected and quantified using LiCor Odyssey scanner and software (22, 25).

3.3.7. Rictor knockdown

Knockdown of rictor protein in HepG2 cells used a siRNA approach. HepG2 cells grown in 12 wells plate to ~30-50% confluent; cells were

transfected with either siRNA rictor or control siRNA (scrambled RNA) at 100 pmole/well plus 2 µl/well of the X-tremeGENE siRNA transfection reagent according to the manufacture's recommendations. Cells were also infected with either Ad-Luc or Ad-Elovl5 (20 IU/cell). Cells were maintained in DMEM + FBS for 72 hours before harvest for protein analysis.

3.3.8. Immunoprecipitation

Mouse liver extracts (1 mg protein/ml) were incubated with 10 µl of antibody conjugated-sepharose beads. The antibodies conjugated to sepharose beads were against rictor or raptor; IgG served as a control. Extracts were incubated with antibody-sepharose beads overnight at 4^0C. Next day, the beads were centrifuged at 14,000 x g for 30 second at 4^0C. The immunoprecipitates were collected and washed with cell lysis buffer five times. The beads were resuspended with protein denaturing buffer containing sodium dodecyl-sulfate (SDS), boiled and centrifuged; the supernatants were applied to SDS-PAGE gels for electrophoresis. Specific proteins were detected by immunoblotting as described above.

3.3.9. Statistical Analysis

The statistical analyses performed in this study included ANOVA plus post hoc Tukey test and Students' t-test by using the statistical software StatView. The comparisons between groups was considered statistically different if $p<0.05$. Data are expressed as mean ± SD.

3.4. Results

3.4.1. Elovl5 regulates Akt2 and FoxO1 phosphorylation in mouse liver and human hepatoma (HepG2) cells

Obese-diabetic mice have levels of hepatic Elovl5 activity that are ~60-75% below levels in livers of lean non-diabetic mice. Infection of obese-diabetic mice with Ad-Elovl5 increases Elovl5 activity ~3-fold; to a level ~50% above the level expressed in livers of lean mice (25). Increased hepatic Elovl5 activity correlated with increased Akt2 and FoxO1 phosphorylation, decreased hepatic Pck1 expression and fasting blood glucose (25). When compared to Ad-Luc infected mice, elevated Elovl5 activity (Ad-Elovl5 infection) significantly increased Akt2-S^{473} and FoxO1-S^{256} phosphorylation, but not Akt-T^{308} phosphorylation, in livers of fasted obese-diabetic mice **(Fig. 3.1, Panel, A and B)**.

Infection of human hepatoma cells, HepG2, with Ad-Elovl5 increased Elovl5 protein ~2-fold (23), and increased Akt2-S^{473} and FoxO1-S^{256}, but not Akt2-T^{308}, phosphorylation **(Fig. 3.1, Panel C and D)**. These results establish that Elovl5 effects on Akt2 phosphorylation status are specific to the Akt-S^{473} site. Thus, Elovl5 activity controls Akt2-S^{473} and FoxO1-S^{256} phosphorylation status in both mouse liver and human hepatoma cells **Fig. 3.1** and (25).

3.4.2. ADA-FoxO1 overrides Elovl5 suppression of GNG genes in HepG2 cells

To determine whether Elovl5 effects on the expression of the gluconeogenic enzymes (i.e., Pck1 and G6Pase) requires FoxO1

phosphorylation, HepG2 cells were infected with Ad-Luc or Ad-Elovl5 in the absence (None) and presence of Ad-ADA-FoxO1. Ad-ADA-FoxO1 expresses a form of FoxO1 that is insensitive to phosphorylation control (69). Infection of HepG2 cells with Ad-Elovl5 significantly decreased Pck1 and G6Pase mRNA abundance by >70% and ~50% respectively **(Fig. 3.2)**. Including Ad-ADA-FoxO1 in the infection scheme induced Pck1 and G6Pase mRNA, and completely abolished Elovl5 regulation of Pck1 and G6Pase mRNA abundance. Thus, Elovl5 control of Pck1 and G6Pase expression in HepG2 cells requires control of FoxO1 phosphorylation status.

3.4.3. Elovl5 control of FoxO1-S^{256} phosphorylation requires Akt2

Akt2 phosphorylates FoxO1-S^{256}. We examined the requirement of active Akt2 in the Elovl5 control of FoxO1-S^{256} phosphorylation. HepG2 cells were first infected with Ad-Luc or Ad-Elovl5 and then treated with vehicle or the Akt1/2 inhibitor [Akti1/2, 3 μM] (137). As expected, infection of HepG2 cells with Ad-Elovl5 significantly increased the phosphorylation of Akt2-S^{473} and FoxO1-S^{256} **(Fig. 3.3, Panel A-C)**. Chemical inhibition of Akt1/2 using Akti1/2 significantly attenuated the Elovl5 mediated increase in Akt2-S^{473} and FoxO1-S^{256} phosphorylation **(Fig. 3.3, Panel A-C)**. Thus, active Akt2 activity is required for Elovl5 control FoxO1-S^{256} phosphorylation. Akti1/2 did not affect the phosphorylation status of Akt2-T^{308} **(Fig. 3.4)**.

3.4.4. The mTORC2 pathway is involved in Elovl5 control of Akt2-S^{473} and FoxO1-S^{256} phosphorylation in mouse liver and HepG2 cells

Elevated activity of hepatic Elovl5 in mouse liver (25) and in HepG2 cells increases the Akt2-S^{473}, a site phosphorylated by mTORC2 (78, 138-140), but not the Akt2-T^{308} site, a target for PI3-kinase-PDK1 **(Fig. 3.1, Panel A-D)**. To assess the role of mTORC2 in the regulation of Akt2-S^{473} phosphorylation status by Elovl5, we first examined the impact of diet on mTORC1 and mTORC2 components, namely raptor, rictor and mTOR **(Fig. 3.5)**.

Using hepatic RNA from lean and obese-diabetic mice infected with either Ad-Luc or Ad-Elovl5 (25), we quantified the mRNA levels of rictor, raptor and mTOR **(Fig. 3.5, Panel A)**. Elevated Elovl5 activity increased rictor and mTOR mRNA in both lean and obese mice $\geq$ 2-fold. Interestingly, raptor mRNA abundance was suppressed by ~70% in livers of obese mice; elevated Elovl5 activity further decreased raptor mRNA. Similar effects were seen in HepG2 cells **(Fig. 3.5, Panel B)**; increased Elovl5 expression induced rictor and mTOR, but suppressed raptor mRNA abundance.

To determine if these changes in mRNA correlated with changes in protein and mTOR phosphorylation status, hepatic extracts from lean and obese mice infected with either Ad-Luc or Ad-Elovl5 (25) were quantified by immunoblotting **(Fig. 3.6)**. Elevated hepatic Elovl5 activity did not significantly increase hepatic mTOR protein abundance **(Fig. 3.6, Panel A)**, an effect that

did not correlate with the changes in mTOR mRNA **(Fig. Fig. 3.5)**. Instead, elevated Elovl5 expression significantly increased phosphorylation of mTOR-S^{2448} in obese, but not lean mice **(Fig. 3.6, Panel A and B)**. Phosphorylated mTOR-S^{2448} is an active kinase (76, 78). The mTORC2 associated regulatory protein, rictor, was significantly induced by increased Elovl5 activity in both lean and obese mice **(Fig. 3.6, Panel C)**, an effect that correlated with Ad-Elovl5-mediated increase in rictor mRNA **(Fig. 3.5)**. While the high fat diet significantly suppressed hepatic raptor protein abundance, elevated Elovl5 activity had no further effect on hepatic raptor content **(Fig. 3.6, Panel A & D)**. Neither diet, nor changes in Elovl5 activity significantly affected hepatic abundance of other mTor-associated proteins, mSIN1 and GβL **(Fig. 3.6)**.

mTOR is the catalytic (kinase) subunit for both mTORC1 and mTORC2 (141, 142). Raptor and rictor play key roles in complex assembly and substrate selection for mTOR-kinase (78, 139). The observed increase in rictor protein abundance with Elovl5 over-expression **(Fig. 3.6)** may facilitate rictor-mTOR interaction. To test this possibility, immunoprecipitation and immunoblotting was used to examine the impact of Elovl5 on mTOR interaction with rictor and raptor. Extracts from diet-induced obese mice infected with Ad-Luc or Ad-Elovl5 were treated with antibodies against rictor (rictor-IP), raptor (raptor-IP); IgG served as a control for non-specific immunoprecipitation. The immune-precipitates were collected, denatured, electrophoresed, immunoblotted and assayed for the presence of rictor, raptor

and mTOR **(Fig. 3.7)**. The rictor sepharose bead conjugated antibody pulled down both rictor and mTOR. Elevated Elovl5 activity increased the immunoprecipitation of both mTOR and rictor. Elovl5 not only increased hepatic levels of rictor protein, Elovl5 promoted the physical interaction of rictor with mTOR. In contrast, raptor sepharose bead conjugated antibody did not pull down raptor or mTOR. The low level of raptor in these hepatic extracts likely explains this result.

3.4.5. Effects of chemical inhibition of mTORC1 and mTORC2 on Elovl5 control of Akt2-S^{473} and FoxO1-S^{256} phosphorylation

To further examine the role of mTORC2 in the Elovl5 control of Akt2-S^{473} and FoxO1-S^{256} phosphorylation, HepG2 cells were infected with Ad-Luc or Ad-Elovl5 and treated with the mTOR inhibitors, rapamycin or PP242 **(Figs. 3.8, 3.9, 3.10 & 3.11)**. Rapamycin inhibits the kinase activity of the rapamycin-sensitive complex mTORC1, whereas PP242 inhibits the kinase activity of both mTORC1 and mTORC2 (143). We are unaware of a mTORC2-specific inhibitor. Treatment of HepG2 cells with rapamycin (100 nM) decreased phosphorylation of mTOR-S^{2448} and its downstream target p70S6-kinase-T^{389} **(Fig. 3.8, Panel A-C)** by $\geq$50% in cells infected with Ad-Luc. In cells infected with Ad-Elovl5, phosphorylation of mTOR-S^{2448} and p70S6-kinase-T^{389} was suppressed by ~15% and 50%, respectively **(Fig. 3.8, Panel A-C)**. Rapamycin did not attenuate Elovl5 induction of Akt2-S^{473} or FoxO1-S^{256} phosphorylation **(Fig. 3.8, Panel A, D and E)**. Rapamycin also had no effect on the protein

abundance of various mTORC1 or mTORC2 components, i.e., raptor, rictor, mSIN1 and GβL **(Fig. 3.9)**.

A similar analysis was carried out using PP242 (500 nM), an inhibitor of both mTORC1 and mTORC2 (143) **(Fig. 3.10)**. PP242 significantly suppressed the phosphorylation of mTOR-S^{2448} and p70S6-kinase-T^{389}, by 70 and 90%, respectively, in both Ad-Luc and Ad-Elovl5 infected cells **(Fig. 3.10, Panel A-C)**. While elevated Elovl5 activity induced Akt2-S^{473} and FoxO1-S^{256} phosphorylation by 2-fold and ~50%, respectively, PP242 completely abolished this response **(Fig. 3.10, Panel A, D and E)**. Interestingly, PP242 significantly attenuated rictor protein abundance ~50%, but had no effect in other mTOR components such as raptor, mSIN1 and GβL **(Fig. 3.11)**. Thus, inhibition of mTORC2, but not mTORC1, blocks Elovl5-mediated control of Akt2 and FoxO1 phosphorylation.

3.4.6. Rictor knockdown (siRNA) attenuates Elovl5 mediated induction of Akt2-S^{473} and FoxO1-S^{256} phosphorylation.

To further verify the role of rictor in Elovl5 control of Akt2 and FoxO1, a siRNA approach was used to knockdown rictor. Transfection of HepG2 cells with rictor-siRNA significantly decreased rictor protein abundance and mTOR-S^{2448} phosphorylation by ~50% **(Fig. 3.12, Panel A-C)**. Increased Elovl5 expression in HepG2 cells significantly induced Akt2-S^{473} and FoxO1-S^{256} phosphorylation by 6- and 3-fold, respectively **(Fig. 3.12, Panel D & E)**. Rictor knockdown, however, attenuated this response by ~50% **(Fig. 3.12, Panel D**

& E). Rictor knockdown had no impact on Akt2-T^{308} phosphorylation **(Fig. 3.13)**. Thus, Elovl5 regulation of rictor protein abundance is required for Elovl5 to induce Akt2-S^{473} and FoxO1-S^{256} phosphorylation.

3.4.7. Elovl5 does not regulate rictor phosphorylation

Rictor has many phosphorylation sites (144-147). One of the kinases phosphorylating rictor is glycogen synthase kinase (GSK3β), a downstream target of Akt. While phosphorylation of GSK3β-S^{9} by Akt inactivates the kinase and increases glycogen synthesis (22), Phosphorylation of GSK3β-Y^{216} activates GSK3β activity (144). GSK3β also negatively regulates Akt activity through rictor (144). Activated GSK3β (phospho-GSK3β-Y^{216}) phosphorylates rictor-S^{1235}, a modification that interferes with rictor binding with Akt and ultimately reducing mTORC2 mediated Akt-S^{473} phosphorylation (144). Unfortunately, no antibody against phospho-rictor-S^{1235} is currently commercially available.

To examine the phosphorylation of GSK3β at both Y^{216} and S^{9} as well as rictor-T^{1135} phosphorylation we used samples from the PP242 study described in **Fig. 3.10**. Elevated Elovl5 expression selectively increased GSK3β-S^{9} phosphorylation, but did not increase GSK3β-Y^{216} phosphorylation **(Fig. 3.14, Panel A-C)**. PP242 inhibited Elovl5 stimulated GSK3β-S^{9} phosphorylation. Moreover, Elovl5 had no effect on rictor-T^{1135} phosphorylation in the presence and absence of PP242 **(Fig. 3.14, Panel D)**.

When combined with the results described in **Figs. 3.5 & 3.6**, these results suggest that Elovl5 does not control rictor phosphorylation.

3.4.8. Inhibition of PP2A synergistically augments Elovl5 induction of FoxO1-S^{256} phosphorylation

Two protein phosphatases (PP2Acat and MKP-3) dephosphorylate FoxO1, thus controlling its function (57, 58). Elovl5 induces the phosphorylation of PP2Acat-Y^{307} (25), an event that inhibits PP2Acat activity. To examine the role of PP2A in the Elovl5 regulation of Akt2-S^{473} and FoxO1-S^{256} phosphorylation, HepG2 cells were infected with Ad-Luc or Ad-Elovl5 and treated with the PP2Acat inhibitor, microcystin-LR [1nM] (148) **(Fig. 3.15)**. Treatment of HepG2 cells with microcystin-LR (1nM), alone did not significantly induce Akt-S^{473} phosphorylation or affect Elovl5 mediated induction of Akt2-S^{473} phosphorylation. In contrast, microcystin-LR significantly increased FoxO1-S^{256} phosphorylation in the absence (3.1-fold) and presence (2.8-fold) of Elovl5. The combination of Elovl5 plus microcystin-LR increased FoxO1-S^{256} phosphorylation nearly 9-fold **(Fig. 3.15, Panel A-C)**. Thus, Elovl5 control of Akt2-S^{473} and PP2Acat-Y^{307} phosphorylation status synergistically elevates FoxO1 phosphorylation.

MKP-3 regulates hepatic GNG by controlling FoxO1 phosphorylation (58). To assess the role of MKP-3 in the Elovl5 control of FoxO1 phosphorylation, we first measured MKP-3 protein in hepatic extracts derived from our previous mouse study (25) and in HepG2 cells. Elevated hepatic

Elovl5 activity had no effect on MKP-3 protein abundance **(Fig. 3.16)**. We next used a short hairpin RNA (shRNA) approach [Ad-shMKP3-24 (58)] to knockdown MKP-3 in HepG2 cells. When compared to no infection or cells infected with Ad-shRNA-Scrambled, Ad-shRNA-MKP3 suppressed MKP-3 protein abundance by ~50% **(Fig. 3.17, Panel A and B)**. The decline in hepatic MKP-3 protein abundance blocked the Elovl-5 mediated induction of Akt2-S^{473} phosphorylation **(Fig. 3.17, Panel A and C)**. While decreasing MKP-3 protein abundance in HepG2 cells significantly increased FoxO1-S^{256} phosphorylation **(Fig. 3.17, Panel A and D)**, knocking down MKP-3 did not increase Elovl5 induction of FoxO1-S^{256} phosphorylation. Finding that MKP-3 knockdown attenuated Elovl5-mediated control of Akt-S^{473} phosphorylation suggests MKP-3 may regulate Elovl5 activity. Both PP2A and MKP-3 control FoxO1 phosphorylation status. Elovl5 control of PP2Acat, but not MKP-3, is required for Elovl5 regulation of FoxO1.

3.5. Discussion

The goal of this study was to clarify the role of specific kinases and phosphatases in the Elovl5 regulation of hepatic FoxO1. This report extends our previous study (25) by establishing that FoxO1 phosphorylation is required for Elovl5 regulation of Pck1 and G6Pase **(Fig. 3.2)**. This is important because, in addition to phosphorylation and ubiquitination, FoxO1 activity is also regulated by acetylation and O-linked β-N-acetyl-glucosamine) (63, 69, 70). We also establish that Elovl5 regulates Akt2 by controlling the

phosphorylation of S^{473} (mTORC2 site) and not T^{308} (PDK1 site). Accordingly, we verified the role of mTORC2 in this regulatory scheme. Elevated Elovl5 activity increased hepatic $C_{20\text{-}22}$ PUFA (25) and increased hepatic rictor protein and mRNA abundance as well as rictor-mTOR interaction (**Fig. 3.5, 3.6, 3.7, 3.18**). Elevated Elovl5 activity does not regulate the abundance of other mTORC2 components (mTOR, mSIN1, GβL) (**Fig. 3.6)**. These results are the first to link PUFA synthesis and Elovl5 to the regulation of rictor and mTORC2.

Raptor and rictor regulate the stability and activity of the mTORC1 and mTORC2 complexes, respectively (56, 78, 139). We discovered, serendipitously, that in the mouse model of diet-induced obesity and diabetes used in this study, mTORC2, and not mTORC1, is the predominant hepatic mTOR complex (**Figs. 3.6 & 3.7**). The low level of hepatic raptor, coupled with the failure of rapamycin (mTORC1 inhibitor) to block Elovl5 induction of Akt2-S^{473} and FoxO1-S^{256} phosphorylation excludes mTORC1 involvement in this regulatory scheme. Future studies will determine if other mouse models of high fat diet-induced obesity and diabetes regulate hepatic raptor.

In contrast to raptor, little information is available on mechanisms controlling rictor expression (76). Recent studies identified the rictor-mTORC2 pathway in the control of GNG, but provided no information about molecular mechanisms controlling rictor (74, 136). Our studies are the first to establish a link between PUFA synthesis, rictor and mTORC2. Elovl5 induces rictor mRNA and rictor protein in mouse liver and in the human hepatoma (HepG2)

cell line. Moreover, Elovl5-mediated induction of rictor was required to increase Akt2-S^{473} and FoxO1-S^{256} phosphorylation. Future studies will focus on defining the molecular basis for Elovl5 control of hepatic rictor mRNA and protein expression.

Our studies reveal a complex regulatory scheme where Elovl5 control of rictor regulates Akt2-S^{473} phosphorylation, which in turn regulates FoxO1-S^{256} and GSK3β-S^{9} phosphorylation. Rictor interaction with mTOR and Akt is regulated by rictor phosphorylation (144-147), e.g., rictor-T^{1135}, rictor-S^{1235} phosphorylation. Rictor-T^{1135} is phosphorylated by p70S6-kinase which possibly interfere with rictor-mTOR interaction (147). Elovl5 does not regulate rictor-T^{1135} phosphorylation (**Fig. 3.14**). GSK3β phosphorylates rictor-S^{1235} in response to elevated ER-stress (144). Elovl5, however, induces GSK3β-S^{9} phosphorylation; phospho-GSK3β-S^{9} is inactive. We previously reported Elovl5 promotes hepatic glycogen accumulation (22). GSK3β-Y^{216}, in contrast, is an active kinase; changes in hepatic Elovl5 activity do not affect GSK3β-Y^{216} phosphorylation (**Fig. 3.14).** Taken together, these results suggest that Elovl5 induces rictor-mTOR interaction **(Fig. 3.7)** by increasing rictor protein abundance (**Figs. 3.6**) and not by regulating rictor phosphorylation.

Rictor was initially identified as a mTOR binding partner involved in controlling cytoskeletal structure (149). Rictor was later established to be an important component of mTORC2 complex regulating the PI3-kinase signaling

pathway (56, 78, 138). As a factor involved in cytoskeletal structure, rictor interacts with integrin and integrin-linked kinase (ILK); ILK phosphorylates Akt-S^{473} in a membrane-associated complex. This event is important for cell survival and cancer cell growth (150). While ILK is present in the mTORC2 immunoprecipitated complex described in **Fig. 3.7**, ILK association with mTOR was not regulated by Elovl5 (data not shown). Finding that rictor knockdown and the dual mTOR inhibitor PP242 blocked Elovl5 induction of Akt-S^{473} and FoxO1-S^{256} phosphorylation argues strongly that rictor-mTORC2 mediated phosphorylation of Akt-S^{473} is the primary target for Elovl5 regulation of Akt and FoxO1 (**Figs. 3.7, 3.8, 3.10, 3.12**). Our results do not support a role for other kinases, i.e., integrin-linked kinase (ILK), MAP kinase-activated protein kinase-2 (MK-2), p38 MAP kinase, protein kinase C (PKCs), NIMA-related kinase-6 (NEK6), double stranded DNA-dependent protein kinase (DNK-PK) and ataxia telangiectasia mutated gene products (73), in Elovl5 regulation of Akt-S^{473} phosphorylation.

We also extended our understanding of the involvement of phosphatases in the Elovl5 control of FoxO1. Both PP2A and MKP-3 remove phosphate from FoxO1; removal of phosphate promotes FoxO1 nuclear accumulation and the induction of GNG (57, 58). Our previous study established that Elovl5 induced PP2Acat-Y^{307} phosphorylation (25) (**Fig. 3.15**); phosphoPP2Acat-Y^{307} is inactive. Herein we establish that inhibition of PP2Acat alone (microcystin-LR) is sufficient to induce FoxO1-S^{256}

phosphorylation ~3-fold. When microcystin-LR inhibition is combined with elevated Elovl5 activity, FoxO1-S^{256} phosphorylation is induced 9-fold. Mechanisms for Elovl5 control of PP2Acat-Y^{307} phosphorylation remain to be established.

Our studies reveal a different role for MKP-3 in the control of Elovl5 and FoxO1. First, Elovl5 does not regulate hepatic MKP-3 protein abundance (**Fig. 3.16**). Moreover, shRNA-knockdown of MKP-3 essentially blocked the Elovl5 regulation of Akt2-S^{473} phosphorylation. As such, MKP-3 knockdown did not augment Elovl5 induction of FoxO1-S^{256} phosphorylation **(Fig. 3.17)**. Whether this outcome reflects MKP-3 control of Elovl5 phosphorylation, per se, or other components in this pathway will require more investigation. Overall, our studies reveal a selective effect of Elovl5 on the control of PP2A, but not MKP-3, in the regulation of FoxO1 and its target genes **(Fig. 3.18)**.

Since Elovl5 increases hepatic $C_{20\text{-}22}$ PUFA in liver and Elovl5 stimulates 18:2,n-6 conversion to $C_{20\text{-}22}$ PUFA (25) (**Fig. 3.18**), an obvious question is whether exogenous fatty acids mimic effects of elevated Elovl5 activity on FoxO1 phosphorylation. Preliminary studies using short term (≤6 hours) treatments with various saturated, mono- and polyunsaturated fatty acids fail to mimic effects with 48 hours of Ad-Elovl5 infection (data not shown). We speculate that Ad-Elovl5 infection channels endogenously generated fatty acids to membrane phospholipids whereas exogenous fatty acids ($\geq$50 μM) are preferentially assimilated into storage lipids (triglycerides

and cholesterol esters). Future studies are required to define how Elovl5 control of membrane lipid content is linked to the regulation of rictor.

In summary, obese and diabetic humans (13, 125-127) and mice (21, 25) display evidence of impaired conversion of C_{18} essential fatty acids to C_{20-22} PUFA, i.e., low plasma ratio of 20:4n-6/18:2n-6. Hepatic Elovl5 expression is attenuated in mice fed high fat-low carbohydrate diets (21, 25). Restoration of Elovl5 activity in livers of obese-diabetic mice lowers hepatic nuclear abundance of FoxO1 through rictor-mTORC2, Akt2, and PP2Acat-dependent mechanisms (**Fig. 3.18**). The consequence of lowering hepatic FoxO1 nuclear abundance is the attenuation of expression of genes involved in GNG and a restoration of euglycemia. Maintenance of blood glucose in euglycemic levels is very important to avoid persistent hyperglycemia related deadly complications. Therefore, results of my studies will eventually be helpful in developing a therapeutic strategy to combat hyperglycemia.

Acknowledgements: The authors thank Dr. Domenico Accili (Columbia University, NYC, NY) for the Ad-ADA-FoxO1 and Dr. Haiyan Xu (Brown Medical School, Providence, RI) for the Ad-shRNA-MKP3-24 and Ad-shRNA-scrambled recombinant adenoviruses used in these studies. This work was supported by the National Institutes of Health grants (DK043220 & DK094600) and the United State Department of Agriculture, National Institute of Food and Agriculture Grant (2009-65200-05846).

Table 3.1. Primers used for qRT-PCR

Gene	Accession No.	Forward	Backward	Species
Elovl5	NM_134382.1	TACCACCATGCCACTATGCT	GACGTGGATGAAGCTGTTGA	Rat
Pck1	NM_002591.3	GGTTCCCAGGGTGCATGAAA	CACGTAGGGTGAATCCGTCAG	Human
G6Pase	NM_138387.3	ATGAGTCTGGTTACTACAGCCA	AAGACAGGGCCGTCATTATGG	Human
mTOR	NM_004958.3	TCTACCACGACAGCCCGGCA	TGGGGGCCCCGTTCCATCAT	Human
Rictor	NM_152756.3	GTCCCGCTGGATCTGACCCGA	GAAGCGCTCGTAGCCCTGCTG	Human
Raptor	NM_020761.2	CGCTTCTGCTGACGGCCACA	TCGCGTCGTTGGCAGCATGT	Human
mTOR	NM_020009.2	CGGGCCTCATTGGCTGGGTG	AACGGCCAGGGAGCGGGTAT	Mouse
Rictor	NM_030168.3	ACCCGGCAGTATGTGCGAGC	ACCTGCCCACGAGCGGAATG	Mouse
Raptor	NM_028898.2	CTGGGCCTTGGCAATATGGCGT	ACTCGCCTGAGGGGCTGCAA	Mouse

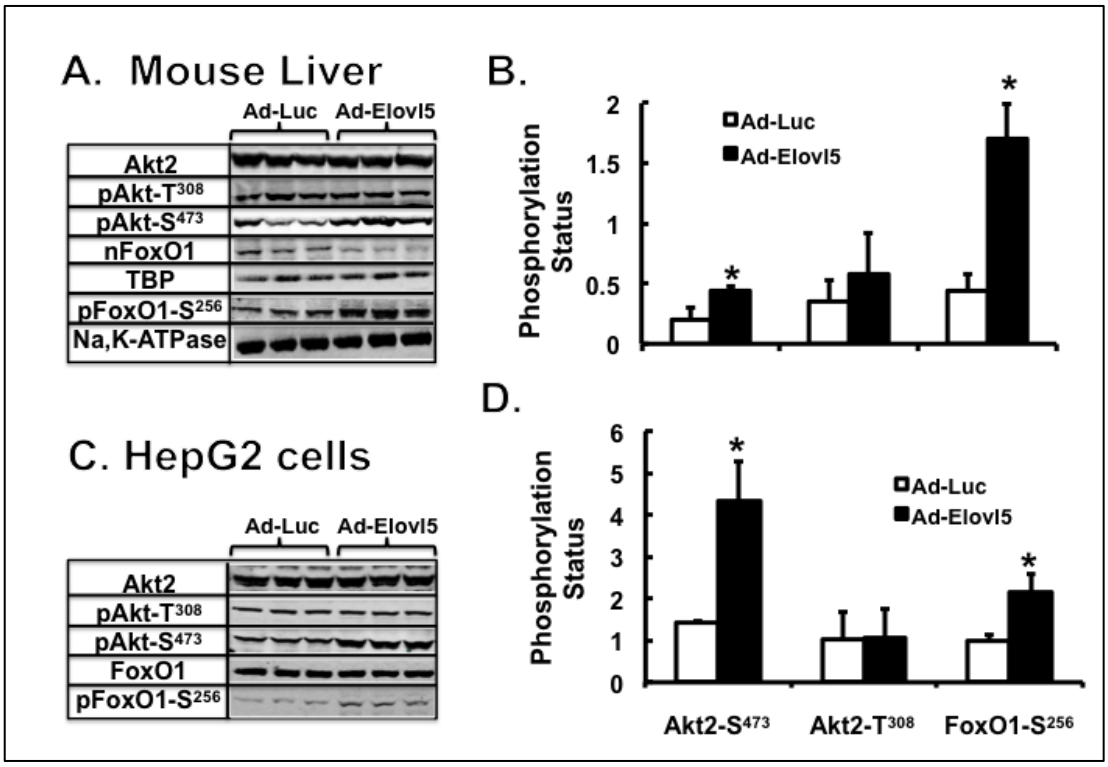

Fig. 3.1. Elovl5 regulates the phosphorylation status of Akt and FoxO1 in mouse liver and HepG2 cells. Panels A & B: Mouse liver extracts from fasted obese-diabetic mice infected with either Ad-Luc or Ad-Elovl5 were prepared and examined for total and phospho-protein abundance. Panel A: Representative immunoblots, n=3 mice per treatment. Panel B: Quantified levels of protein phosphorylation for Akt2-S^{473}, Akt2-T^{308} and FoxO1-S^{256}. Results are from 2 separate studies and are expressed as mean ± SD, n=6. *, $p \leq 0.05$ versus Ad-Luc. Phosphorylation status is based on the ratio of phosphoprotein divided by total protein as quantified by immunoblot and Licor Odyssey software. Panels C and D: HepG2 cells infected with Ad-Luc or Ad-Elovl5 for 48 hours were serum starved overnight. The next day cells were harvested to prepare total cell extracts and quantify levels of total and phospho-Akt and FoxO1. Panel C: Representative immunoblots for total and phospho-Akt2-S^{473}, Akt2-T^{308} and FoxO1-S^{256}. Panel D: Phosphorylation status was quantified as above. Results are representative of 3 separate studies; results are expressed as mean ± SD, n=3. *, $p \leq 0.05$ versus Ad-Luc.

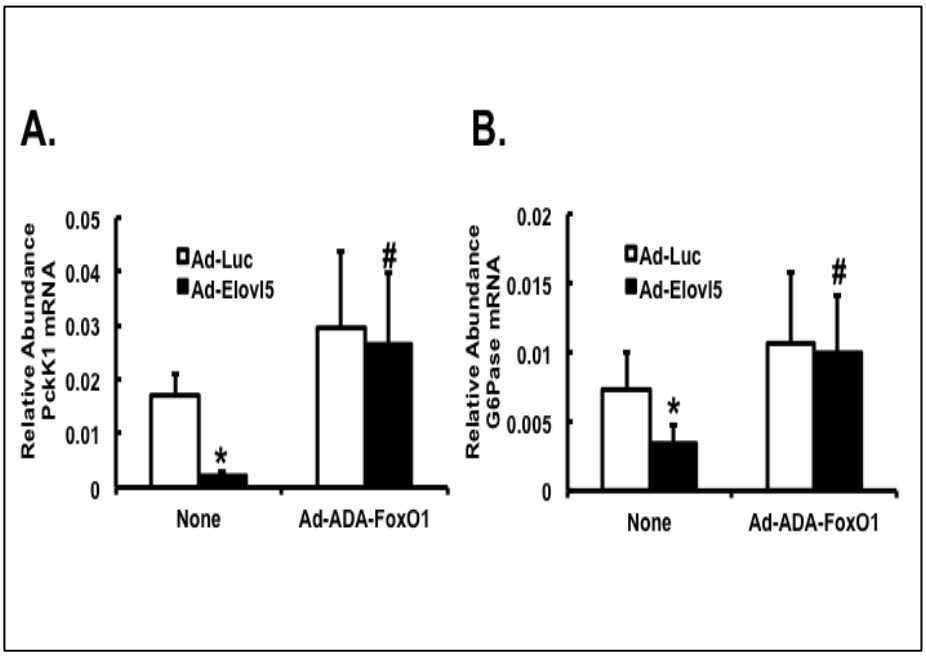

Fig. 3.2. Effects of phosphorylation resistant form of FoxO1 on Elovl5 control of Pck1 and G6Pase expressions in HepG2 cells. HepG2 cells were infected with Ad-Luc (control virus) and Ad-Elovl5 in the absence and presence of Ad-ADA-FoxO1 for 48 hours. ADA-FoxO1 is insensitive to phosphorylation control. Cells were infected for 48 hours and serum-starved overnight and harvested the next day for RNA extraction and quantitation of Pck1 (Panel A), G6Pase (Panel B) and cyclophilin mRNA by qRT-PCR. Results are representative of 3 separate studies; results are expressed as mean ± SD, n=3. *, $p \leq 0.05$ versus Ad-Luc; #, $p \leq 0.05$ versus No Ad-ADA-FoxO1 (None)

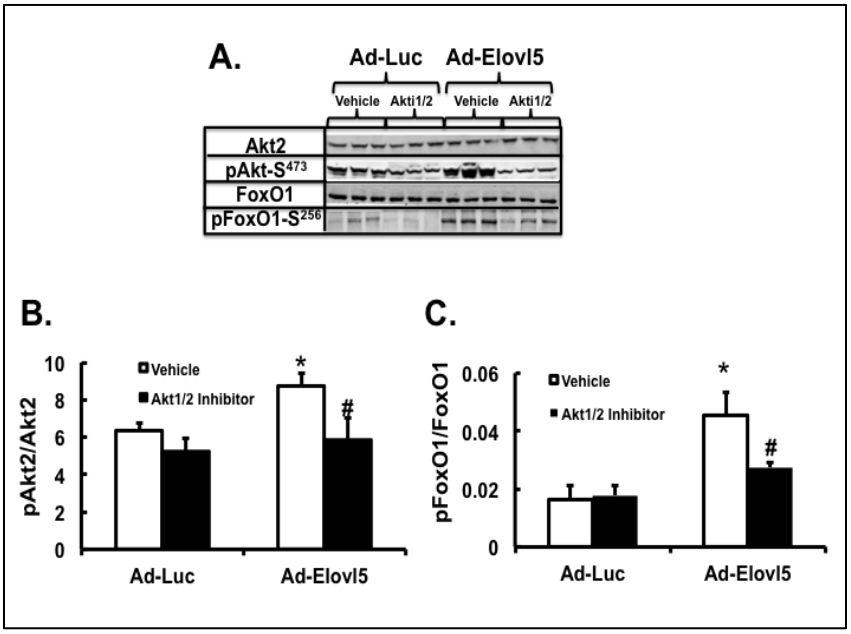

Fig. 3.3. Effect of Akt1/2 inhibitor on Elovl5 control of FoxO1-S^{256} phosphorylation in HepG2 cells. HepG2 cells were infected with Ad-Luc or Ad-Elovl5 for 48 hours and starved overnight as described above in Figs. 3.1 & 3.2. Cells were treated with vehicle (DMSO) or the Akt1/2 inhibitor (Akti1/2, 3μM) for 30 minutes. Proteins were extracted and protein abundance of Akt2, Phospho-Akt1/2/3-S^{473}, FoxO1 and Phospho-FoxO1-S^{256} was measured by immunoblot and Licor Odyssey software. Panel A: Representative Immunoblots, n=3 per treatment; Panel B, Phosphorylation status of Akt2-S^{473}; Panel C, Phosphorylation status of FoxO1-S^{256}. Results are representative of 3 separate studies; results are expressed as mean ± SD, n=3. *, $p \leq 0.05$ versus Ad-Luc; #, $p \leq 0.05$ versus Vehicle.

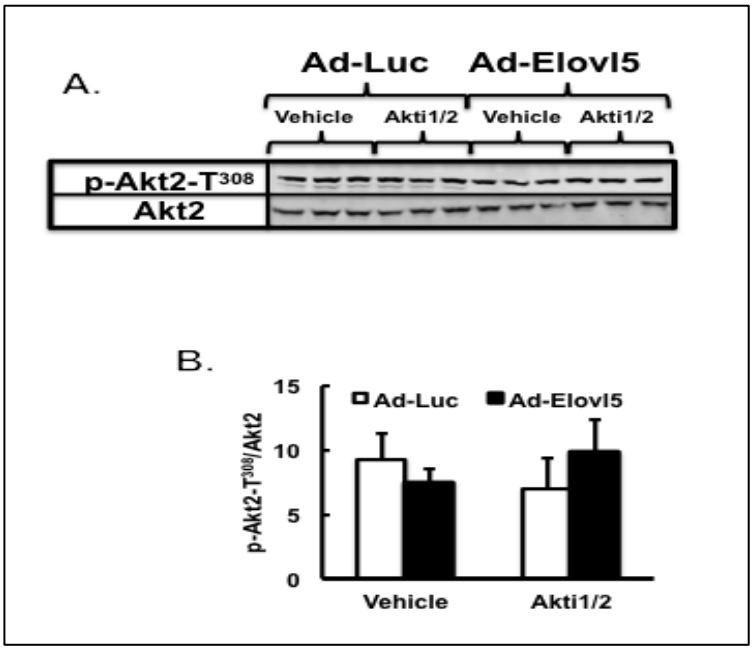

Fig. 3.4. **The effect of the Akt inhibitor (Akti1/2) on Akt-T^{308} phosphorylation status in HepG2 cells.** HepG2 cells were infected with either Ad-Luc or Ad-Elovl5. Forty eight hours later cells were serum starved overnight and treated with DMSO (Vehicle) or Akt1/2 inhibitor [Akti1/2, 3μM] for 30 minutes in the absence of insulin. Cells were harvested for protein extraction and immunoblotting. A) Immunoblot for pAkt-T^{308} and total Akt2. B) Quantitation of immunoblots. Results are representative of 3 separate studies; results are expressed as mean ± SD, n=3.

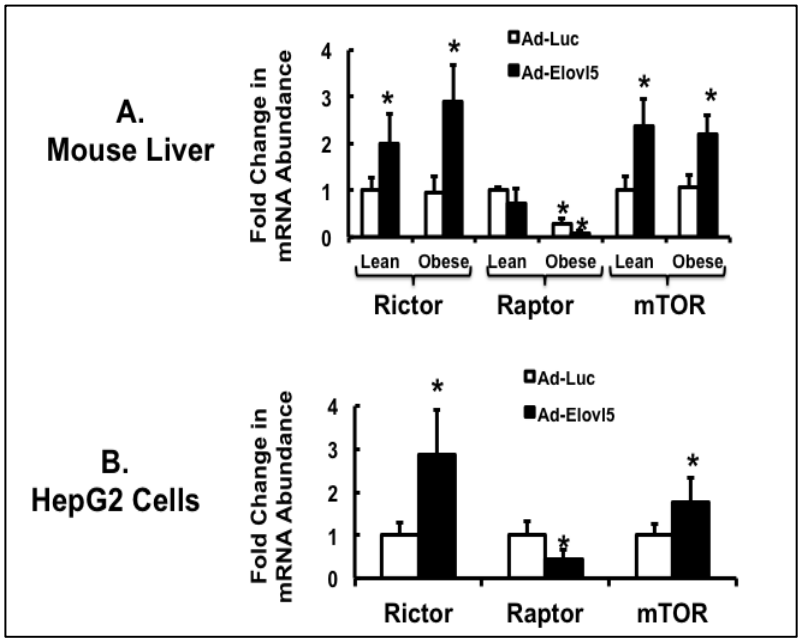

Fig. 3.5. Effects of Elovl5 overexpression on abundance of rictor and mTOR at the pretranslational level in mouse liver and HepG2 cells. Panel A: RNA was extracted from livers of lean and obese mice. mRNA abundance was measured by qRT-PCR using the primers for rictor, raptor, mTOR and cyclophilin. Cyclophilin was used as a house-keeping gene. Panel A: mRNA abundance in livers of lean and obese mice infected with either Ad-Luc or Ad-Elovl5. Results are expressed as Fold Change, relative to the abundance of the mRNA in lean Ad-Luc livers. Results are from 2 separate studies and are expressed as the mean $\pm$ SD, n=6. Panel B: mRNA abundance of HepG2 cells infected with either Ad-Luc or Ad-Elovl5. Results are expressed as Fold Change, relative to the abundance of the mRNA in cells infected with Ad-Luc. Results are representative of 3 separate studies; results are expressed as mean ± SD, n=3. *, $p \leq 0.05$ versus Ad-Luc.

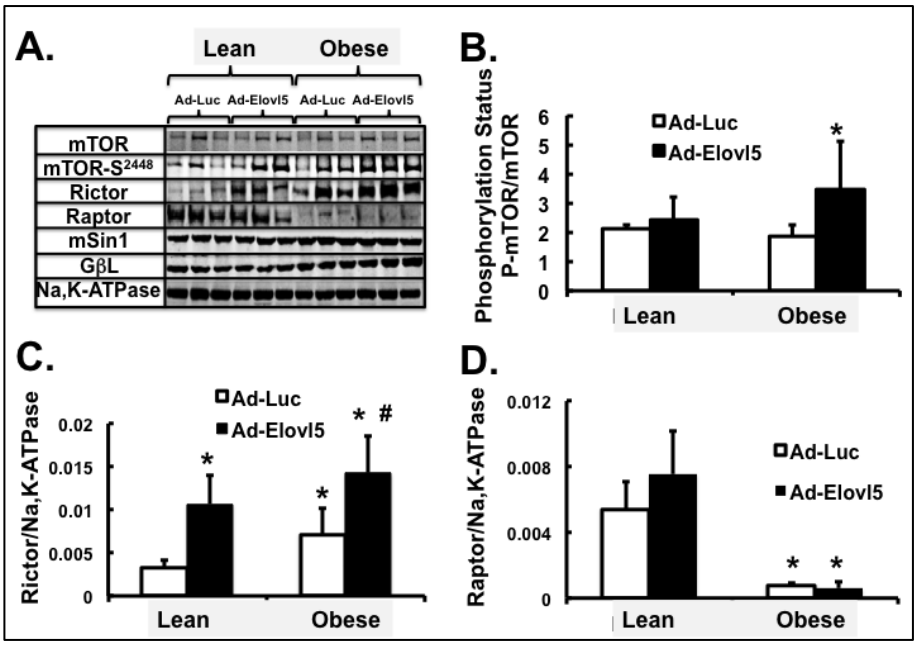

Fig. 3.6. Diet and Elovl5 regulate hepatic mTOR, Rictor and Raptor protein levels in C57BL/6J mice. C57BL/6J mice were fed a low fat (10% calories as fat diet) [Lean] or a high fat (60% calories as fat diet) [Obese] for 12 weeks. Mice were infected with Ad-Luc or Ad-Elovl5 five days prior to termination of the experiment. Five days after infection, mice were fasted overnight and euthanized the next day. Hepatic protein extracts were assayed for protein levels of mTOR, mTOR-S^{2448} phosphorylation, rictor, raptor, mSIN1, GβL and Na,K-ATPase. Panel A: Representative immunoblots, n=3 separate mouse liver extracts per treatment. Panel B: Phosphorylation status of mTOR at S^{2448}. Hepatic protein abundance of rictor (Panel C) and raptor (Panel D). Results are from 2 separate studies and are expressed as mean ± SD, n=6. *, $p \leq 0.05$ versus Lean Ad-Luc; #, $p \leq 0.05$ versus obese, Ad-Luc.

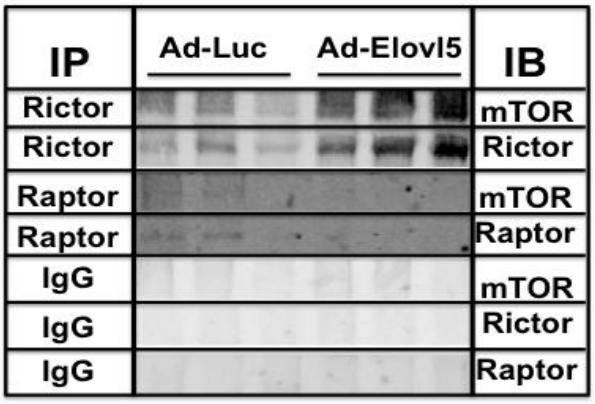

Fig. 3.7. Elovl5 effects on Rictor-mTOR interaction in livers of obese mice. Hepatic extracts from fasted obese C57BL/6J mice infected with Ad-Luc or Ad-Elovl5 (Materials and methods, Fig. 3.6) were treated with antibodies against rictor and raptor. IgG was used as a control for non-specific immunoprecipitation. Immunoprecipitates (IP) were collected and proteins separated for immunoblotting (IB) with antibodies against mTOR, rictor and raptor. The immunoblot data is from hepatic extracts from 3 separate mice infected with either Ad-Luc or Ad-Elovl5 and is representative of 2 separate studies.

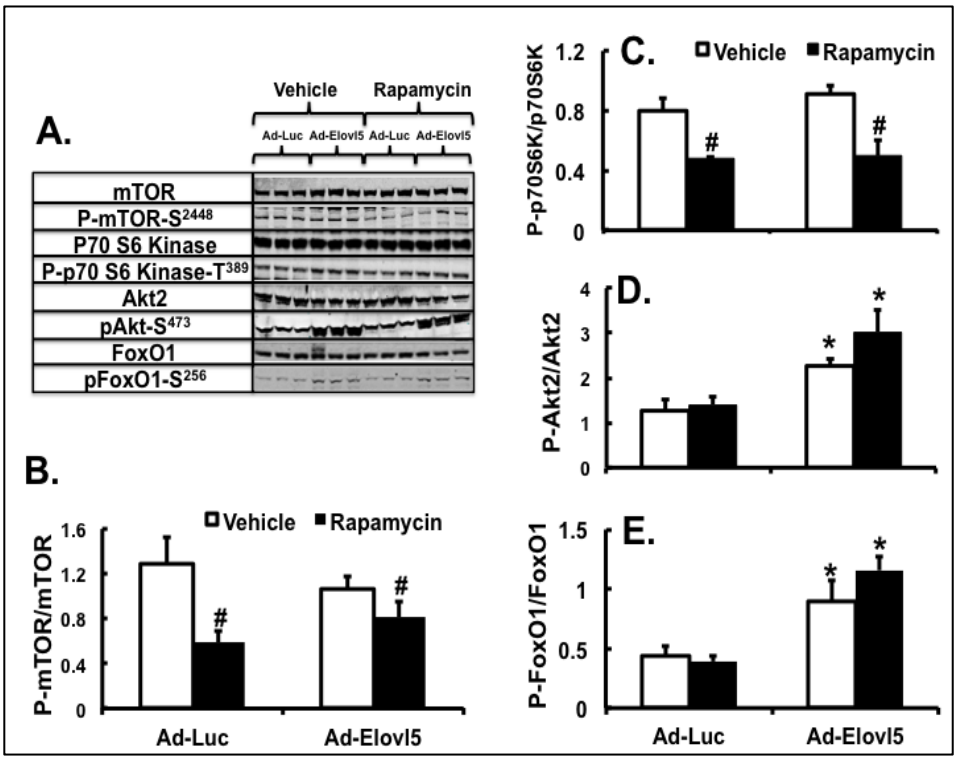

Fig. 3.8. Effects of rapamycin, the mTORC1 inhibitor, on Elovl5 induction of Akt2-S^{473} and FoxO1-S^{256} phosphorylation in HepG2 cells. HepG2 cells were infected with Ad-Luc or Ad-Elovl5 for 48 hours and serum starved overnight. Cells were treated with vehicle (ethanol) or the mTORC1 inhibitor, rapamycin (100 nM) for 30 minutes in the absence of insulin. Proteins were extracted and protein abundance of mTOR, p70S6kinase, phospho-p70S6kinase-T^{389}, phospho-mTOR-S^{2448}, Akt2, phospho-Akt1/2/3-S^{473}, FoxO1 and phospho-FoxO1-S^{256} was measured and quantified as described above. Panel A: Representative immunoblots, 3 cell extracts per treatment. Panels B-E: Phosphorylation status of mTOR-S^{2448}, p70S6 kinase-T^{389}; Akt2-S^{473} and FoxO1-S^{256}, respectively. Results are representative of 3 separate studies; results are expressed as mean ± SD, n=3. *, $p \leq 0.05$ versus Ad-Luc; #, $p \leq 0.05$ versus vehicle.

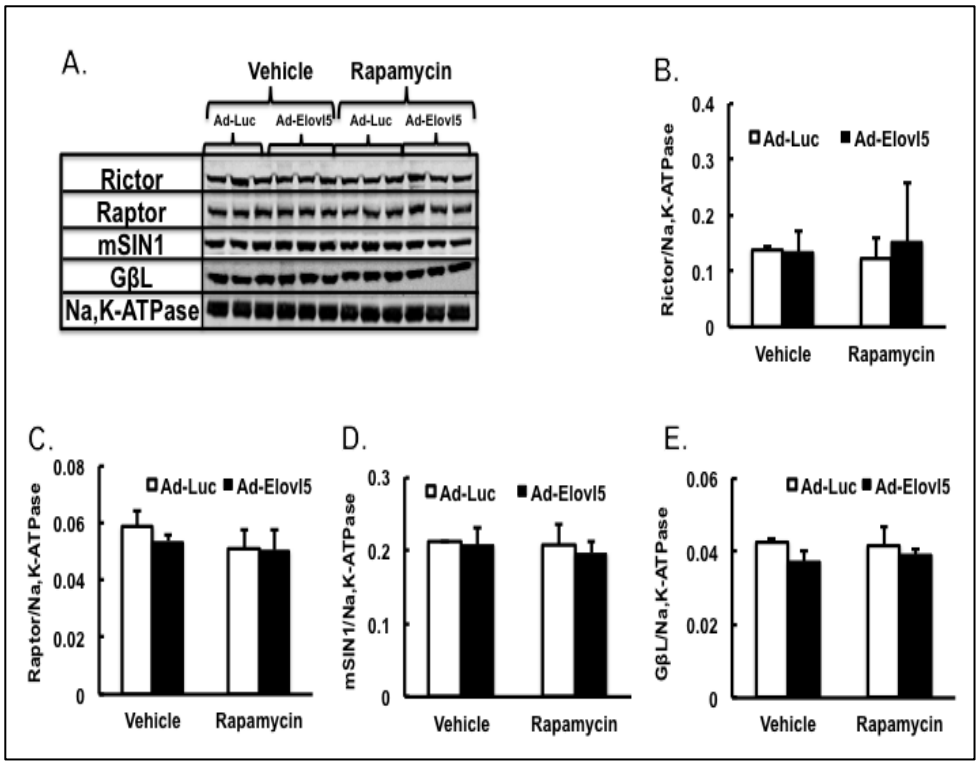

Fig. 3.9. mTORC1 inhibitor (rapamycin) effects on protein abundance of various components of mTORC1 and mTORC2 in HepG2 cells. HepG2 cells were infected with Ad-Luc or Ad-Elovl5. Forty eight hours later cells were serum-starved overnight and then treated with rapamycin (mTORC1 inhibitor, 100 nM for 30 minutes) in the absence of insulin. Whole cell protein extracts were prepared and rictor, raptor, GβL and mSIN1 protein abundance was measured by immunoblotting. A) Immunoblots of rictor, raptor, mSin1, GβL and Na,K-ATPase (loading control). Levels of proteins were quantified and expressed relative to Na,K-ATPase abundance. B) Rictor/Na,K-ATPase; C) Raptor/Na,K-ATPase; D) mSIN1/Na,K-ATPase; E) GβL/Na,K-ATPase. The results are representative of 3 separate studies and are expressed as mean ± SD, n=3.

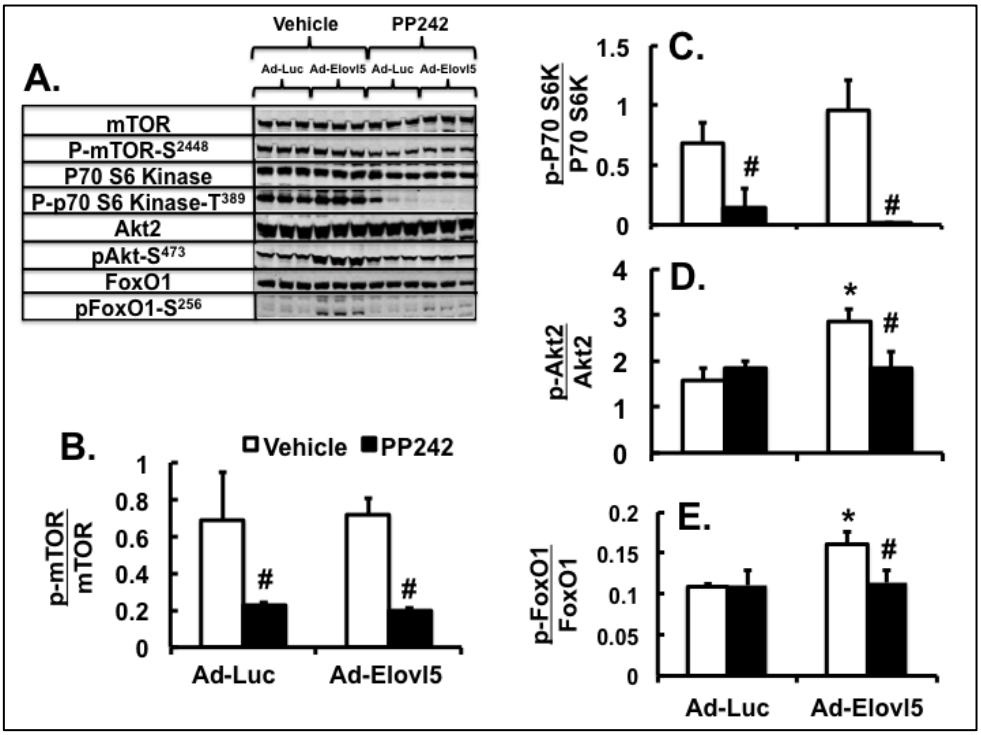

Fig. 3.10. Effects of PP242, the mTORC1 and mTORC2, on Elovl5 control of Akt2-S^{473} and FoxO1-S^{256} phosphorylation in HepG2 cells. HepG2 cells were infected with Ad-Luc or Ad-Elovl5 for 48 hours and serum starved overnight as described above. Cells were treated with vehicle (DMSO) and the mTORC1 and mTORC2 inhibitor, PP242 (500 nM) for 30 minutes in the absence of insulin. Proteins were extracted and the abundance of mTOR, Phospho-mTOR-S^{2448}, p70S6kinase, phospho-p70S6kinase-T^{389}, Akt2, Phospho-Akt1/2/3-S^{473}, FoxO1 and Phospho-FoxO1-S^{256} was quantified as described above. Panel A: Immunoblots, 3 extracts per treatment. Panels B-E: Phosphorylation status of mTOR at S^{2448}, p70 S6 kinase (p70 S6K) at T^{389}; Akt2 at S^{473}, and FoxO1 at S^{256}, respectively. Results are representative of 3 separate studies; results are expressed as mean ± SD, n=3. *, $p \leq 0.05$ versus Ad-Luc; #, $p \leq 0.05$ versus Vehicle.

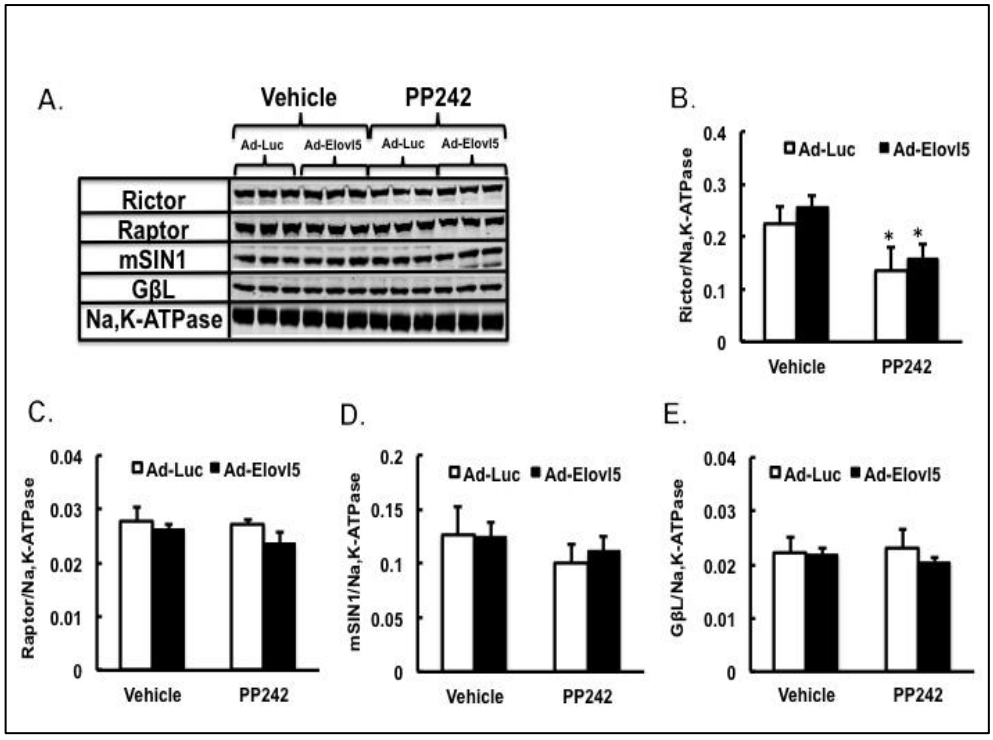

Fig. 3.11. Effects of mTORC1 and mTORC2 inhibitor, PP242, on protein abundance of various components of mTORC1 and mTORC2 in HepG2 cells. HepG2 cells were infected with Ad-Luc or Ad-Elovl5. Forty eight hours later cells were serum-starved overnight and then treated with PP242 (mTORC1 & mTORC2 inhibitor, 500 nM for 30 minutes) in the absence of insulin. Whole cell protein extracts were prepared and rictor, raptor, GβL and mSIN1 protein abundance was measured by immunoblotting. A) Immunoblots of rictor, raptor, mSin1, GβL and Na,K-ATPase (loading control). Levels of proteins were quantified and expressed relative to Na,K-ATPase abundance. B) Rictor/Na,K-ATPase; C) Raptor/Na,K-ATPase; D) mSIN1/Na,K-ATPase; E) GβL/Na,K-ATPase. The results are representative of 3 separate studies and are expressed as mean ± SD, n=3. *, $p \leq 0.05$ versus vehicle.

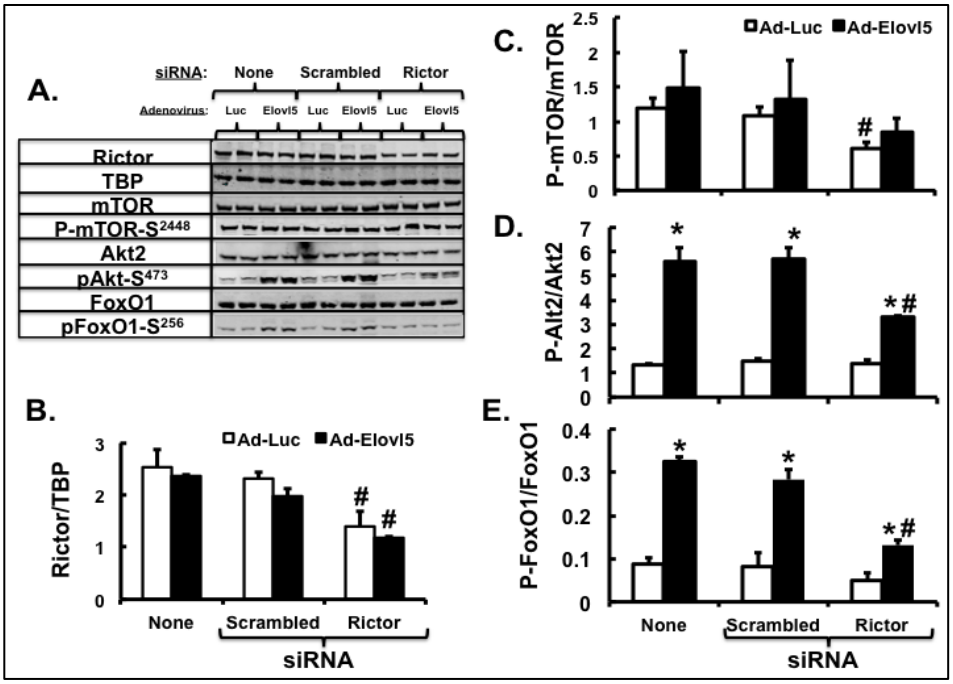

Fig. 3.12. Effects of siRNA knockdown of rictor on Elovl5 control of Akt2-S^{473} and FoxO1-S^{256} phosphorylation in HepG2 cells. HepG2 cells were infected with either Ad-Luc or Ad-Elovl5. Both groups of cells received either no siRNA, scrambled-siRNA or siRNA-Rictor. After 72 hours, cells were serum starved overnight and harvested the next day for protein extraction and immunoblotting. Levels of rictor, Akt2, Phospho-Akt1/2/3-S^{473}, FoxO1, Phospho-FoxO1-S^{256}, mTOR and Phospho-mTOR-S^{2448} and TBP (loading control) were measured as described above. Panel A: Immunoblots, 2 extracts per treatment. Panel B: Rictor protein abundance, Panels C-E: phosphorylation status of mTOR-S^{2448}, Akt2-S^{473} and FoxO1-S^{256}. Results are representative of 3 separate studies; results are expressed as mean ± SD, n=3. *, $p \leq 0.05$ versus Ad-Luc; #, $p \leq 0.05$ versus Ad-Luc + Scrambled siRNA.

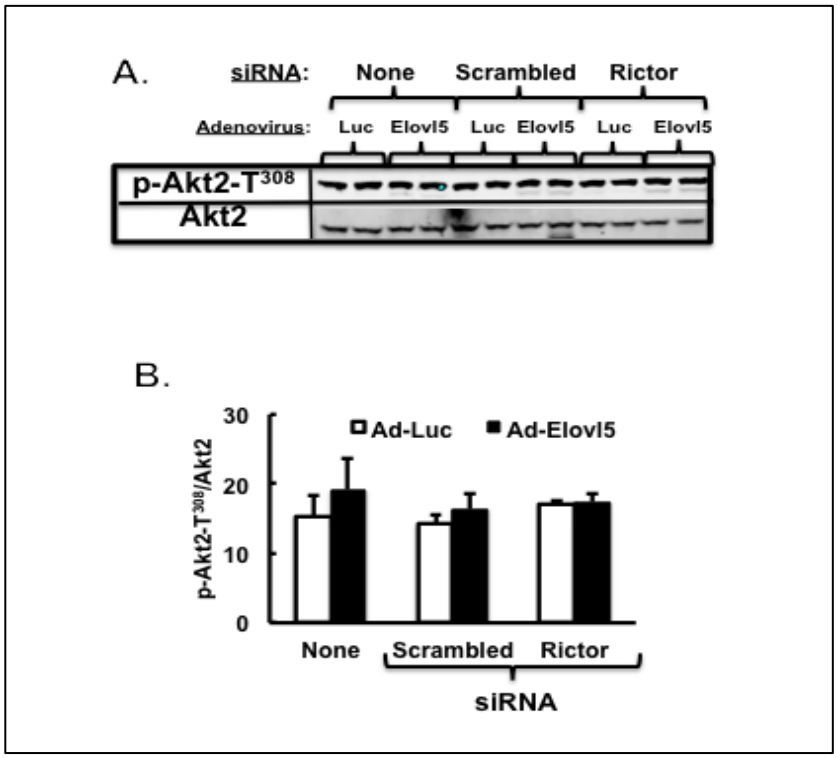

Fig. 3.13. **The effect of siRNA knockdown of rictor on Akt-T^{308} phosphorylation status in HepG2 cells.** HepG2 cells were infected with either Ad-Luc or Ad-Elovl5 in the absence of siRNA or the presence of Scrambled siRNA or Rictor siRNA. After 72 hours, cells were harvested for protein extraction. Immunoblot for p-Akt-T^{308} and total Akt2. B) Quantitation of immunoblots. Results are representative of 3 separate studies and are expressed as mean ± SD, n=3.

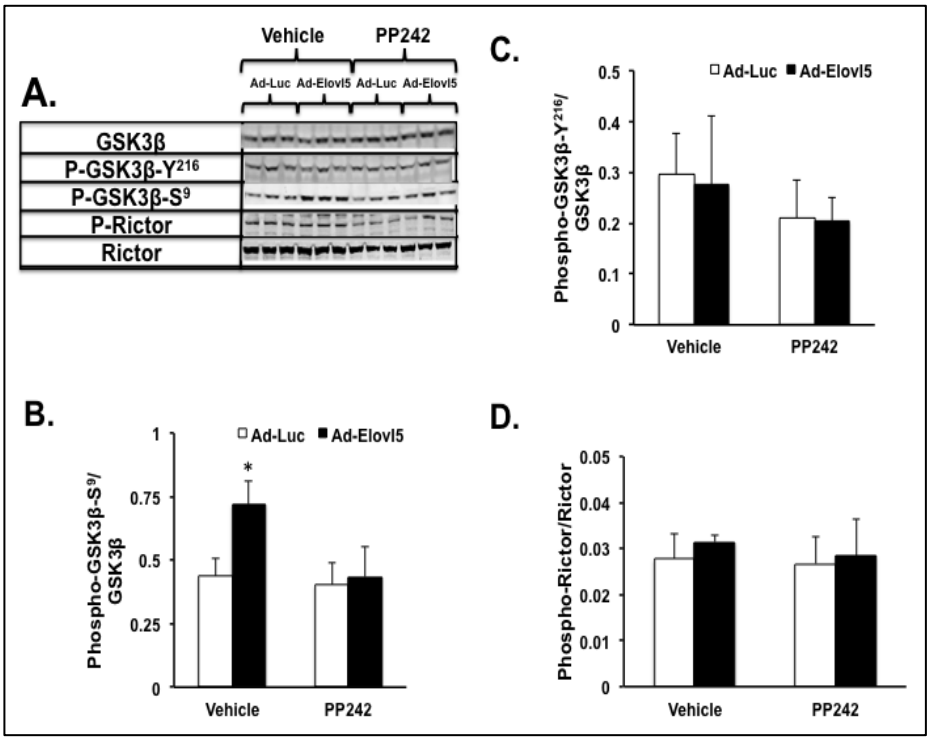

Fig. 3.14. Effects of Elovl5 on rictor phosphorylation in HepG2 cells. HepG2 cells were infected with Ad-Luc or Ad-Elovl5 for 48 hours and serum starved overnight as described above. Cells were treated with vehicle (DMSO) and the mTORC1 and mTORC2 inhibitor, PP242 (500 nM) for 30 minutes in the absence of insulin. Proteins were extracted and the abundance of GSK3β, Phospho-GSK3β-S^9, Phospho-GSK3β-Y^{216}, Rictor and Phospho-Rictor was quantified as described above. Panel A: Immunoblots, 3 extracts per treatment. Panels B-D: Phosphorylation status of GSK3β at S^9, GSK3β at Y^{216}; Rictor espectively. Results are representative of 3 separate studies; results are expressed as mean ± SD, n=3. *, $p \leq 0.05$ versus all other groups.

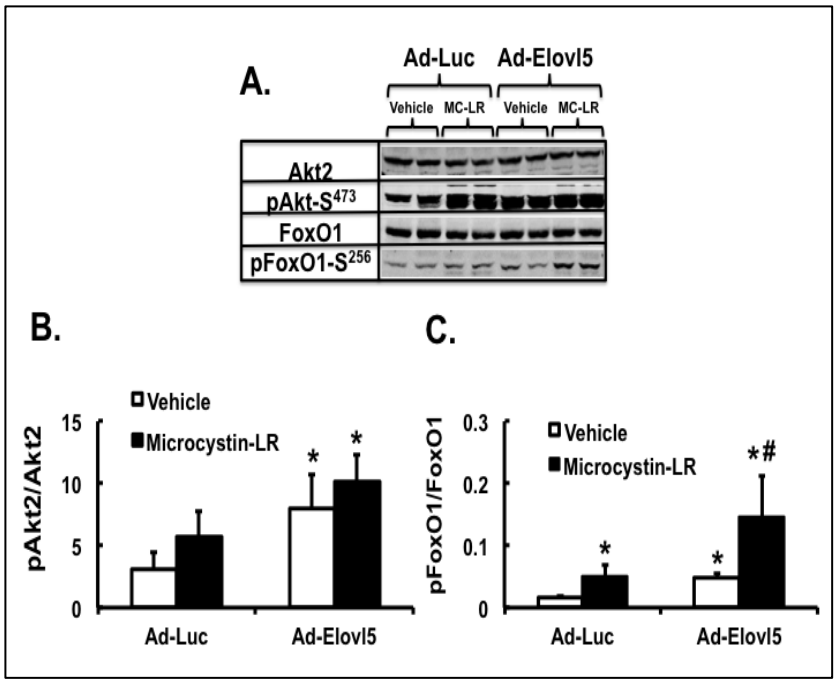

Fig. 3.15. Inhibition of PP2A catalytic unit effects on Elovl5 induction of FoxO1-S^{256} phosphorylation in HepG2 cells. HepG2 cells were infected with Ad-Luc or Ad-Elovl5 as described above. Forty-eight hours after infection, cells were treated with ethanol (Vehicle) or microcystin-LR (PP2A-cat inhibitor, 1 nM) for 30 mins. As above, proteins were extracted and levels of total and phospho-Akt2, and total and phospho-FoxO1-S^{256} were quantified. Panel A: Representative Immunoblots, n=2 per treatment; Panel B: Phosphorylation status of Akt2-S^{473}; Panel C: Phosphorylation status of FoxO1-S^{256}. Results are representative of 3 separate studies; results are expressed as mean ± SD, n=3. *, $p \leq 0.05$ versus Ad-Luc; #, $p \leq 0.05$ versus Vehicle.

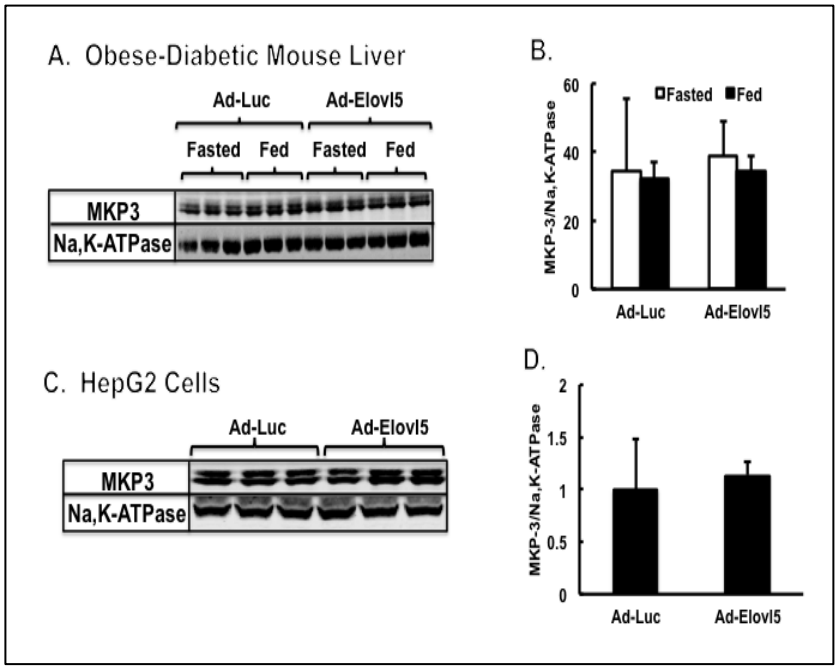

Fig. 3.16. MKP-3 protein abundance in livers of obese-diabetic C57BL/6J mice and in HepG2 cells. Upper Panels [A & B]. Obese-diabetic C57BL/6J mice were fasted (fasted) or fasted and refed (Fed) as described in Methods. Hepatic extracts were assayed for MKP-3 and Na,K-ATPase (loading control) by immunoblotting (A); results are quantified in (B). Results are representative of 2 separate studies and are expressed as mean ± SD, n=6.Lower Panels [C & D]. HepG2 cells were infected with either Ad-Luc or Ad-Elovl5 as described in Methods, serum starved overnight and extracted for total protein. HepG2 whole cell extracts were assayed for MKP-3 and Na,K-ATPase by immunoblot. The results are representative of 3 separate studies and are expressed as mean ± SD, n=3.

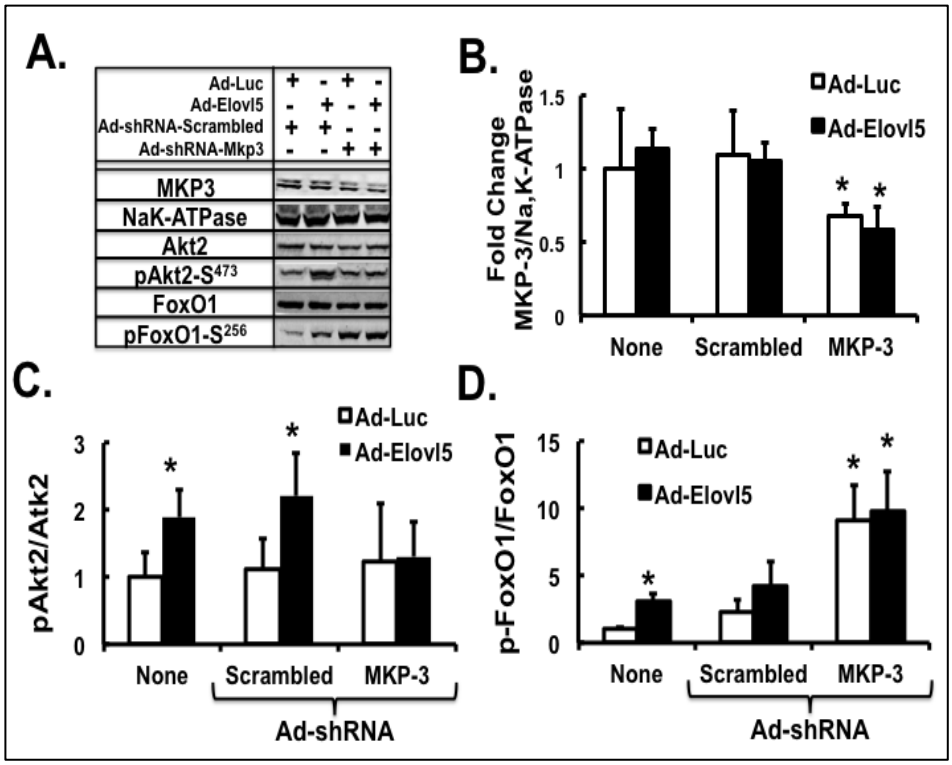

Fig. 3.17. Effects of knockdown of the dual function protein phosphatase MKP-3 on Elovl5 induction of FoxO1-S^{256} phosphorylation in HepG2 cells. HepG2 cells were infected with Ad-Luc or Ad-Elovl5 in the absence or presence of adenovirus expressing shRNA-scrambled or shRNA-MKP3-24. After 48 hours of infection, cells were serum starved overnight. The next day, cells were harvested for protein extraction and quantitation of MKP-3, Na,K-ATPase, Akt2, Phospho-Akt1/2/3-S^{473}, FoxO1 and Phospho-FoxO1-S^{256} by immunoblotting. Panel A: Representative immunoblots; n=1 per treatment. Panel B: MKP-3 protein abundance normalized to the loading control, Na,K-ATPase. Phosphorylation status of Akt2-S^{473} (Panel C) and FoxO1-S^{256} (Panel D). Results are representative of 3 separate studies; results are expressed as mean ± SD, n=3. *, $p \leq 0.05$ versus Ad-Luc + Ad-shRNA-scrambled.

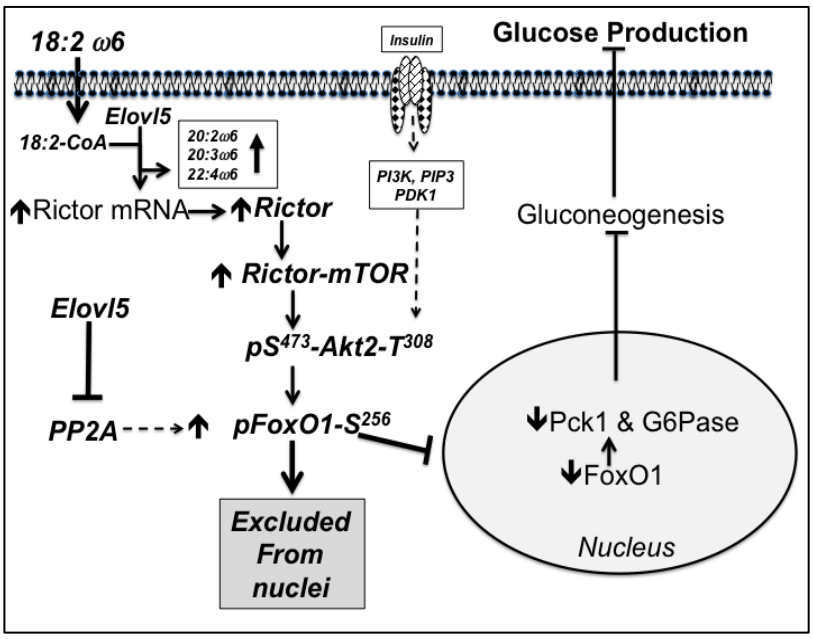

Fig. 3.18. Molecular mechanism for Elovl5 control of FoxO1-S^{256} phosphorylation and hepatic gluconeogenesis. Elovl5 uses two mechanisms to increase FoxO1 phosphorylation such as rictor-Akt mediated increased phosphorylation FoxO1 by induction of rictor and decreased FoxO1 dephosphorylation by inhibition of PP2A. Ultimately, increased phosphorylation of FoxO1 leads to decreased expression of GNG genes such as Pck1 and G6Pase.

Chapter 4

Conclusion

T2DM is a progressive and complex metabolic disorder characterized by persistent hyperglycemia. Presence of chronic hyperglycemia in T2DM further leads to deadly complications such as chronic renal failure, adult blindness, limb amputation, and poses risk for heart disease, stroke, fatty liver diseases and birth defects (1, 2, 7). Thus, maintenance of blood glucose close to normal levels is a major goal for every individual with diabetes. Population studies revealed that individuals with type 2 diabetes have another clinical feature; low tissue and plasma PUFA concentrations, an effect often attributed to impairment in endogenous PUFA synthesis (13, 125, 126, 151-154). Rodent studies from our lab also suggested an inverse link between blood glucose and PUFA synthesis, particularly dependent upon expression and activity of Elovl5, an enzyme involved in endogenous PUFA synthesis pathway (21).

Fatty acids (SFAs, MUFAs and PUFAs) are synthesized endogenously via multiple pathways including *DNL (synthesis of fatty acids from glucose)*, elongation and desaturation (21, 22) with the involvement of enzymes FAS, ACC 1 & 2, SCD-1 and Elovl6 during SFA and MUFA synthesis, and Elovl2, Elovl5, FADS1 and FADS2 during PUFA synthesis (21, 22). Genetic ablation or overexpression studies in rodents have revealed the significance of these enzymes in diabetes and its associated complications (22, 32, 35, 37-39, 44, 155-159). Overall rodent studies suggest that overexpression or increase activity of ACC, FAS, SCD-1 and Elovl6 have detrimental effect from insulin resistance, fatty liver and obesity, whereas, Elovl5 has beneficial effect in

attenuating fatty liver and blood glucose. While, the above studies suggest a possible beneficial role of PUFA synthesis in T2DM and its related complications, none of these studies actually provided confirmatory results on the role of PUFA synthesis in carbohydrate metabolism during T2DM.

Our previous study (22) on the effect of Elovl5 on carbohydrate metabolism identified a possible link between endogenous PUFA synthesis and blood glucose control in C57BL/6J chow fed mice. Over expression of hepatic Elovl5 improved PUFA synthesis, decreased fasting blood glucose and increased hepatic fasting glycogen content in mice fed standard chow diet (22). In addition, elevated hepatic Elovl5 activity increased the phosphorylation of Akt and GSK3β, key components of insulin signaling pathways controlling glucose and glycogen synthesis (22). Thus, this study found key observations that identified the role of Elovl5 in hepatic carbohydrate metabolism.

It is evident that feeding high fat diets to rodents induces obesity, diabetes, hyperglycemia and insulin resistance (21, 22). The fact that Elovl5 activity and expression is suppressed in diabetes raises the question of whether chronic changes in Elovl5 activity contribute to impaired carbohydrate metabolism associated with diet-induced diabetes (21). My preliminary data identified the role of Elovl5 in blood glucose control in normal healthy chow fed mice (22). I further examined the role of Elovl5 or hepatic PUFA synthesis in regulation of blood glucose in the high fat diet induced obese-diabetic C57BL/6J mouse model. Briefly, C57BL/6J mice fed a high fat diet for 12

weeks were obese-hyperglycemic and developed insulin resistance and fatty liver (25). They had low hepatic levels of C_{20-22} PUFAs, particularly, C20:2,n-6, C20:3,n-6, C22:4,n-6, and C22:3,n-3 fatty acids which are mainly generated through endogenous PUFA synthesis pathways. The low levels of these hepatic C_{20-22} PUFAs were significantly associated with decreased expression and activity of Elovl5, whereas, other enzymes in that pathway such as FADS1, FADS2 and Elovl2 were unaffected by high fat diet. Moreover, in these mice, over expression of Elovl5 by recombinant adenovirus increased hepatic Elovl5 activity by 2-3 fold in 5 days. Elevated hepatic Elovl5 activity increased the hepatic contents of C_{20-22} PUFAs, an indication of improved endogenous PUFA synthesis, and decreased the fasting blood glucose to normal level without having any effect on body weight and food intake (25). Thus, my studies provided strong evidence that Elovl5 corrects high fat diet induced hyperglycemia in obese-diabetic mice. The control of blood glucose by Elovl5 was linked to increased phosphorylation of hepatic FoxO1-S^{256}, Akt-S^{473} and PP2A-Y^{307}, and decreased expression of key regulators of GNG and glucose production enzymes such as Pck1 and G6Pase (25). Active Akt (phospho-Akt) phosphorylates FoxO1 leading to its exclusion from nuclei, ubiquitination and proteasomal degradation (25, 57, 62-65). The suppression of nuclear FoxO1 abundance results in down regulation of Pck1 and G6Pase and the suppression of GNG and glucose production (25). Elevated hepatic Elovl5 increased phosphorylation of PP2A-cat-Y^{307}, which has been linked to

decreased phosphatase activity of Akt and FoxO1 (57). This event leads to increased phosphorylation of FoxO1 and promotes its proteosomal degradation. Elevated hepatic Elovl5 activity had no impact on other transcription factors involved in GNG including CREB, CRTC2, PPARα and HNF4α. Thus, this study suggested that the insulin mimetic effect of Elovl5 on GNG and hepatic glucose production involves multiple components such as FoxO1, Akt and PP2A (25).

My second goal was to define the molecular mechanism regulating Elovl5 mediated FoxO1 control of GNG signaling pathway. I selected HepG2 cells to define the GNG pathway because 1) HepG2 cells are insulin responsive cell line and used as an alternative to primary hepatocytes and 2) Elovl5 over-expression in HepG2 cells recapitulated our in vivo obese-diabetic mice observations such as increased Akt-S^{473} and FoxO1-S^{256} phosphorylation. Further examination of Akt-FoxO1 pathway by using obese-diabetic mouse liver extracts and HepG2 cells protein extracts revealed that elevated hepatic Elovl5 selectively increased Akt2 phosphorylation at S^{473} site (mTORC2 site) and has no impact on phosphorylation at T^{308} site (PI3-kinase-PDK1 pathway targeted site). This observation correlates with the data we have reported that elevated Elovl5 activity has no effect on phosphorylation status of components upstream of Akt, i.e., IRS1/2 (insulin receptor substrate 1-2) and PDK1/2 (phosphoinositide-dependent kinase 1-2) **(Fig. 2.6)**. Akt-S^{473} site is a target of mTORC2 (76, 133). Thus, I have determined the involvement

of mTORC2 pathway in the Elovl5 regulation of Akt2-S^{473} and FoxO1-S^{256} phosphorylation by using chemical inhibitors and siRNA knock down approach in HepG2 cells. Phosphatases such as PP2A (25) and MKP-3 (58) are reported as the regulators of FoxO1 phosphorylation. As such, I used a chemical inhibitor for PP2A inhibition and shRNA mediated knock down approach to knock down MKP-3 for the assessment of the MKP-3 role in Elovl5 mediated Akt-S^{473} and FoxO1-S^{256} phosphorylation in HepG2 cells. Thus, my mechanistic studies defined the requirement for FoxO1-S^{256} & Akt2-S^{473} phosphorylation, mTORC2 pathway and PP2A inhibition in Elovl5 mediated suppression of GNG genes.

Briefly, the results of my mechanistic studies discussed in chapter 3 showed that treatment of HepG2 cells with adenovirus expressing a phosphorylation resistant form of FoxO1 (ADA-FoxO1; a form does not get phosphorylated, resides in nucleus and promotes GNG gene expression) and chemical inhibitor of Akt1/2 (chemical inhibitor of Akt decreases Akt phosphorylation) confirmed that Elovl5 control of FoxO1-S^{256} phosphorylation requires Akt2-S^{473} and Elovl5 mediated suppression of GNG genes requires FoxO1-S^{256} phosphorylation. To assess the involvement of mTOR pathway, I measured the phosphorylation status of mTOR and protein abundance of various components of mTORC1 and mTORC2 in our obese-diabetic mouse liver extracts. My data showed that elevated Elovl5 activity increased phosphorylation of mTOR and increased the mRNA and protein content of

rictor, the regulatory component of mTORC2, but suppressed mRNA expression of raptor, the regulatory component of mTORC1. We have further shown that elevated Elovl5 hepatic activity promoted rictor-mTOR association. mTOR binding with rictor is essential for mTORC2 complex stability and mTOR kinase activity in mTORC2 regulated signaling pathways (133, 138). Thus, our results provided strong evidence that supports a role for the mTORC2 pathway in Elovl5 mediated Akt-S^{473} and FoxO1-S^{256} phosphorylation. HepG2 cells treated with mTORC1 and mTORC2 inhibitor, PP242 or mTORC1 inhibitor, rapamycin showed that PP242, but not rapamycin, blocked Elovl5 regulated Akt2-S^{473} and FoxO1-S^{256} phosphorylation, confirming the role of mTORC2 pathway in Elovl5 mediated Akt-S^{473} and FoxO1-S^{256} phosphorylation. Transient knockdown of rictor attenuated the Elovl5 mediated increase in Akt2-S^{473} and FoxO1-S^{256} phosphorylation in HepG2 cells, establishing rictor is the target of Elovl5 for the inhibition of GNG.

To assess the involvement of PP2A and MKP-3 on Elovl5 control of FoxO1-S^{256} phosphorylation, a chemical inhibitor, microcystin-LR or an adenovirus expressing sh-MKP3, respectively were used in HepG2 cells. These studies revealed that PP2A inhibition synergistically increased FoxO1-S^{256} phosphorylation and had no impact on Elovl5 induction of Akt2-S^{473} phosphorylation. Transient knockdown of MKP-3 showed that reduction in MKP-3 protein abundance in HepG2 cells significantly increased FoxO1-S^{256}

phosphorylation, but did not increase Elovl5 induction of FoxO1-S^{256} phosphorylation.

While studies in the present work confirmed and established that elevated Elovl5 activity corrects high fat diet induced hyperglycemia in mice via rictor-Akt-FoxO1 pathway, many questions still remain unanswered. We have observed that over-expression of Elovl5 increased rictor mRNA and protein abundance and mTOR-rictor association; required events for Akt-S^{473} phosphorylation. But these data did not show how a change in hepatic Elovl5 activity increases rictor mRNA abundance. More studies are needed to identify the molecular mechanism through which Elovl5 increases rictor mRNA abundance. FoxO1 control of GNG involves many covalent modifications such as phosphorylation, acetylation and O-linked-β-N-acetyl-glucosamine. Studies described here only addressed the role of FoxO1 phosphorylation in Elovl5 control of GNG genes. Future studies are very essential to evaluate the role of other covalent modifications such as acetylation, O-linked-β-N-acetyl-glucosamine of FoxO1 in GNG. Another important question that must be addressed is the role of exogenous PUFA in suppression of GNG similar to that of Elovl5. Although preliminary studies showed that exogenous PUFA did not suppress GNG, more studies are required to have clear answer about the differential effect of dietary PUFA and Elovl5 in control of GNG. A membrane phospholipid analysis can answer this question. Therefore, future studies will be directed towards membrane phospholipid analysis.

In conclusion, the present work established a critical role of Elovl5 in correcting high fat diet induced fasting hyperglycemia in C57BL/6J mice. Results presented in the various studies above have shown the role of mTORC2-Akt-FoxO1 pathway in Elovl5 mediated suppression of GNG and hepatic glucose production in diet induced obese-diabetic mouse model. Elovl5 utilizes two mechanisms to control GNG, FoxO1 phosphorylation and its nuclear abundance **(refer Fig. 3.18)**. The first mechanism involves Elovl5 mediated increase in Akt2-S^{473} and FoxO1-S^{256} phosphorylation via mTORC2/rictor pathway, whereas the second mechanism involves Elovl5 mediated attenuation of de-phosphorylation of FoxO1 via PP2A inhibition. Together, these mechanisms increase FoxO1 phosphorylation status in livers of fasted obese mice, which lowers hepatic FoxO1 nuclear abundance and FoxO1 capacity to sustain transcription of GNG genes. The dual mechanism (increased phosphorylation, inhibited de-phosphorylation) controlling Akt2 and FoxO1 phosphorylation status explains how elevated hepatic PUFA synthesis (Elovl5) inhibits GNG and restores blood glucose levels in fasted obese mice. The molecular mechanism of Elovl5/PUFA synthesis control of GNG in obese-diabetic mice identified in this work will certainly be helpful in developing a therapeutic target to combat hyperglycemia.

Bibliography

1. Doria, A., Patti, M.E., and Kahn, C.R. 2008. The emerging genetic architecture of type 2 diabetes. *Cell Metabolism* 8:186-200.
2. Cusi, K. 2009. Nonalcoholic fatty liver disease in type 2 diabetes mellitus. *Current Opinion in Endocrinology, Diabetes and Obesity* 16:141-149.
3. Leavens, K.F., and Birnbaum, M.J. 2011. Insulin signaling to hepatic lipid metabolism in health and disease. *Critical Reviews in Biochemistry and Molecular Biology* 46:200-215.
4. Parekh, S., and Anania, F.A. 2007. Abnormal lipid and glucose metabolism in obesity: implications for nonalcoholic fatty liver disease. *Gastroenterology* 132:2191-2207.
5. Biddinger, S.B., and Kahn, C.R. 2006. From mice to men: insights into the insulin resistance syndromes. *Annual Review of Physiology* 68:123-158.
6. Xie, J., and Herbert, T.P. 2012. The role of mammalian target of rapamycin (mTOR) in the regulation of pancreatic beta-cell mass: implications in the development of type-2 diabetes. *Cellular and Molecular Life Sciences* 69:1289-1304.

7. Ali, T.K., and El-Remessy, A.B. 2009. Diabetic retinopathy: current management and experimental therapeutic targets. *Pharmacotherapy* 29:182-192.

8. Qian, H., and Ripps, H. 2011. Neurovascular interaction and the pathophysiology of diabetic retinopathy. *Experimental Diabetes Research* 2011:693426.

9. Madsen-Bouterse, S.A., and Kowluru, R.A. 2008. Oxidative stress and diabetic retinopathy: pathophysiological mechanisms and treatment perspectives. *Reviews in Endocrinology and Metabolic Disorder* 9:315-327.

10. Harris, W.S., Mozaffarian, D., Rimm, E., Kris-Etherton, P., Rudel, L.L., Appel, L.J., Engler, M.M., Engler, M.B., and Sacks, F. 2009. Omega-6 fatty acids and risk for cardiovascular disease: a science advisory from the American Heart Association Nutrition Subcommittee of the Council on Nutrition, Physical Activity, and Metabolism; Council on Cardiovascular Nursing; and Council on Epidemiology and Prevention. *Circulation* 119:902-907.

11. Hartweg, J., Perera, R., Montori, V., Dinneen, S., Neil, H.A., and Farmer, A. 2008. Omega-3 polyunsaturated fatty acids (PUFA) for type 2 diabetes mellitus. *Cochrane Database of Systematic Reviews*:CD003205.

12. Jump, D.B. 2008. N-3 polyunsaturated fatty acid regulation of hepatic gene transcription. *Current Opinion in Lipidology* 19:242-247.

13. Warensjo, E., Riserus, U., Gustafsson, I.B., Mohsen, R., Cederholm, T., and Vessby, B. 2008. Effects of saturated and unsaturated fatty acids on estimated desaturase activities during a controlled dietary intervention. *Nutrition, Metabolism and Cardiovascular Diseases* 18:683-690.

14. Fernandez-Real, J.M., Broch, M., Vendrell, J., and Ricart, W. 2003. Insulin resistance, inflammation, and serum fatty acid composition. *Diabetes Care* 26:1362-1368.

15. Kotronen, A., Seppanen-Laakso, T., Westerbacka, J., Kiviluoto, T., Arola, J., Ruskeepaa, A.L., Yki-Jarvinen, H., and Oresic, M. 2010. Comparison of lipid and fatty acid composition of the liver, subcutaneous and intra-abdominal adipose tissue, and serum. *Obesity (Silver Spring)* 18:937-944.

16. Sjogren, P., Sierra-Johnson, J., Gertow, K., Rosell, M., Vessby, B., de Faire, U., Hamsten, A., Hellenius, M.L., and Fisher, R.M. 2008. Fatty acid desaturases in human adipose tissue: relationships between gene expression, desaturation indexes and insulin resistance. *Diabetologia* 51:328-335.

17. Martin de Santa Olalla, L., Sanchez Muniz, F.J., and Vaquero, M.P. 2009. N-3 fatty acids in glucose metabolism and insulin sensitivity. *Nutricion Hospitalaria* 24:113-127.

18. Mustad, V.A., Demichele, S., Huang, Y.S., Mika, A., Lubbers, N., Berthiaume, N., Polakowski, J., and Zinker, B. 2006. Differential effects of n-3 polyunsaturated fatty acids on metabolic control and vascular reactivity in the type 2 diabetic ob/ob mouse. *Metabolism: Clinical and Experimental* 55:1365-1374.

19. Jump, D.B. 2002. The biochemistry of n-3 polyunsaturated fatty acids. *Journal of Biological Chemistry* 277:8755-8758.

20. Wang, Y., Botolin, D., Christian, B., Busik, J., Xu, J., and Jump, D.B. 2005. Tissue-specific, nutritional, and developmental regulation of rat fatty acid elongases. *Journal of Lipid Research* 46:706-715.

21. Wang, Y., Botolin, D., Xu, J., Christian, B., Mitchell, E., Jayaprakasam, B., Nair, M.G., Peters, J.M., Busik, J.V., Olson, L.K., et al. 2006. Regulation of hepatic fatty acid elongase and desaturase expression in diabetes and obesity. *Journal of Lipid Research* 47:2028-2041.

22. Wang, Y., Torres-Gonzalez, M., Tripathy, S., Botolin, D., Christian, B., and Jump, D.B. 2008. Elevated hepatic fatty acid elongase-5 activity affects multiple pathways controlling hepatic lipid and carbohydrate composition. *Journal of Lipid Research* 49:1538-1552.

23. Jump, D.B., Torres-Gonzalez, M., and Olson, L.K. 2011. Soraphen A, an inhibitor of acetyl CoA carboxylase activity, interferes with fatty acid elongation. *Biochemical Pharmacology* 81:649-660.

24. Jump, D.B. 2009. Mammalian Fatty Acid elongases. *Methods in Molecular Biology* 579:375-389.

25. Tripathy, S., Torres-Gonzalez, M., and Jump, D.B. 2010. Elevated hepatic fatty acid elongase-5 activity corrects dietary fat-induced hyperglycemia in obese C57BL/6J mice. *Journal of Lipid Research* 51:2642-2654.

26. Pawar, A., and Jump, D.B. 2003. Unsaturated fatty acid regulation of peroxisome proliferator-activated receptor alpha activity in rat primary hepatocytes. *Journal of Biological Chemistry* 278:35931-35939.

27. Botolin, D., Wang, Y., Christian, B., and Jump, D.B. 2006. Docosahexaneoic acid (22:6,n-3) regulates rat hepatocyte SREBP-1 nuclear abundance by Erk- and 26S proteasome-dependent pathways. *Journal of Lipid Research* 47:181-192.

28. Chinetti-Gbaguidi, G., Fruchart, J.C., and Staels, B. 2005. Role of the PPAR family of nuclear receptors in the regulation of metabolic and cardiovascular homeostasis: new approaches to therapy. *Current Opinion in Pharmacology* 5:177-183.

29. Kalaany, N.Y., Gauthier, K.C., Zavacki, A.M., Mammen, P.P., Kitazume, T., Peterson, J.A., Horton, J.D., Garry, D.J., Bianco, A.C., and

Mangelsdorf, D.J. 2005. LXRs regulate the balance between fat storage and oxidation. *Cell Metabolism* 1:231-244.

30. Kakuma, T., Lee, Y., Higa, M., Wang, Z., Pan, W., Shimomura, I., and Unger, R.H. 2000. Leptin, troglitazone, and the expression of sterol regulatory element binding proteins in liver and pancreatic islets. *Proceedings of the National Academy of Sciences of the United States of America* 97:8536-8541.

31. Towle, H.C. 2005. Glucose as a regulator of eukaryotic gene transcription. *Trends in Endocrinology and Metabolism* 16:489-494.

32. Abu-Elheiga, L., Matzuk, M.M., Kordari, P., Oh, W., Shaikenov, T., Gu, Z., and Wakil, S.J. 2005. Mutant mice lacking acetyl-CoA carboxylase 1 are embryonically lethal. *Proceedings of the National Academy of Sciences of the United States of America* 102:12011-12016.

33. Mao, J., DeMayo, F.J., Li, H., Abu-Elheiga, L., Gu, Z., Shaikenov, T.E., Kordari, P., Chirala, S.S., Heird, W.C., and Wakil, S.J. 2006. Liver-specific deletion of acetyl-CoA carboxylase 1 reduces hepatic triglyceride accumulation without affecting glucose homeostasis. *Proceedings of the National Academy of Sciences of the United States of America* 103:8552-8557.

34. Oh, W., Abu-Elheiga, L., Kordari, P., Gu, Z., Shaikenov, T., Chirala, S.S., and Wakil, S.J. 2005. Glucose and fat metabolism in adipose tissue of acetyl-CoA carboxylase 2 knockout mice. *Proceedings of the*

National Academy of Sciences of the United States of America 102:1384-1389.

35. Abu-Elheiga, L., Oh, W., Kordari, P., and Wakil, S.J. 2003. Acetyl-CoA carboxylase 2 mutant mice are protected against obesity and diabetes induced by high-fat/high-carbohydrate diets. *Proceedings of the National Academy of Sciences of the United States of America* 100:10207-10212.

36. Miyazaki, M., Flowers, M.T., Sampath, H., Chu, K., Otzelberger, C., Liu, X., and Ntambi, J.M. 2007. Hepatic stearoyl-CoA desaturase-1 deficiency protects mice from carbohydrate-induced adiposity and hepatic steatosis. *Cell Metabolism* 6:484-496.

37. Flowers, M.T., Miyazaki, M., Liu, X., and Ntambi, J.M. 2006. Probing the role of stearoyl-CoA desaturase-1 in hepatic insulin resistance. *Journal of Clinical Investigation* 116:1478-1481.

38. Brown, J.M., Chung, S., Sawyer, J.K., Degirolamo, C., Alger, H.M., Nguyen, T., Zhu, X., Duong, M.N., Wibley, A.L., Shah, R., et al. 2008. Inhibition of stearoyl-coenzyme A desaturase 1 dissociates insulin resistance and obesity from atherosclerosis. *Circulation* 118:1467-1475.

39. Matsuzaka, T., Shimano, H., Yahagi, N., Kato, T., Atsumi, A., Yamamoto, T., Inoue, N., Ishikawa, M., Okada, S., Ishigaki, N., et al. 2007. Crucial role of a long-chain fatty acid elongase, Elovl6, in obesity-induced insulin resistance. *Nature Medicine* 13:1193-1202.

40. Murakami, K., Sasaki, S., Takahashi, Y., Uenishi, K., Watanabe, T., Kohri, T., Yamasaki, M., Watanabe, R., Baba, K., Shibata, K., et al. 2008. Lower estimates of delta-5 desaturase and elongase activity are related to adverse profiles for several metabolic risk factors in young Japanese women. *Nutrition Research* 28:816-824.

41. Salomaa, V., Ahola, I., Tuomilehto, J., Aro, A., Pietinen, P., Korhonen, H.J., and Penttila, I. 1990. Fatty acid composition of serum cholesterol esters in different degrees of glucose intolerance: a population-based study. *Metabolism: Clinical and Experimental* 39:1285-1291.

42. Hulbert, A.J., Turner, N., Storlien, L.H., and Else, P.L. 2005. Dietary fats and membrane function: implications for metabolism and disease. *Biological Reviews of the Cambridge Philosophical Society* 80:155-169.

43. Hall, D., Poussin, C., Velagapudi, V.R., Empsen, C., Joffraud, M., Beckmann, J.S., Geerts, A.E., Ravussin, Y., Ibberson, M., Oresic, M., et al. 2010. Peroxisomal and microsomal lipid pathways associated with resistance to hepatic steatosis and reduced pro-inflammatory state. *Journal of Biological Chemistry* 285:31011-31023.

44. Moon, Y.A., Hammer, R.E., and Horton, J.D. 2009. Deletion of ELOVL5 leads to fatty liver through activation of SREBP-1c in mice. *Journal of Lipid Research* 50:412-423.

45. Stroud, C.K., Nara, T.Y., Roqueta-Rivera, M., Radlowski, E.C., Lawrence, P., Zhang, Y., Cho, B.H., Segre, M., Hess, R.A., Brenna,

J.T., et al. 2009. Disruption of FADS2 gene in mice impairs male reproduction and causes dermal and intestinal ulceration. *Journal of Lipid Research* 50:1870-1880.

46. Stoffel, W., Holz, B., Jenke, B., Binczek, E., Gunter, R.H., Kiss, C., Karakesisoglou, I., Thevis, M., Weber, A.A., Arnhold, S., et al. 2008. Delta6-desaturase (FADS2) deficiency unveils the role of omega3- and omega6-polyunsaturated fatty acids. *EMBO Journal* 27:2281-2292.

47. Nakamura, M.T., and Nara, T.Y. 2004. Structure, function, and dietary regulation of delta6, delta5, and delta9 desaturases. *Annual Review of Nutrition* 24:345-376.

48. Bevan, P. 2001. Insulin signalling. *Journal of Cell Science* 114:1429-1430.

49. Rojas, F.A., Hirata, A.E., and Saad, M.J. 2001. Regulation of IRS-2 tyrosine phosphorylation in fasting and diabetes. *Molecular and Cellular Endocrinology* 183:63-69.

50. Rojas, F.A., Hirata, A.E., and Saad, M.J. 2003. Regulation of insulin receptor substrate-2 tyrosine phosphorylation in animal models of insulin resistance. *Endocrine* 21:115-122.

51. Sajan, M.P., Standaert, M.L., Nimal, S., Varanasi, U., Pastoor, T., Mastorides, S., Braun, U., Leitges, M., and Farese, R.V. 2009. The critical role of atypical protein kinase C in activating hepatic SREBP-1c and NFkappaB in obesity. *Journal of Lipid Research* 50:1133-1145.

52. Cai, D., Yuan, M., Frantz, D.F., Melendez, P.A., Hansen, L., Lee, J., and Shoelson, S.E. 2005. Local and systemic insulin resistance resulting from hepatic activation of IKK-beta and NF-kappaB. *Nature Medicine* 11:183-190.

53. Sabio, G., Das, M., Mora, A., Zhang, Z., Jun, J.Y., Ko, H.J., Barrett, T., Kim, J.K., and Davis, R.J. 2008. A stress signaling pathway in adipose tissue regulates hepatic insulin resistance. *Science* 322:1539-1543.

54. Dentin, R., Liu, Y., Koo, S.H., Hedrick, S., Vargas, T., Heredia, J., Yates, J., 3rd, and Montminy, M. 2007. Insulin modulates gluconeogenesis by inhibition of the coactivator TORC2. *Nature* 449:366-369.

55. Grasfeder, L.L., Gaillard, S., Hammes, S.R., Ilkayeva, O., Newgard, C.B., Hochberg, R.B., Dwyer, M.A., Chang, C.Y., and McDonnell, D.P. 2009. Fasting-induced hepatic production of DHEA is regulated by PGC-1alpha, ERRalpha, and HNF4alpha. *Molecular Endocrinology* 23:1171-1182.

56. Guertin, D.A., Stevens, D.M., Thoreen, C.C., Burds, A.A., Kalaany, N.Y., Moffat, J., Brown, M., Fitzgerald, K.J., and Sabatini, D.M. 2006. Ablation in mice of the mTORC components raptor, rictor, or mLST8 reveals that mTORC2 is required for signaling to Akt-FOXO and PKCalpha, but not S6K1. *Developmental Cell* 11:859-871.

57. Yan, L., Lavin, V.A., Moser, L.R., Cui, Q., Kanies, C., and Yang, E. 2008. PP2A regulates the pro-apoptotic activity of FOXO1. *Journal of Biological Chemistry* 283:7411-7420.

58. Wu, Z., Jiao, P., Huang, X., Feng, B., Feng, Y., Yang, S., Hwang, P., Du, J., Nie, Y., Xiao, G., et al. 2010. MAPK phosphatase-3 promotes hepatic gluconeogenesis through dephosphorylation of forkhead box O1 in mice. *Journal of Clinical Investigation* 120:3901-3911.

59. Koo, S.H., Satoh, H., Herzig, S., Lee, C.H., Hedrick, S., Kulkarni, R., Evans, R.M., Olefsky, J., and Montminy, M. 2004. PGC-1 promotes insulin resistance in liver through PPAR-alpha-dependent induction of TRB-3. *Nature Medicine* 10:530-534.

60. Li, X., Monks, B., Ge, Q., and Birnbaum, M.J. 2007. Akt/PKB regulates hepatic metabolism by directly inhibiting PGC-1alpha transcription coactivator. *Nature* 447:1012-1016.

61. Lin, H.V., and Accili, D. 2011. Hormonal regulation of hepatic glucose production in health and disease. *Cell Metabolism* 14:9-19.

62. Guo, S., Rena, G., Cichy, S., He, X., Cohen, P., and Unterman, T. 1999. Phosphorylation of serine 256 by protein kinase B disrupts transactivation by FKHR and mediates effects of insulin on insulin-like growth factor-binding protein-1 promoter activity through a conserved insulin response sequence. *Journal of Biological Chemistry* 274:17184-17192.

63. Aoki, M., Jiang, H., and Vogt, P.K. 2004. Proteasomal degradation of the FoxO1 transcriptional regulator in cells transformed by the P3k and Akt oncoproteins. *Proceedings of the National Academy of Sciences of the United States of America* 101:13613-13617.

64. Matsumoto, M., Pocai, A., Rossetti, L., Depinho, R.A., and Accili, D. 2007. Impaired regulation of hepatic glucose production in mice lacking the forkhead transcription factor Foxo1 in liver. *Cell Metabolism* 6:208-216.

65. Puigserver, P., Rhee, J., Donovan, J., Walkey, C.J., Yoon, J.C., Oriente, F., Kitamura, Y., Altomonte, J., Dong, H., Accili, D., et al. 2003. Insulin-regulated hepatic gluconeogenesis through FOXO1-PGC-1alpha interaction. *Nature* 423:550-555.

66. Altomonte, J., Richter, A., Harbaran, S., Suriawinata, J., Nakae, J., Thung, S.N., Meseck, M., Accili, D., and Dong, H. 2003. Inhibition of Foxo1 function is associated with improved fasting glycemia in diabetic mice. *American Journal of Physiology-Endocrinology and Metabolism* 285:E718-728.

67. Sparks, J.D., and Sparks, C.E. 2008. Overindulgence and metabolic syndrome: is FoxO1 a missing link? *Journal of Clinical Investigation* 118:2012-2015.

68. Yoon, J.C., Puigserver, P., Chen, G., Donovan, J., Wu, Z., Rhee, J., Adelmant, G., Stafford, J., Kahn, C.R., Granner, D.K., et al. 2001.

Control of hepatic gluconeogenesis through the transcriptional coactivator PGC-1. *Nature* 413:131-138.

69. Qiang, L., Banks, A.S., and Accili, D. 2010. Uncoupling of acetylation from phosphorylation regulates FoxO1 function independent of its subcellular localization. *Journal of Biological Chemistry* 285:27396-27401.

70. Housley, M.P., Rodgers, J.T., Udeshi, N.D., Kelly, T.J., Shabanowitz, J., Hunt, D.F., Puigserver, P., and Hart, G.W. 2008. O-GlcNAc regulates FoxO activation in response to glucose. *Journal of Biological Chemistry* 283:16283-16292.

71. Yang, J., Cron, P., Thompson, V., Good, V.M., Hess, D., Hemmings, B.A., and Barford, D. 2002. Molecular mechanism for the regulation of protein kinase B/Akt by hydrophobic motif phosphorylation. *Molecular Cell* 9:1227-1240.

72. Dormond, O., Madsen, J.C., and Briscoe, D.M. 2007. The effects of mTOR-Akt interactions on anti-apoptotic signaling in vascular endothelial cells. *Journal of Biological Chemistry* 282:23679-23686.

73. Dong, L.Q., and Liu, F. 2005. PDK2: the missing piece in the receptor tyrosine kinase signaling pathway puzzle. *American Journal of Physiology-Endocrinology and Metabolism* 289:E187-196.

74. Zhang, C., Wendel, A.A., Keogh, M.R., Harris, T.E., Chen, J., and Coleman, R.A. 2012. Glycerolipid signals alter mTOR complex 2

(mTORC2) to diminish insulin signaling. *Proceedings of the National Academy of Sciences of the United States of America* 109:1667-1672.

75. Wang, R.H., Kim, H.S., Xiao, C., Xu, X., Gavrilova, O., and Deng, C.X. 2011. Hepatic Sirt1 deficiency in mice impairs mTorc2/Akt signaling and results in hyperglycemia, oxidative damage, and insulin resistance. *Journal of Clinical Investigation* 121:4477-4490.

76. Zoncu, R., Efeyan, A., and Sabatini, D.M. 2011. mTOR: from growth signal integration to cancer, diabetes and ageing. *Nature Reviews Molecular Cell Biology* 12:21-35.

77. Wullschleger, S., Loewith, R., and Hall, M.N. 2006. TOR signaling in growth and metabolism. *Cell* 124:471-484.

78. Hresko, R.C., and Mueckler, M. 2005. mTOR.RICTOR is the Ser473 kinase for Akt/protein kinase B in 3T3-L1 adipocytes. *Journal of Biological Chemistry* 280:40406-40416.

79. Chen, J., Parsons, S., and Brautigan, D.L. 1994. Tyrosine phosphorylation of protein phosphatase 2A in response to growth stimulation and v-src transformation of fibroblasts. *Journal of Biological Chemistry* 269:7957-7962.

80. Xu, H., Yang, Q., Shen, M., Huang, X., Dembski, M., Gimeno, R., Tartaglia, L.A., Kapeller, R., and Wu, Z. 2005. Dual specificity MAPK phosphatase 3 activates PEPCK gene transcription and increases

gluconeogenesis in rat hepatoma cells. *Journal of Biological Chemistry* 280:36013-36018.

81. Mills, E., Kuhn, C.M., Feinglos, M.N., and Surwit, R. 1993. Hypertension in CB57BL/6J mouse model of non-insulin-dependent diabetes mellitus. *American Journal of Physiology* 264:R73-78.

82. Surwit, R.S., Feinglos, M.N., Rodin, J., Sutherland, A., Petro, A.E., Opara, E.C., Kuhn, C.M., and Rebuffe-Scrive, M. 1995. Differential effects of fat and sucrose on the development of obesity and diabetes in C57BL/6J and A/J mice. *Metabolism: Clinical and Experimental* 44:645-651.

83. West, D.B., Waguespack, J., and McCollister, S. 1995. Dietary obesity in the mouse: interaction of strain with diet composition. *American Journal of Physiology* 268:R658-665.

84. Buettner, R., Scholmerich, J., and Bollheimer, L.C. 2007. High-fat diets: modeling the metabolic disorders of human obesity in rodents. *Obesity (Silver Spring)* 15:798-808.

85. Gao, D., Nong, S., Huang, X., Lu, Y., Zhao, H., Lin, Y., Man, Y., Wang, S., Yang, J., and Li, J. 2010. The effects of palmitate on hepatic insulin resistance are mediated by NADPH Oxidase 3-derived reactive oxygen species through JNK and p38MAPK pathways. *Journal of Biological Chemistry* 285:29965-29973.

86. Okamoto, T., Kanemoto, N., Ban, T., Sudo, T., Nagano, K., and Niki, I. 2009. Establishment and characterization of a novel method for evaluating gluconeogenesis using hepatic cell lines, H4IIE and HepG2. *Archives of Biochemistry and Biophysics* 491:46-52.

87. Lusis, A.J., Attie, A.D., and Reue, K. 2008. Metabolic syndrome: from epidemiology to systems biology. *Nature Reviews Genetics* 9:819-830.

88. Cinti, D.L., Cook, L., Nagi, M.N., and Suneja, S.K. 1992. The fatty acid chain elongation system of mammalian endoplasmic reticulum. *Progress in Lipid Research* 31:1-51.

89. Jakobsson, A., Westerberg, R., and Jacobsson, A. 2006. Fatty acid elongases in mammals: their regulation and roles in metabolism. *Progress in Lipid Research* 45:237-249.

90. Leonard, A.E., Pereira, S.L., Sprecher, H., and Huang, Y.S. 2004. Elongation of long-chain fatty acids. *Progress in Lipid Research* 43:36-54.

91. Denic, V., and Weissman, J.S. 2007. A molecular caliper mechanism for determining very long-chain fatty acid length. *Cell* 130:663-677.

92. Moon, Y.A., and Horton, J.D. 2003. Identification of two mammalian reductases involved in the two-carbon fatty acyl elongation cascade. *Journal of Biological Chemistry* 278:7335-7343.

93. Moon, Y.A., Shah, N.A., Mohapatra, S., Warrington, J.A., and Horton, J.D. 2001. Identification of a mammalian long chain fatty acyl elongase

regulated by sterol regulatory element-binding proteins. *Journal of Biological Chemistry* 276:45358-45366.

94. Wang, Y., Botolin, D., Xu, J., Christian, B., Mitchell, E., Jayaprakasam, B., Nair, M.G., Peters, J.M., Busik, J.V., Olson, L.K., et al. 2006. Regulation of hepatic fatty acid elongase and desaturase expression in diabetes and obesity. *Journal of Lipid Research* 47:2028-2041.

95. Sprecher, H. 2000. Metabolism of highly unsaturated n-3 and n-6 fatty acids. *Biochimica et Biophysica Acta* 1486:219-231.

96. Westerberg, R., Mansson, J.E., Golozoubova, V., Shabalina, I.G., Backlund, E.C., Tvrdik, P., Retterstol, K., Capecchi, M.R., and Jacobsson, A. 2006. ELOVL3 is an important component for early onset of lipid recruitment in brown adipose tissue. *Journal of Biological Chemistry* 281:4958-4968.

97. Jump, D.B., Botolin, D., Wang, Y., Xu, J., Demeure, O., and Christian, B. 2008. Docosahexaenoic acid (DHA) and hepatic gene transcription. *Chemistry and Physics of Lipids* 153:3-13.

98. Jump, D.B. 2004. Fatty acid regulation of gene transcription. *Critical Reviews in Clinical Laboratory Sciences* 41:41-78.

99. Yang, J., Kong, X., Martins-Santos, M.E., Aleman, G., Chaco, E., Liu, G.E., Wu, S.Y., Samols, D., Hakimi, P., Chiang, C.M., et al. 2009. Activation of SIRT1 by resveratrol represses transcription of the gene for the cytosolic form of phosphoenolpyruvate carboxykinase (GTP) by

deacetylating hepatic nuclear factor 4alpha. *Journal of Biological Chemistry* 284:27042-27053.

100. Rhee, J., Inoue, Y., Yoon, J.C., Puigserver, P., Fan, M., Gonzalez, F.J., and Spiegelman, B.M. 2003. Regulation of hepatic fasting response by PPARgamma coactivator-1alpha (PGC-1): requirement for hepatocyte nuclear factor 4alpha in gluconeogenesis. *Proceedings of the National Academy of Sciences of the United States of America* 100:4012-4017.

101. Zhang, W., Patil, S., Chauhan, B., Guo, S., Powell, D.R., Le, J., Klotsas, A., Matika, R., Xiao, X., Franks, R., et al. 2006. FoxO1 regulates multiple metabolic pathways in the liver: effects on gluconeogenic, glycolytic, and lipogenic gene expression. *Journal of Biological Chemistry* 281:10105-10117.

102. Cassuto, H., Kochan, K., Chakravarty, K., Cohen, H., Blum, B., Olswang, Y., Hakimi, P., Xu, C., Massillon, D., Hanson, R.W., et al. 2005. Glucocorticoids regulate transcription of the gene for phosphoenolpyruvate carboxykinase in the liver via an extended glucocorticoid regulatory unit. *Journal of Biological Chemistry* 280:33873-33884.

103. Potthoff, M.J., Inagaki, T., Satapati, S., Ding, X., He, T., Goetz, R., Mohammadi, M., Finck, B.N., Mangelsdorf, D.J., Kliewer, S.A., et al. 2009. FGF21 induces PGC-1alpha and regulates carbohydrate and fatty acid metabolism during the adaptive starvation response.

Proceedings of the National Academy of Sciences of the United States of America 106:10853-10858.

104. An, J., Muoio, D.M., Shiota, M., Fujimoto, Y., Cline, G.W., Shulman, G.I., Koves, T.R., Stevens, R., Millington, D., and Newgard, C.B. 2004. Hepatic expression of malonyl-CoA decarboxylase reverses muscle, liver and whole-animal insulin resistance. *Nature Medicine* 10:268-274.

105. Inagaki, T., Dutchak, P., Zhao, G., Ding, X., Gautron, L., Parameswara, V., Li, Y., Goetz, R., Mohammadi, M., Esser, V., et al. 2007. Endocrine regulation of the fasting response by PPARalpha-mediated induction of fibroblast growth factor 21. *Cell Metabolism* 5:415-425.

106. Raymer, B., Kavana, M., Price, A., Wang, B., Corcoran, L., Kulathila, R., Groarke, J., and Mann, T. 2009. Synthesis and characterization of a BODIPY-labeled derivative of Soraphen A that binds to acetyl-CoA carboxylase. *Bioorganic and Medicinal Chemistry Letters* 19:2804-2807.

107. Daitoku, H., Yamagata, K., Matsuzaki, H., Hatta, M., and Fukamizu, A. 2003. Regulation of PGC-1 promoter activity by protein kinase B and the forkhead transcription factor FKHR. *Diabetes* 52:642-649.

108. Matsuzaki, H., Daitoku, H., Hatta, M., Tanaka, K., and Fukamizu, A. 2003. Insulin-induced phosphorylation of FKHR (Foxo1) targets to proteasomal degradation. *Proceedings of the National Academy of Sciences of the United States of America* 100:11285-11290.

109. Du, K., Herzig, S., Kulkarni, R.N., and Montminy, M. 2003. TRB3: a tribbles homolog that inhibits Akt/PKB activation by insulin in liver. *Science* 300:1574-1577.

110. Maira, S.M., Galetic, I., Brazil, D.P., Kaech, S., Ingley, E., Thelen, M., and Hemmings, B.A. 2001. Carboxyl-terminal modulator protein (CTMP), a negative regulator of PKB/Akt and v-Akt at the plasma membrane. *Science* 294:374-380.

111. Ugi, S., Imamura, T., Maegawa, H., Egawa, K., Yoshizaki, T., Shi, K., Obata, T., Ebina, Y., Kashiwagi, A., and Olefsky, J.M. 2004. Protein phosphatase 2A negatively regulates insulin's metabolic signaling pathway by inhibiting Akt (protein kinase B) activity in 3T3-L1 adipocytes. *Molecular and Cellular Biology* 24:8778-8789.

112. Chen, J., Martin, B.L., and Brautigan, D.L. 1992. Regulation of protein serine-threonine phosphatase type-2A by tyrosine phosphorylation. *Science* 257:1261-1264.

113. Zhou, Y., Li, L., Liu, Q., Xing, G., Kuai, X., Sun, J., Yin, X., Wang, J., Zhang, L., and He, F. 2008. E3 ubiquitin ligase SIAH1 mediates ubiquitination and degradation of TRB3. *Cellular Signalling* 20:942-948.

114. Stulnig, T.M., Huber, J., Leitinger, N., Imre, E.M., Angelisova, P., Nowotny, P., and Waldhausl, W. 2001. Polyunsaturated eicosapentaenoic acid displaces proteins from membrane rafts by

altering raft lipid composition. *Journal of Biological Chemistry* 276:37335-37340.

115. Chen, W., Jump, D.B., Esselman, W.J., and Busik, J.V. 2007. Inhibition of cytokine signaling in human retinal endothelial cells through modification of caveolae/lipid rafts by docosahexaenoic acid. *Investigative Ophthalmology and Visual Science* 48:18-26.

116. Chen, W., Esselman, W.J., Jump, D.B., and Busik, J.V. 2005. Anti-inflammatory effect of docosahexaenoic acid on cytokine-induced adhesion molecule expression in human retinal vascular endothelial cells. *Investigative Ophthalmology and Visual Science* 46:4342-4347.

117. Chen, W., Jump, D.B., Grant, M.B., Esselman, W.J., and Busik, J.V. 2003. Dyslipidemia, but not hyperglycemia, induces inflammatory adhesion molecules in human retinal vascular endothelial cells. *Investigative Ophthalmology and Visual Science* 44:5016-5022.

118. Tikhonenko, M., Lydic, T.A., Wang, Y., Chen, W., Opreanu, M., Sochacki, A., McSorley, K.M., Renis, R.L., Kern, T., Jump, D.B., et al. 2010. Remodeling of retinal Fatty acids in an animal model of diabetes: a decrease in long-chain polyunsaturated fatty acids is associated with a decrease in fatty acid elongases Elovl2 and Elovl4. *Diabetes* 59:219-227.

119. Sakamoto, K., McCarthy, A., Smith, D., Green, K.A., Grahame Hardie, D., Ashworth, A., and Alessi, D.R. 2005. Deficiency of LKB1 in skeletal

muscle prevents AMPK activation and glucose uptake during contraction. *EMBO Journal* 24:1810-1820.

120. Samuel, V.T., Beddow, S.A., Iwasaki, T., Zhang, X.M., Chu, X., Still, C.D., Gerhard, G.S., and Shulman, G.I. 2009. Fasting hyperglycemia is not associated with increased expression of PEPCK or G6Pc in patients with Type 2 Diabetes. *Proceedings of the National Academy of Sciences of the United States of America* 106:12121-12126.

121. Burgess, S.C., He, T., Yan, Z., Lindner, J., Sherry, A.D., Malloy, C.R., Browning, J.D., and Magnuson, M.A. 2007. Cytosolic phosphoenolpyruvate carboxykinase does not solely control the rate of hepatic gluconeogenesis in the intact mouse liver. *Cell Metabolism* 5:313-320.

122. Chevalier, S., Burgess, S.C., Malloy, C.R., Gougeon, R., Marliss, E.B., and Morais, J.A. 2006. The greater contribution of gluconeogenesis to glucose production in obesity is related to increased whole-body protein catabolism. *Diabetes* 55:675-681.

123. Kamagate, A., Qu, S., Perdomo, G., Su, D., Kim, D.H., Slusher, S., Meseck, M., and Dong, H.H. 2008. FoxO1 mediates insulin-dependent regulation of hepatic VLDL production in mice. *Journal of Clinical Investigation* 118:2347-2364.

124. Altomonte, J., Cong, L., Harbaran, S., Richter, A., Xu, J., Meseck, M., and Dong, H.H. 2004. Foxo1 mediates insulin action on apoC-III and

triglyceride metabolism. *Journal of Clinical Investigation* 114:1493-1503.

125. Warensjo, E., Ohrvall, M., and Vessby, B. 2006. Fatty acid composition and estimated desaturase activities are associated with obesity and lifestyle variables in men and women. *Nutrition, Metabolism and Cardiovascular Diseases* 16:128-136.

126. Warensjo, E., Riserus, U., and Vessby, B. 2005. Fatty acid composition of serum lipids predicts the development of the metabolic syndrome in men. *Diabetologia* 48:1999-2005.

127. Zhu, Q.Q., Lou, D.J., Si, X.W., Guan, L.L., You, Q.Y., Yu, Z.M., Zhang, A.Z., and Li, D. 2010. [Serum omega-3 polyunsaturated fatty acid and insulin resistance in type 2 diabetes mellitus and non-alcoholic fatty liver disease]. *Zhonghua Nei Ke Za Zhi* 49:305-308.

128. Cho, H., Mu, J., Kim, J.K., Thorvaldsen, J.L., Chu, Q., Crenshaw, E.B., 3rd, Kaestner, K.H., Bartolomei, M.S., Shulman, G.I., and Birnbaum, M.J. 2001. Insulin resistance and a diabetes mellitus-like syndrome in mice lacking the protein kinase Akt2 (PKB beta). *Science* 292:1728-1731.

129. Brozinick, J.T., Jr., and Birnbaum, M.J. 1998. Insulin, but not contraction, activates Akt/PKB in isolated rat skeletal muscle. *Journal of Biological Chemistry* 273:14679-14682.

130. Kohn, A.D., Summers, S.A., Birnbaum, M.J., and Roth, R.A. 1996. Expression of a constitutively active Akt Ser/Thr kinase in 3T3-L1 adipocytes stimulates glucose uptake and glucose transporter 4 translocation. *Journal of Biological Chemistry* 271:31372-31378.

131. Liao, J., Barthel, A., Nakatani, K., and Roth, R.A. 1998. Activation of protein kinase B/Akt is sufficient to repress the glucocorticoid and cAMP induction of phosphoenolpyruvate carboxykinase gene. *Journal of Biological Chemistry* 273:27320-27324.

132. Cho, H., Thorvaldsen, J.L., Chu, Q., Feng, F., and Birnbaum, M.J. 2001. Akt1/PKBalpha is required for normal growth but dispensable for maintenance of glucose homeostasis in mice. *Journal of Biological Chemistry* 276:38349-38352.

133. Sarbassov, D.D., Guertin, D.A., Ali, S.M., and Sabatini, D.M. 2005. Phosphorylation and regulation of Akt/PKB by the rictor-mTOR complex. *Science* 307:1098-1101.

134. Zong, H., Bastie, C.C., Xu, J., Fassler, R., Campbell, K.P., Kurland, I.J., and Pessin, J.E. 2009. Insulin resistance in striated muscle-specific integrin receptor beta1-deficient mice. *Journal of Biological Chemistry* 284:4679-4688.

135. Pearce, L.R., Huang, X., Boudeau, J., Pawlowski, R., Wullschleger, S., Deak, M., Ibrahim, A.F., Gourlay, R., Magnuson, M.A., and Alessi, D.R.

2007. Identification of Protor as a novel Rictor-binding component of mTOR complex-2. *Biochemical Journal* 405:513-522.

136. Hagiwara, A., Cornu, M., Cybulski, N., Polak, P., Betz, C., Trapani, F., Terracciano, L., Heim, M.H., Ruegg, M.A., and Hall, M.N. 2012. Hepatic mTORC2 Activates Glycolysis and Lipogenesis through Akt, Glucokinase, and SREBP1c. *Cell Metabolism* 15:725-738.

137. Lindsley, C.W., Zhao, Z., Leister, W.H., Robinson, R.G., Barnett, S.F., Defeo-Jones, D., Jones, R.E., Hartman, G.D., Huff, J.R., Huber, H.E., et al. 2005. Allosteric Akt (PKB) inhibitors: discovery and SAR of isozyme selective inhibitors. *Bioorganic and Medicinal Chemistry Letters* 15:761-764.

138. Moore, S.F., Hunter, R.W., and Hers, I. 2011. mTORC2 protein-mediated protein kinase B (Akt) serine 473 phosphorylation is not required for Akt1 activity in human platelets. *Journal of Biological Chemistry* 286:24553-24560.

139. Gu, Y., Lindner, J., Kumar, A., Yuan, W., and Magnuson, M.A. 2011. Rictor/mTORC2 is essential for maintaining a balance between beta-cell proliferation and cell size. *Diabetes* 60:827-837.

140. Breuleux, M., Klopfenstein, M., Stephan, C., Doughty, C.A., Barys, L., Maira, S.M., Kwiatkowski, D., and Lane, H.A. 2009. Increased AKT S473 phosphorylation after mTORC1 inhibition is rictor dependent and

does not predict tumor cell response to PI3K/mTOR inhibition. *Molecular Cancer Therapeutics* 8:742-753.

141. Efeyan, A., and Sabatini, D.M. 2010. mTOR and cancer: many loops in one pathway. *Current Opinion in Cell Biology* 22:169-176.

142. Emerling, B.M., and Akcakanat, A. 2011. Targeting PI3K/mTOR signaling in cancer. *Cancer Research* 71:7351-7359.

143. Feldman, M.E., Apsel, B., Uotila, A., Loewith, R., Knight, Z.A., Ruggero, D., and Shokat, K.M. 2009. Active-site inhibitors of mTOR target rapamycin-resistant outputs of mTORC1 and mTORC2. *PLoS Biol*ogy 7:e38.

144. Chen, C.H., Shaikenov, T., Peterson, T.R., Aimbetov, R., Bissenbaev, A.K., Lee, S.W., Wu, J., Lin, H.K., and Sarbassov dos, D. 2011. ER stress inhibits mTORC2 and Akt signaling through GSK-3beta-mediated phosphorylation of rictor. *Science Signaling* 4:ra10.

145. Dibble, C.C., Asara, J.M., and Manning, B.D. 2009. Characterization of Rictor phosphorylation sites reveals direct regulation of mTOR complex 2 by S6K1. *Molecular and Cellular Biology* 29:5657-5670.

146. Julien, L.A., Carriere, A., Moreau, J., and Roux, P.P. 2010. mTORC1-activated S6K1 phosphorylates Rictor on threonine 1135 and regulates mTORC2 signaling. *Molecular and Cellular Biology* 30:908-921.

147. Treins, C., Warne, P.H., Magnuson, M.A., Pende, M., and Downward, J. 2010. Rictor is a novel target of p70 S6 kinase-1. *Oncogene* 29:1003-1016.

148. Honkanen, R.E., Zwiller, J., Moore, R.E., Daily, S.L., Khatra, B.S., Dukelow, M., and Boynton, A.L. 1990. Characterization of microcystin-LR, a potent inhibitor of type 1 and type 2A protein phosphatases. *Journal of Biological Chemistry* 265:19401-19404.

149. Sarbassov, D.D., Ali, S.M., Kim, D.H., Guertin, D.A., Latek, R.R., Erdjument-Bromage, H., Tempst, P., and Sabatini, D.M. 2004. Rictor, a novel binding partner of mTOR, defines a rapamycin-insensitive and raptor-independent pathway that regulates the cytoskeleton. *Current Biology* 14:1296-1302.

150. McDonald, P.C., Oloumi, A., Mills, J., Dobreva, I., Maidan, M., Gray, V., Wederell, E.D., Bally, M.B., Foster, L.J., and Dedhar, S. 2008. Rictor and integrin-linked kinase interact and regulate Akt phosphorylation and cancer cell survival. *Cancer Research* 68:1618-1624.

151. Borkman, M., Storlien, L.H., Pan, D.A., Jenkins, A.B., Chisholm, D.J., and Campbell, L.V. 1993. The relation between insulin sensitivity and the fatty-acid composition of skeletal-muscle phospholipids. *New England Journal of Medicine* 328:238-244.

152. Pan, D.A., Lillioja, S., Milner, M.R., Kriketos, A.D., Baur, L.A., Bogardus, C., and Storlien, L.H. 1995. Skeletal muscle membrane lipid

composition is related to adiposity and insulin action. *Journal of Clinical Investigation* 96:2802-2808.

153. Vessby, B., Aro, A., Skarfors, E., Berglund, L., Salminen, I., and Lithell, H. 1994. The risk to develop NIDDM is related to the fatty acid composition of the serum cholesterol esters. *Diabetes* 43:1353-1357.

154. Vessby, B., Tengblad, S., and Lithell, H. 1994. Insulin sensitivity is related to the fatty acid composition of serum lipids and skeletal muscle phospholipids in 70-year-old men. *Diabetologia* 37:1044-1050.

155. Brown, J.M., Chung, S., Sawyer, J.K., Degirolamo, C., Alger, H.M., Nguyen, T.M., Zhu, X., Duong, M.N., Brown, A.L., Lord, C., et al. 2010. Combined therapy of dietary fish oil and stearoyl-CoA desaturase 1 inhibition prevents the metabolic syndrome and atherosclerosis. *Arteriosclerosis, Thrombosis, and Vascular Biology* 30:24-30.

156. Chirala, S.S., Chang, H., Matzuk, M., Abu-Elheiga, L., Mao, J., Mahon, K., Finegold, M., and Wakil, S.J. 2003. Fatty acid synthesis is essential in embryonic development: fatty acid synthase null mutants and most of the heterozygotes die in utero. *Proceedings of the National Academy of Sciences of the United States of America* 100:6358-6363.

157. Flowers, M.T., Groen, A.K., Oler, A.T., Keller, M.P., Choi, Y., Schueler, K.L., Richards, O.C., Lan, H., Miyazaki, M., Kuipers, F., et al. 2006. Cholestasis and hypercholesterolemia in SCD1-deficient mice fed a

low-fat, high-carbohydrate diet. *Journal of Lipid Research* 47:2668-2680.

158. Gutierrez-Juarez, R., Pocai, A., Mulas, C., Ono, H., Bhanot, S., Monia, B.P., and Rossetti, L. 2006. Critical role of stearoyl-CoA desaturase-1 (SCD1) in the onset of diet-induced hepatic insulin resistance. *Journal of Clinical Investigation* 116:1686-1695.

159. Harada, N., Oda, Z., Hara, Y., Fujinami, K., Okawa, M., Ohbuchi, K., Yonemoto, M., Ikeda, Y., Ohwaki, K., Aragane, K., et al. 2007. Hepatic de novo lipogenesis is present in liver-specific ACC1-deficient mice. *Molecular and Cellular Biology* 27:1881-1888.